uOttawa

L'Université canadienne
Canada's university

FACULTÉ DES ÉTUDES SUPÉRIEURES ET POSTOCTORALES

uOttawa

L'Université canadienne
Canada's university

FACULTY OF GRADUATE AND POSDOCTORAL STUDIES

Louise Gariépy-Boudreault
AUTEUR DE LA THÈSE / AUTHOR OF THESIS

Ph.D. (Cellular and Molecular Medicine)
GRADE / DEGREE

Department of Cellular and Molecular Medicine
FACULTÉ, ÉCOLE, DÉPARTEMENT / FACULTY, SCHOOL, DEPARTMENT

Sk_{ATP} Channels Protect Skeletal Muscles Against Fibre Damage During Fatigue by Preventing Excessive Increases in $[Ca^{2+}]i$

TITRE DE LA THÈSE / TITLE OF THESIS

Jean-Marc Renaud
DIRECTEUR (DIRECTRICE) DE LA THÈSE / THESIS SUPERVISOR

CO-DIRECTEUR (CO-DIRECTRICE) DE LA THÈSE / THESIS CO-SUPERVISOR

Paul Albert

Micheal Jonz

Antony Krantis

Brian MacIntosh (University of Calgary)

Gary W. Slater
Le Doyen de la Faculté des études supérieures et postdoctorales / Dean of the Faculty of Graduate and Postdoctoral Studies

sK_{ATP} CHANNELS PROTECT SKELETAL MUSCLE AGAINST FIBRE DAMAGE DURING FATIGUE BY PREVENTING EXCESSIVE INCREASES IN $[Ca^{2+}]i$

by

Louise Gariépy-Boudreault

Thesis submitted to the Faculty of Graduate and Postdoctoral Studies as a partial fulfillment of the Ph.D. program in Cellular and Molecular Medicine.

Submitted: March 30, 2010

Department of Cellular and Molecular Medicine
Faculty of Medicine
University of Ottawa

Your file Votre référence
ISBN: 978-0-494-66001-0
Our file Notre référence
ISBN: 978-0-494-66001-0

ABSTRACT

Opening sarcolemmal ATP-sensitive potassium channels (sKATP channels) contributes to increasing the rate of fatigue in skeletal muscle by reducing action potential amplitude. However, in previous studies, when sKATP channel activity was abolished, the rate of fatigue was not decreased; rather, the muscles developed significant contractile dysfunctions including greater unstimulated force, reduced force recovery and fibre damage. The aim of this study was to determine how abolishing sKATP channel activity during fatigue results in a faster rate of fatigue compared to wild type muscle. Single fibres and small bundles from the flexor digitorum brevis (FDB) muscle were utilized. sKATP channel activity was abolished pharmacologically using glibenclamide and genetically using Kir6.2$^{-/-}$ mice. This study demonstrated for the first time that abolishing sKATP channel activity at 37°C resulted in faster decreases in peak $Ca^{2+}i$ and tetanic force than in wild type fibres. Furthermore, several contractile dysfunctions were observed in sKATP channel deficient muscle fibres. They included partially or completely supercontracted single muscle fibres, large membrane depolarizations, greater increases in unstimulated $Ca^{2+}i$ and unstimulated force, and lower force recovery. The application of verapamil prevented the development of several of the contractile dysfunctions by reducing [Ca^{2+}] influx. Furthermore, application of ROS scavengers in sKATP channel deficient muscle reduced the extent of the contractile dysfunctions, suggesting that the rise in [Ca^{2+}]i can lead to deleterious ROS production. This study also demonstrated a novel phenomenon in which one fatigue bout at 37°C improves, within 30 min, fatigue resistance during a second fatigue bout. Furthermore, muscles no longer depended on sKATP channels to protect them against functional impairment and fibre damage during

the second fatigue bout. The phenomenon was defined as 'fatigue pre-conditioning', and does not follow the same signaling pathway as ischemic preconditioning (IPC) observed in heart and skeletal muscle. Thus, it appears that sKATP channels are necessary for myoprotection during a single fatigue bout, and blocking channel activity leads to development of contractile dysfunctions and an apparent faster fatigue rate. However, during subsequent fatigue bouts separated by short time periods, the reliance on sKATP channels for myoprotection is abolished.

TABLE OF CONTENTS

LIST OF FIGURES

LIST OF TABLES

LIST OF ABBREVIATIONS

AP	Action potential
CLC	Chloride channel
DHP	Dihydropyridine
E_{Cl}	Reversal potential of Cl^-
EDL	Extensor digitorum longus
E_K	Reversal potential of K^+
E_M	Membrane potential
E_{Na}	Reversal potential of Na^+
FDB	Flexor digitorum brevis
G_{Cl}	Chloride conductance
G_K	Potassium conductance
G_M	Membrane conductance
H_2O_2	Hydrogen peroxide
Kir	Potassium inward rectifier
Kv	Voltage sensitive K^+ channel
MHC	Myosin heavy chain
mK_{ATP}	Mitochondrial ATP-sensitive K^+ channel
NAC	N-acetyl-cysteine
Nav	Voltage sensitive Na^+ channel
OH•	Hydroxyl radical
P_o	Open probability
ROS	Reactive oxygen species
RYR	Ryanodine receptor
sK_{ATP}	Sarcolemmal ATP-sensitive K^+ channel
SR	Sarcoplasmic reticulum
SUR	Suronylurea receptor

ACKNOWLEDGMENTS

There are so many people that I owe my deepest gratitude to. In my 4+ years here, I know that I would not have gotten this far without you.

First and foremost, Jean-Marc, thank you for being the supervisor that you are. I have witnessed your passion for your students, and your willingness to do anything for them. So many times you helped me. I will miss your daily bombardments of teasing, knowing that as you always say, you only do it because you like me.

To all my committee, always I looked forward to my meetings with you. You made me think outside the box, and challenged me to expand my knowledge. But, Dr. Staines, I don't think I'll ever know you're joking and when you're serious!

To all my labmates, past and present. I've worked with 19 of you, just too many names to list. I helped you, you helped me. May you always be grateful for your time in this lab and the supervisor you have. Take every opportunity you are given and run with it. May the force be with you.

It's easy to forget how many other people play a small but very significant role in completing such a project as this. And so, to Kim, Rainy and Mingying, thank you. Many, many times over. And same to Donna, Sylvie and Blanche. To all the animal care staff, you taught me about mouse habits, breeding, and tail-lifting. Without these mice, I wouldn't have gotten any work done. To every other person in this building who I have gotten to know – those in other labs, purchasing and receiving, health and safety, and those who I don't know who you are, but I smile at when I see you, thank you. Every day, you made my work here a bit more enjoyable.

To both of my families, you all think I'm crazy to stay in school this long. Oh well, I did it anyway. But I promise I'm done now.

To my dear friends Brent, Joe and Tom – you guys truly believed in me. You listened to me rant, you pushed me to do my best, and always made me laugh. To every training buddy I've swam, biked or run with, you all provided entertaining diversions from my lab work for a few hours. Without you, I would not have completed 3 marathons, two ironmans, and a whole slew of other races during my time here.

And lastly, to the one person who, without him, I could not have done this. Alex, every single day you helped me get this far. You cooked and cleaned, made lunches and cleaned litterboxes when I was too busy or too tired. You accepted my drive to succeed, and you never complained about my lack of paycheque. I love you more than you can imagine. I promise that I will learn french now that I'm done school.

CHAPTER 1 - INTRODUCTION

During muscle exercise, energy demand increases 20- to 100- fold, depending on fibre type and activity intensity (Gibbs, 1987). With an increased energy demand, ATP production must increase in order to avoid deleterious ATP depletion, which can lead to impaired muscle function and integrity. One protective mechanism against ATP depletion involves the sarcolemmal ATP-sensitive potassium channel (sKATP channel), which was named upon discovery that ATP binds to the intracellular side to close the channel (Noma, 1983). During fatigue, opening sKATP channels reduces action potential amplitude (Gong *et al.*, 2003), and as a consequence less SR Ca^{2+} is released (Burton & Smith, 1997a). The result is a faster rate of fatigue and preservation of ATP by reduced myosin ATPase and SR Ca^{2+} ATPase activity. Thus, sKATP channels are proposed to link the metabolic status of the muscle fibres to the electrical activity of the cell membrane.

Since activating sKATP channels results in an increased K^+ conductance causing reduced AP amplitude, and therefore faster decreases in rate of fatigue, one would therefore expect that abolishing sKATP channel activity would result in a slower rate of fatigue. However, i*n vitro* studies have shown that abolishing sKATP channel activity results in large membrane depolarization between contractions under metabolic inhibition, (Gramolini & Renaud, 1997) and large increases in unstimulated force during fatigue, which develops when muscle fails to completely relax between contractions (Gong, Miki et al. 2000; Matar, Nosek et al. 2000). Recently, evidence for mild to severe fibre damage in sKATP channel deficient mice following treadmill running (Thabet *et al.*, 2005) and swimming (Kane *et al.*, 2004) was observed.

Therefore, it appears that the effect of sKATP channel activity on the rate of fatigue is a function of the balance between the slower decreases in action potential amplitude and the development of contractile dysfunctions. In particular, these contractile dysfunctions can include both the reduced AP amplitude during a contraction due to excessive membrane depolarization causing Na^+ channel inactivation, as suggested by Gong *et al* (Gong *et al.*, 2003), and possible L-type Ca^{2+} channel activation between contractions, causing deleterious Ca^{2+} influx leading to fibre damage and subsequently reduced force generation, as demonstrated in cardiac muscle when sKATP channel activity is abolished (Zingman *et al.*, 2002). The objective of this study was, therefore, to examine how sKATP channel activity protects skeletal muscle during fatigue.

Muscle contraction cycle

For skeletal muscle to generate force, it must undergo an excitation-contraction coupling cycle consisting of an electrical and mechanical phase. Each muscle contraction is generated by an action potential that originates at the neuromuscular junction, which is a specialized synapse between the α-motoneuron and the muscle fibre. At this junction, the motoneuron releases acetylcholine (Ach) which binds to the ligand-sensitive Ach-receptors (Westerblad *et al.*, 1991). This allows for opening of the Ach-receptor pores to allow for an influx of Na^+, depolarizing the cell membrane and activating neighbouring voltage-sensitive Na^+ channels, permitting a more rapid influx of Na^+ into the cell. The action potential (AP) is conducted along the cell membrane and into the transverse tubules (t-tubules), which are invaginations of the cell membrane. As the t-tubules depolarize, the L-type calcium channels (also known as dihydropyridine (DHP) receptors) undergo a conformational change to allow interaction with the sarcoplasmic

reticulum (SR) Ca^{2+} release channels, the ryanodine receptors (RYRs) (Westerblad *et al.*, 1991). When activated, the RYRs open, allowing for Ca^{2+} to flow into the cytosol.

In skeletal muscle, the sarcomere is comprised of the thick filaments, containing myosin and titin, and the thin filaments, containing desmin (nebulin), troponin, tropomyosin, and actin. These filaments make up the contractile unit for generation of force. About one-third along the length of each tropomyosin molecule is a complex of three globular proteins, troponin C, I and T. The rise in intracellular Ca^{2+} ($Ca^{2+}i$) following an action potential results in binding of Ca^{2+} to troponin C, which triggers a slight movement of tropomyosin and exposure of the myosin binding sites along actin. This allows for cross-bridge formation between actin and myosin, with myosin executing a power-stroke to pull the actin towards the centre of the sarcomere, allowing for the generation of force (via an isometric contraction) and / or shortening of the sarcomere through the length of the fibre (via an isotonic contraction). Upon membrane repolarization, Ca^{2+} disassociates from troponin C, causing the return of tropomyosin to the myosin binding sites on actin. The excess Ca^{2+} is transported back into the SR by the Ca^{2+} ATPase pump, allowing for muscle relaxation.

Membrane potential and ion flux at rest and during a single action potential

At rest. Resting membrane potential (E_m) of skeletal muscle is between -80 and -70 mV. E_m is generated by the movement of ions across the membrane. Both ion concentration and the open probability (P_o) of each ion channel determines ion permeability. Resting intracellular and interstitial ionic concentrations can vary slightly due to fibre type differences. $[Na^+]i$ and $[K^+]i$ are ~6 mM and ~160 mM, while interstitial $[Na^+]$ and $[K^+]$ are 140 mM and 4 mM (Sjogaard, Adams et al. 1985; Green, Bulow et al.

1999; Green, Langberg et al. 2000; Nielsen, Ortenblad et al. 2004; Street, Nielsen et al. 2005). $[Cl^-]i$ is ~12 - 20 mM, while $[Cl^-]int$ is ~130 mM (Lindinger & Heigenhauser, 1988). P_o is a function of each channel's characteristics. At rest, the ratio of $P_K:P_{Cl}:P_{Na}$ is 1 : 10 : 0.005, such that E_m is primarily controlled by the movement of K^+ and Cl^-. Given that the equilibrium potential of K^+ (E_K) is -100 mV and Cl^- (E_{Cl}) is -66 mV in skeletal muscle, it is the movement of these two ions that maintains E_m at the resting potential of -80 to -70 mV (Dulhunty, 1979; Jurkat-Rott *et al.*, 2006). Cl^- is known to be extremely important to stabilize E_m, and any mutation resulting in abolished CLC-1 channel activity will lead to muscle hyperexcitability, as seen in patients suffering from myotonia congenita (McComas & Mrozek, 1968; Bryant & Morales-Aguilera, 1971; Pusch, 2002). Another contributor to E_m at rest is the Na^+K^+ pump, which pumps out 3 Na^+ in exchange for 2 K^+ to maintain concentration gradients (due to the small channel leakage at rest) while generating a net outward current.

During a single action potential. During an AP, the slight depolarization by the Na^+ influx through the ligand-sensitive Ach receptors is large enough to activate the neighboring voltage-sensitive Na^+ channels. These channels open immediately, creating a large increase in Na^+ conductance (G_{Na}) allowing for influx of Na^+ and thus a greater, more rapid depolarization of the membrane. This depolarization propagates along the membrane surface and into the t-tubules. As the depolarization continues, Na^+ channels rapidly inactivate within 1 - 2 ms, but at the same time, the delayed voltage-sensitive K^+ (K_V) channels open. The eventual net result is a peak in action potential amplitude of ~+30 mV, a function of the relationship between Na^+ and Cl^- influx and K^+ efflux (Adrian 1956; Yonemura 1967; Mainwood and Renaud 1985; Juel 1986; Lannergren and

Westerblad 1987; Matar, Nosek et al. 2000). Subsequent rapid repolarization follows due to continued K^+ efflux; as E_m approaches resting potential, K_v channels close and the $Na_v1.4$ channels transform from an inactivated state to a closed state.

Muscle fatigue

Fatigue is described as a decrease in force or work generating capacity with repetitive stimulation. The cause of fatigue is multifactorial, and can be due to a failure anywhere along the path of events from the central nervous system to the sarcomere. Early landmark research demonstrated that a reduced force production by humans caused by high-intensity voluntary contractions could not be improved by direct motor nerve stimulation (Merton, 1954). Therefore, fatigue is an intrinsic property of the muscle itself.

Changes in metabolites during fatigue

During muscular activity, there is an increase in metabolic rate of up to 100-fold over rest (Gibbs, 1987). Adenosine triphosphate (ATP) is the only direct source of energy utilized during a muscle contraction, and is used mainly by three different ATPases: 1. myosin ATPase, which transforms the chemical energy of ATP into mechanical work during the power stroke of the excitation-contraction coupling cycle; 2. the Ca^{2+}-ATPase pump, which allows for re-uptake of the Ca^{2+} into the SR to allow for muscle relaxation; and 3. the Na^+ K^+ ATPase pump, which pumps Na^+ out of the cell in exchange for K^+ in order to maintain the concentration and electrical gradients necessary for the generation of action potentials (Gibbs, 1987; Clausen, 1996). Of the three ATPases, the myosin ATPase was originally believed to account for 50-80% of all ATP consumption during

the muscle contraction cycle (Baker *et al.*, 1994; Szentesi *et al.*, 2001). However, these experiments were carried out at temperatures that are below the physiological range. A recent study conducted at the physiological temperature of 37°C showed that in mouse EDL muscle myosin ATPase may account for only 20% of the total ATP consumption, leading the authors to suggest that the major ATP energy consuming processes involve ion pumps (Zhang *et al.*, 2006a).

It is vital that [ATP]i does not decrease, as this can lead to muscle function impairment, cellular damage or even cell death. Therefore, four ATP production pathways exist to meet the energy demands of the cell. The high-energy phosphocreatine system, glycolysis, and oxidative phosphorylation are the three primary chemical pathways that allow for the formation of ATP by phosphorylating ADP. The relative importance of each of the ATP generating pathways is dependent on: 1. exercise intensity; 2. exercise duration; and 3. muscle fibre type recruitment. High intensity, short duration exercise such as sprinting and weightlifting relies on glycolysis and the phosphocreatine system to rapidly generate ATP, while low intensity, long duration exercise such as marathon running relies predominantly on oxidative phosphorylation.

However, production of ATP through these pathways and the subsequent breakdown of ATP to ADP + P_i results in the generation of several metabolic by-products, some of which can affect force production and lead to fatigue. The majority of studies report that during fatigue, intracellular ATP concentration does not change (Jansson *et al.*, 1987; Vollestad *et al.*, 1988; Cady *et al.*, 1989; Hancock *et al.*, 2005), while some report only a very small decrease of up to 20% (Jacobs *et al.*, 1982; Chasiotis *et al.*, 1987; Bangsbo *et al.*, 1990; Giannesini *et al.*, 2001). One study, however,

measured an 80% decline in [ATP] in Type IIX fibres in humans following maximal cycling exercise (Karatzaferi *et al.*, 2001). At 25°C, Godt and Nosek (1989) observed that a small decrease in MgATP from 6.18 to 4.7 mM (as observed during fatigue and hypoxia) actually increased force development, as did the increase in ADP and AMP at the level of the sarcomere (Godt & Nosek, 1989). On the other hand, an increase in Pi from the breakdown of PCr to Cr and Pi led to significant force depression by decreasing the Ca^{2+} sensitivity of the myofilaments, and in skinned muscle fibres the accumulation of H^+ ions (and therefore a decrease in pHi) from glycolysis reduced the binding of Ca^{2+} to troponin C at 25°C (Blanchard & Solaro, 1984). The combination of lowered pH and greater Pi appear to act independently on force production in slow twitch muscle (Nosek *et al.*, 1990); in fast-twitch muscle, some researchers report an independent effect (Chase & Kushmerick, 1988), while others report a synergistic effect on force (Nosek *et al.*, 1987; Nosek *et al.*, 1990).

However, at 37°C, the increased production of these adenylates (ATP, ADP, and AMP) that occurs during fatigue do not appear to contribute to the onset of fatigue. Furthermore, the effects of Pi and H^+ are abolished when experiments were performed at 37°C (Westerblad, Bruton et al. 1997; Debold, Romatowski et al. 2006). Overall, it appears that the decreased force production during fatigue is not due to changes in metabolic by-products acting at the sarcomere level. Rather, fatigue must be due to an upstream effect, either an altered Ca^{2+} handling or decreased membrane excitability.

Role of Ca^{2+} in muscle fatigue

When considering the effect of changes in Ca^{2+}i on muscle force production, it must be considered that three things may be occurring concurrently: 1. a decrease in Ca^{2+}

release from the SR; 2. a decrease in the Ca^{2+} sensitivity of the myofibrillar proteins, and 3. a decrease in maximum Ca^{2+}-activated force (Westerblad & Allen, 1993). #2 and #3 can be eliminated as discussed above, whereby changes in Ca^{2+} sensitivity and maximum force due to the rise in Pi and H^+ were observed only at 25°C, while at 37°C, these effects were minimal (Godt & Nosek, 1989; Allen *et al.*, 1995; Westerblad *et al.*, 1997; Debold *et al.*, 2006).

On the other hand, there is strong evidence for decreased Ca^{2+} release from the SR as a major mechanism of muscle fatigue (Allen *et al.*, 2008). Eberstein and Sandow (1962) were first to show that when isolated frog muscle fibres that had been stimulated to exhaustion were treated with either 100 mM KCl (to directly depolarize the t-tubules and activate the DHP receptors) or caffeine (to activate RYRs), force was largely restored (Eberstein & Sandow, 1962), suggesting that SR Ca^{2+} release was decreased during fatigue. Allen *et al,* in 1989, were the first to use a Ca^{2+} photoprotein to measure changes in free $[Ca^{2+}]i$ at rest and during stimulation. They demonstrated that during prolonged repetitive stimulation, tetanic $[Ca^{2+}]i$ initially increased and then decreased significantly during repeated tetani, which corresponded to development of fatigue (see Fig. 1.1) (Allen *et al.*, 1989). The initial increase in tetanic $[Ca^{2+}]i$ was ~10 – 40%, depending on muscle preparation, but the final decrease was ~50%, which corresponds to the ~50% decrease in tetanic force (Allen *et al.*, 2002). The question is, why is Ca^{2+} release from the SR decreased during fatigue?

The application of caffeine in unfatigued muscle increased Ca^{2+} release slightly, without affecting force, suggesting that the contractile proteins were maximally activated (Fig 1.1a) (Westerblad & Allen, 1991). However, in fatigued muscle, the application of

caffeine was shown to overcome much, but not all, of the decline in Ca^{2+} release and force generation (Fig 1.1b) (Westerblad & Allen, 1991, 1993), suggesting that the decrease in SR Ca^{2+} release was so large that contractile proteins were no longer maximally activated, and hence the reduced force generation. The fact that the application of caffeine at the end of the fatigue bout did not result in Ca^{2+} release similar to that observed in unfatigued muscles (Fig. 1.1b) suggests that there is a depletion of available Ca^{2+} in the SR for release.

Using skinned muscle fibres, Fryer *et al* (1995) proposed that Pi is able to enter the SR and when large enough, CaP would precipitate within the SR, thus lowering the amount of free Ca^{2+} available for release (Fryer *et al.*, 1995). Further evidence for precipitation was found when muscle from creatine kinase knock-out mice ($CK^{-/-}$ mice) did not show an increase in Pi during intense exercise, and the muscle fibres were considerably more resistant to fatigue (Dahlstedt *et al.*, 2000). However, while a number of studies support this theory of precipitation (Cady, Jones et al. 1989; Kabbara and Allen 1999; Dahlstedt, Katz et al. 2000; Kabbara and Allen 2001; Dutka, Cole et al. 2005), there are those that refute it (Cady *et al.*, 1989; Laver *et al.*, 2001) since the decrease in Ca^{2+} release occurs much more rapidly than the rate of CaP precipitation. It is also possible that the decline in SR free [Ca^{2+}] may also be due to a decreased SR ATPase activity due to metabolite changes occurring during fatigue, thereby reducing Ca^{2+} reuptake into the SR (Fabiato & Fabiato, 1978; Lamb *et al.*, 1992; Duke & Steele, 2001; Steele & Duke, 2003).

FIGURE 1.1

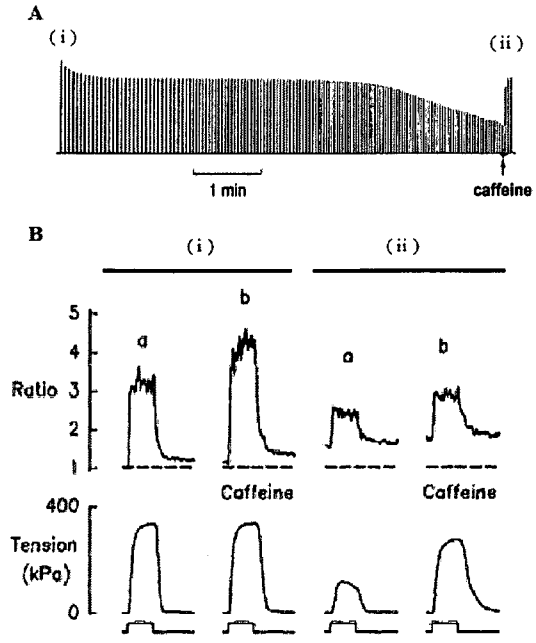

Fig. 1.1. Contribution of impaired SR Ca^{2+} release to muscle fatigue. A) force record of repeated, short tetani continued until force had declined 40%. The final three tetani in A show the effect of rapid application of 10 mM caffeine. B) tetanic Ca^{2+}i ratio from tetani illustrated in A. *(i)* and *(ii)* indicates a representative force tetani whose tetanic Ca^{2+}i ratio are shown beneath. *(a)* and *(b)* represent the absence and presence of 10 mM caffeine. Dashed lines represent resting ratio in control; stimulation periods are displayed below tension records. Note the fall in tetanic Ca^{2+}i ratio from *i* to *ii*, which is associated with the reduced force at time point *ii*. Furthermore, the tetanic Ca^{2+}i ratio induced by caffeine at the end of the fatigue stimulation was accompanied by a substantially enhanced tension production, whereas tension was not markedly affected by the increased Ca^{2+} release at rest. Modified from (Allen *et al.*, 1989; Westerblad & Allen, 1991; Allen *et al.*, 2008).

While Ca^{2+} release is reduced during fatigue, the application of high K^+ to activate the L-type Ca^{2+} channels via a large t-tubular depolarization, or caffeine to directly activate the RYRs, resulted in improved Ca^{2+} release and force recovery in fatigued muscle fibres (Eberstein and Sandow 1962; Westerblad and Allen 1991; Allen and Westerblad 1995). Importantly, this suggests that 1. there was still sufficient SR Ca^{2+} for release to generate maximal force; and 2. there is a failure in Ca^{2+} release from the SR during fatigue that is not due to L-type Ca^{2+} channel or RYR failure, but rather a loss of t-tubular excitability so that the L-type Ca^{2+} channels are not properly activated.

Changes in ion gradients and membrane excitability during fatigue

During fatigue, there is a shift in ion concentration due to passive Na^+ influx and K^+ efflux during an AP, exceeding the capacity of the Na^+K^+ pump to maintain concentration gradients. The shift of K^+ from the intracellular to the interstitial space can cause K^+ levels to reach values from ~4mM up to 11 – 13 mM (Sjogaard *et al.*, 1985; Green *et al.*, 1999; Green *et al.*, 2000; Juel *et al.*, 2000; Nielsen *et al.*, 2004), which is expected to be even larger in the t-tubules. Na^+i will increases slightly from ~ 6mM to 10 – 25 mM, depending on fibre type (Street *et al.*, 2005). Plasma $[Na^+]$ changes very little due to the shift in plasma volume; i.e. the movement of fluid from the blood to the interstitial space balances the movement of sodium into the intracellular space (McKenna, 1992). This shift results in a rundown of sarcolemmal Na^+ and K^+ concentration gradients, with a concurrent loss of membrane excitability (Sejersted and Sjogaard 2000; Clausen 2003) as the large change in $[K^+]e/[K^+]i$ results in a membrane depolarization of ~10 – 15 mV at 37°C, which is sufficient to cause $Na_v1.4$ channel inactivation and reduced action potential amplitude (Adrian 1956; Hodgkin and

Horowicz 1959; Dulhunty 1978; Renaud and Light 1992; Cairns, Flatman et al. 1995; Cairns, Hing et al. 1997; Yensen, Matar et al. 2002).

There are numerous studies examining the reduction of force that occurs with elevated $[K^+]e$. As shown in Fig 1.2, when $[K^+]e$ reaches a critical level in unfatigued muscle, force will decline due to the altered effects of membrane excitability (i.e. level of K^+ sensitivity). In skeletal muscle, this level of K^+ sensitivity can be modulated. In resting muscle, there is evidence for numerous mechanisms to protect skeletal muscle from K^+-induced membrane inexcitability. Given that Na^+K^+ pump activity is highly driven by $[Na^+]i$, a rise in $[Na^+]i$ will increase pump activity (Bouclin *et al.*, 1995; Nielsen *et al.*, 2004). In addition, the presence of circulating catecholamines will stimulate greater Na^+K^+ pump activity (Clausen *et al.*, 1993; Clausen, 2003; Mikkelsen *et al.*, 2005). Furthermore, an increase in pump content, a well-known adaptation to chronic exercise training, also occurs. The net result of elevated content and activity is membrane hyperpolarization to counteract the K^+-induced depolarization and force depression. Recently, Pedersen *et al* demonstrated that in resting muscle, an increased [lactate]i and decreased pHi were shown to independently decrease G_{Cl} (Pedersen *et al.*, 2004; Pedersen *et al.*, 2005). They also showed that at the onset of repetitive stimulation, G_{Cl} also decreases by ~70% (Pedersen *et al.*, 2009). At high $[K^+]e$, this improves force generation by reducing the amount of inward current required for membrane depolarization (Pedersen *et al.*, 2004; Pedersen *et al.*, 2005; de Paoli *et al.*, 2007).

FIGURE 1.2

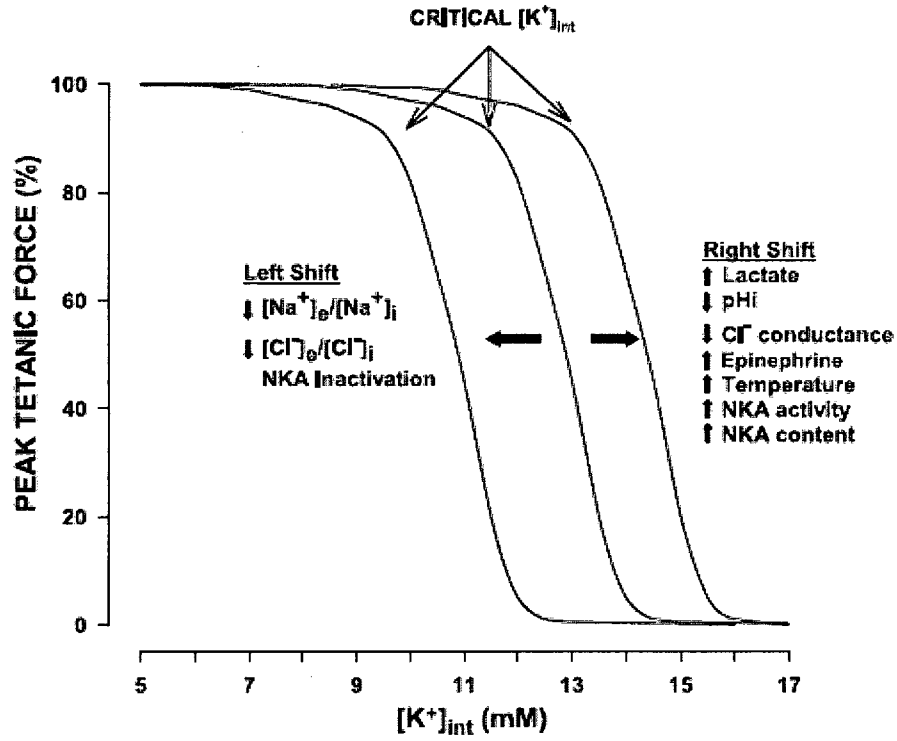

Fig. 1.2. Peak tetanic force-[K^+]int relationship in skeletal muscle. Figure indicates the critical [K^+]int, the precipitous decline in force, and the modulation of the relationship by other ions and by Na^+K^+ pump. Critical [K^+]int is defined at the interstitial [K^+] at which peak tetanic force starts to decline abruptly. Taken from (McKenna *et al.*, 2008).

These mechanisms to decrease K^+ sensitivity are critical at the initial onset of exercise, when elevated K^+ is necessary for vasodilation and improved cardiovascular output, both of which will improve blood flow to the working muscles. The reduced sensitivity also allows for greater force maintenance, an important outcome to achieve a rapid "fight-or-flight" response.

However, the protective measures against K^+-induced force depression do not persist during fatigue, and as such, there is a leftward shift in the K^+-force generation relationship. Firstly, as the ratio of $[Na^+]e/[Na^+]i$ decreases, there is a reduced driving force of Na^+ influx during an action potential. In fact, a decrease in $[Na^+]e$ with a concurrent rise in $[K^+]e$ will have a synergistic effect to suppress force (i.e. force depression is greater than the sum of individual effects) (Bouclin *et al.*, 1995). Secondly, decreasing the ratio of $[Cl^-]e/[Cl^-]i$ will also reduce the driving force of Cl^- as E_{Cl} will be reduced, and thus cause membrane depolarization. Thirdly, a decrease in Na^+K^+ pump activity occurs with prolonged fatigue (Fowles *et al.*, 2002; Fraser *et al.*, 2002; Leppik *et al.*, 2004; Petersen *et al.*, 2005; Sandiford *et al.*, 2005; McKenna *et al.*, 2006), which will cause further membrane depolarization as its electrogenic effect on E_m is reduced (Fowles *et al.*, 2002; Leppik *et al.*, 2004; Murphy *et al.*, 2004; Sandiford *et al.*, 2005; Aughey *et al.*, 2007).

Lastly, Pedersen *et al.* demonstrated that following the rapid decrease of G_{Cl} at the early onset of repetitive stimulation is followed by a 3-fold rise in resting G_{Cl} as stimulation continues (Pedersen *et al.*, 2009), which they proposed is a possible means of myoprotection. That is, given that G_{Cl} can affect membrane excitability, and is partially regulated by [ATP]i, G_{Cl} may increase during fatigue to prevent deleterious [ATP]i

depletion (Bennetts *et al.*, 2007). This leads to the question of whether other ion channels, along with CLC-1, may also alter membrane excitability to protect against contractile dysfunctions.

Since K^+ is able to alter E_m, it is very likely that K^+ channels can play a role. In fact, along with an increased G_{Cl} with repetitive stimulation, Pederson *et al* (Pedersen *et al.*, 2009) measured a synchronous 14-fold increase in G_K, such that G_m increased by ~400% over rest. This increase in G_K could be significantly blocked by the presence of glibenclamide, providing evidence for the opening of sarcolemmal ATP-sensitive K^+ (sK_{ATP}) channels. Similar to CLC-1 channels, sK_{ATP} channels are sensitive to the metabolic state of the cell, and can alter membrane excitability by increasing K^+ efflux. Furthermore, other K^+ channels, such at BKCa and Kir2.1, have also been shown to affect the fatigue process. Evidence for an increased $BKCa^{2+}$ (KCa1.1) channel conductance was suggested by Tricarico *et al* in 2005 (Tricarico *et al.*, 2005) due to its activation factors; i.e. E_m depolarization and increased $[Ca^{2+}]i$ (Jacquemond & Allard, 1998; Mallouk & Allard, 2000). Its close proximity to the DHP receptors (Nielsen *et al.*, 2003), coupled with its activation characteristics suggests that this channel is important in controlling membrane excitability. When muscle was incubated with a $BKCa^{2+}$ channel opener, there was a faster reduction in peak tetanic force during *in vitro* stimulation (Kristensen *et al.*, 2006). Inhibiting Kir2.1 and the Na^+-K^+-$2Cl^-$ cotransporter (NKCC1), which assists the Na^+K^+ pump in K^+ reuptake during contractions, further increasing the rate of fatigue by increasing t-tubular K^+ accumulation (Kristensen *et al.*, 2006). However, given the large contribution of the sK_{ATP} channel to increasing G_K during

fatigue, and their ability to link the energy status of a fibre to its electrical activity, it appears that this channel is of primary importance in myoprotection.

sKATP channels

The sKATP channel was first discovered by Noma in 1983 (Noma, 1983). It derives its name from the fact that the binding of ATP on the cytosolic side results in the closure of the channel. sKATP channels are expressed ubiquitously throughout the body, including cardiac, skeletal and smooth muscle cells (Noma, 1983; Spruce *et al.*, 1987; Standen *et al.*, 1989), as well as pancreatic β-cells and glucose sensing neurons (Cook & Hales, 1984; Ashford *et al.*, 1988).

Molecular structure

In skeletal muscle, the sKATP channel is comprised of two primary protein subunits: a Kir6.2 and a SUR2A sulfonylurea receptor (SUR) subunit (Ashcroft & Gribble, 1998; Seino, 1999). The Kir6.2 subunit belongs to the Kir6.x inwardly-rectifying potassium channel superfamily, and forms the pore of the channel (Seino, 1999). The SUR2A subunit belongs to the ATP-binding cassette (ABC) transporter superfamily, which modulates channel function and can be controlled by pharmaceutical applications (Aguilar-Bryan *et al.*, 1995; Chutkow *et al.*, 1996; Ashcroft & Gribble, 1998; Seino, 1999). Each SUR subunit contains two nucleotide binding folds (NBF) on the intracellular side, which are thought to play a role in nucleotide regulation of subunit activity (Tusnady *et al.*, 1997). The two Kir and SUR subunits are combined in a 4:4 stoichiometry to form an octameric channel through which the K^+ can move through the

cell membrane (Clement *et al.*, 1997; Inagaki *et al.*, 1997; Seino & Miki, 2003). There is a small amount of expression of both Kir6.1 and SUR2B subunits in hindlimb rat muscle, and the SUR1 subunit expression was found in FDB (Tricarico *et al.*, 2006). Since sKATP channels are inward rectifiers, their outward currents are significantly smaller than their inward currents (Ashcroft, 2000). It is primarily the presence of intracellular Mg^{2+} that causes the inward rectification.

sKATP channel regulation

In the resting state, sKATP channels exist in the closed position due to a conformational change from the binding of ATP on the intracellular face of the Kir subunit (Tucker *et al.*, 1997; Antcliff *et al.*, 2005). ADP can also bind to the Kir subunit to close the channel, but with a much lower affinity than ATP (Ki for ADP is 500 μM vs. 172 μM for ATP). In combination with the SUR subunit, the Ki for ATP is reduced to ~10 μM (Tucker *et al.*, 1997). However, it is known that during situations of fatigue, metabolic inhibition, hypoxia and ischemia, these channels are open, even though the [ATP]i decreases only slightly to ~3 – 5 mM (McPherson *et al.*, 1993; Gramolini & Renaud, 1997).

However, [ATP]i is not the only regulator of sKATP channels, as in all these cases [ATP]i far exceeds the Ki value (Fitts, 1994; Fitts & Balog, 1996). A decrease in intracellular pH to 6.2 – 6.4 (Davies *et al.*, 1992) along with corresponding increases in extracellular adenosine (Barrett-Jolley *et al.*, 1996) and intracellular lactate of 20 – 40 mM (in cardiac cells only) (Keung & Li, 1991), will also lead to channel opening. More importantly, these changes occur under physiological conditions, such as during fatigue, suggesting their importance in metabolic regulation. Furthermore, Mg·ADP activates

channels (as opposed to free ADP causing closure), even those inhibited by ATP (Vivaudou *et al.*, 1991). This is thought to occur since ATP binds to SUR NBF1 and Mg·ADP binds to NBF2, and the balance of the two regulates sKATP channel activity (Walker *et al.*, 1982; Miki *et al.*, 1999; Ueda *et al.*, 1999). Indeed, the ratio of ATP to ADP is accepted to regulate the channel by regulating SUR activity, altering its interaction with Kir6.2 by reducing the binding affinity of Kir6.2 for ATP, thus determining the opening probability of Kir6.2 (Ueda *et al.*, 1999).

Thus, given the strong evidence of metabolites and metabolic by-products to regulate sKATP channel activity, it has been proposed that sKATP channels link the metabolic status of the muscle fibres to the electrical activity of the cell membrane (Renaud, 2002; Thabet *et al.*, 2005).

General physiological function of the sKATP channels

The sKATP channels play three distinct functions depending on the tissue they are expressed in. Firstly, they are involved in glucose homeostasis by being one mechanism for regulation of insulin and glucagon secretion by pancreatic β-cells and α-cells (Miki *et al.*, 1999; Ashcroft, 2006), modulating activity of glucose sensory neurons in the hypothalamus (Taborsky *et al.*, 1998; Miki *et al.*, 2001), and modulating glucose uptake in adipose tissue and skeletal muscle (Chutkow *et al.*, 2001; Miki *et al.*, 2002). Secondly, sKATP channels regulate systemic blood pressure by their effects on vascular smooth muscle cells. Lastly, in cardiac and skeletal muscle, they respond to catecholamines during stress (cardiac) to alter cardiac function and aid in myoprotection against fibre damage during metabolic stressors such as hypoxia, ischemia, exercise and fatigue (cardiac and skeletal). It is this latter role in skeletal muscle that is the focus of this thesis.

Function of sKATP channels in cardiomyocyte protection

In cardiac ventricular myocytes, the AP duration under normal physiological conditions is approximately 400 ms due to the delay in K_V channel activation. Activation of sKATP channels during hypoxia or ischemia by adenosine receptor stimulation (Light *et al.*, 2000; Light *et al.*, 2001) results in shortening of AP duration, preventing Ca^{2+} overload and preserving energy (Nichols & Lederer, 1991; Nichols *et al.*, 1991; Findlay, 1994). Zingman et al (Zingman *et al.*, 2002) demonstrated that Kir6.2$^{-/-}$ mice (null mice for the pore of the sKATP channel) undergoing treadmill running failed to sustain performance due to non-shortening of the action potential duration, opposite to what they observed with wild type mice. In fact, their exercise capacity was ~3-fold lower than that of wild type. Furthermore, Zane *et al* (2006) noted impaired contractility, left ventricular necrosis and hypertrophy related to the Ca^{2+}i overload under similar exercise conditions in Kir6.2$^{-/-}$ mice (Kane *et al.*, 2004). They further observed that the application of verapamil, an L-type Ca^{2+} channel blocker, reduced mortality by ~65% in these stressed Kir6.2$^{-/-}$ mice (Kane *et al.*, 2006) by preventing the large influx of Ca^{2+}.

Therefore, the mechanism of sKATP channel action in cardiac myocytes is prevention of excessive membrane depolarization, which will have two effects (Zingman *et al.*, 2002; Baczko *et al.*, 2004; Baczko *et al.*, 2005): 1. prevention of L-type Ca^{2+} activation and consequent Ca^{2+} influx; and 2. prevention of $Na_V1.5$ channel inactivation and membrane inexcitability. The net result is prevention of impaired contractility and cell death (Bolli & Marban, 1999; Piper & Garcia-Dorado, 1999; Light *et al.*, 2001). In addition, the repolarizing effects of sKATP channel activation reduced the activity of the

reverse-mode Na^+/Ca^{2+} exchanger, which is highly active during ischemia-reperfusion due to impaired Na^+ handling (Baczko *et al.*, 2003).

Function of sKATP channels in skeletal myocyte protection

In resting skeletal muscle *in vitro*, sKATP channels are in a closed state (Light *et al.*, 1994). When these channels are activated, such as during fatigue or metabolic inhibition, there is a greater K^+ efflux into the t-tubular and interstitial space (Pedersen *et al.*, 2009). In cardiac muscle, opening of sKATP channels reduces AP duration, whereas in skeletal muscle, the use of channel openers have shown that the main effect of sKATP channels is to reduce AP amplitude (Gong *et al.*, 2003); albeit, in frog sartorius muscle the application of glibenclamide (a sKATP channel blocker) results in a longer AP duration both at rest and following fatigue.

The reduced AP amplitude is accomplished through two mechanisms. Firstly, opening sKATP channels directly increase K^+ conductance, allowing for a greater efflux of K^+ out of the cell to counteract the Na^+ influx and reducing the extent of membrane depolarization (Gramolini & Renaud, 1997). Secondly, opening sKATP channels allows for greater increases in $[K^+]e$, resulting in membrane depolarization (Gramolini & Renaud, 1997; Matar *et al.*, 2001) and resulting in Na^+ channel inactivation (Lannergren & Westerblad, 1986, 1987). Reducing AP amplitude was shown to be directly related to a reduced Ca^{2+} release by the SR (Duty & Allen, 1995), which provides two main benefits (Burton & Smith, 1997b). First, there is preservation of ATP by reduction of Ca^{2+}-ATPase pump activity. The second is the reduction in the number of cross-bridges formed, and therefore a reduction in myosin ATPase activity. So, the final result of sKATP

channel activation is thus a faster decrease in force production during fatigue (Matar *et al.*, 2000) and a preservation of ATP.

So, if activating sKATP channels results in a faster rate of fatigue due to the increased K^+ conductance causing reduced AP amplitude, and therefore faster rates of fatigue, one would therefore expect that abolishing sKATP channel activity would result in a slower rate of fatigue. However, the opposite of this was observed *in vivo,* and furthermore, *in vitro*, Gong *et* al (2003) observed no effect of abolishing sKATP channel activity on rate of fatigue in mouse EDL or soleus muscle

When Kir6.2$^{-/-}$ mice were elicited to run on treadmills, they demonstrated a faster rate of fatigue during a single bout of running, tolerating only an average of 0.9 km of running at 20 m/min at 0° incline, versus 2.2 km of their wild type counterparts. Following a four-week training span of daily running at 24 m/min and 20° incline, compared to their wild type counterparts (Thabet *et al.*, 2005), ~25% of EDL and ~12% of plantaris and tibialis Kir6.2$^{-/-}$ fibres showed signs of regeneration (as evident from the presence of nuclei). Of those damaged fibres, 99% were Type IIB. It is very likely that this fibre damage was one cause of the apparent faster rate of fatigue. In SUR2 mutant mice (which also have nonfunctional sKATP channels), a similar response to a single bout of training was observed, along with a failure to increase their exercise capacity above baseline (Stoller *et al.*, 2009). In addition, hindlimb muscle damage was observed after the four-week running, although the severity of the damage was reduced (< 5% vs. 25% of EDL fibres being damaged). However, these mice started with a baseline skeletal myopathy, which was not observed in Kir6.2$^{-/-}$ mice.

It cannot be denied that Kir6.2$^{-/-}$ have a reduced cardiovascular and respiratory capacity with chronic exercise, which could also have led to the reduced exercise output (Zingman *et al.*, 2002; Thabet *et al.*, 2005). In fact, following the four weeks of running, there was significant damage to the Kir6.2$^{-/-}$ diaphragm as shown by mononucleated fibres, severe loss of fibres and collagen infiltration (Thabet *et al.*, 2005). Interestingly, the damage was not particular to a fibre type as observed in hindlimb muscle. Nevertheless, it still supports the importance of sKATP channels in skeletal muscle protection *in vivo*.

In vitro, evidence for sKATP channel myoprotection was demonstrated using both pharmacological and genetic approaches. During fatigue and metabolic inhibition, sKATP channel deficient fibres developed significant unstimulated force (Gramolini & Renaud, 1997; Gong *et al.*, 2000; Matar *et al.*, 2000; Gong *et al.*, 2003) and lowered force recovery following fatigue (Light *et al.*, 1994; Comtois *et al.*, 1995; Gong *et al.*, 2000; Matar *et al.*, 2000; Gong *et al.*, 2003). During metabolic inhibition, excessive membrane depolarization of 30 – 50 mV also occurred (Light *et al.*, 1994), which is sufficient to cause Na^+ channel inactivation (Ruff, 1999) and subsequent membrane inexcitability.

Therefore, it appears that the effect of sKATP channel activity on the rate of fatigue is a function of the balance between the slower decreases in action potential amplitude and the development of contractile dysfunctions. These contractile dysfunctions (defined as any event from the generation of action potentials to the actin–myosin interaction that is depressed in a manner not associated with the normal process of fatigue (or any metabolic stress), and that eventually incapacitate muscle from generating force) can include both the reduced AP amplitude during a contraction due to

excessive membrane depolarization causing Na^+ channel inactivation, as suggested by Gong *et al* (Gong *et al.*, 2003), and possible L-type Ca^{2+} channel activation between contractions, causing deleterious Ca^{2+} influx leading to fibre damage and subsequently reduced force generation, as demonstrated in cardiac muscle when sKATP channel activity is abolished (Zingman *et al.*, 2002; Kane *et al.*, 2004; Kane *et al.*, 2006).

Possible role of calcium in functional impairment

It is well known that an excessive rise in Ca^{2+}i can lead to fibre damage by (Jackson *et al.*, 1984; Jackson, 2009): 1. activation of proteases (or calpains) (Belcastro *et al.*, 1998; Allen *et al.*, 2005) which damages the contractile proteins; and 2. increasing reactive oxygen species (ROS) production by the mitochondria (Vercesi *et al.*, 1997; Inoue *et al.*, 2003; Brookes *et al.*, 2004).

Eccentric damage, which causes a prolonged rise in $[Ca^{2+}]$i for 60+ minutes (Balnave & Allen, 1995; Lynch *et al.*, 1997; Warren *et al.*, 2002), led to calpain activation in both skinned EDL and soleus muscle fibres (Murphy & Lamb, 2009) and human vastus lateralis muscle (Murphy *et al.*, 2007). This would explain the disrupted Z-lines and breakdown of sarcomeric proteins (titin, desmin) (Goll *et al.*, 2003; Murphy *et al.*, 2006) and membrane integrity (by infiltration of fibronectin), and the resulting muscle weakness (Ingalls *et al.*, 1998; Murphy *et al.*, 2007).

ROS can affect muscle activity by numerous mechanisms. ROS can cause an increased open probability of the RYR1 (Anzai *et al.*, 2000; Hamilton & Reid, 2000) and a decreased rate of reuptake by the SR Ca^{2+}-ATPase pump (Lee & Okabe, 1995; Davidson & Berman, 1996; Senisterra *et al.*, 1997), along with an increased leak of Ca^{2+} through the SR Ca^{2+} pump. The net effect of all this is a greater rise in $[Ca^{2+}]$i. In

addition, Ca^{2+} sensitivity of the contractile proteins is reduced, as shown using single FDB and EDL muscle fibres (Moopanar & Allen, 2005, 2006; Bruton *et al.*, 2008; Murphy *et al.*, 2008), and therefore force production is reduced.

OBJECTIVE AND HYPOTHESES – STUDIES ONE TO THREE

The function of sKATP channels during a contraction is now established whereby it reduces AP amplitude and decreases force production during fatigue *in vitro*, and prevents fibre damage *in vivo* during treadmill running. The questions are: 1. how does abolishing sKATP channel activity lead to the development of the contractile dysfunctions during fatigue; and 2. if the contractile dysfunctions are prevented, what effect will it have on the rate of fatigue. Thus, the **overall objective** of this study was to examine how sKATP channel activity protects skeletal muscle during fatigue. **Aim #1** will demonstrate that abolishing sKATP channel activity led to the development of several contractile dysfunctions including faster decreases in peak Ca^{2+} and tetanic force, greater increases in unstimulated Ca^{2+} and force, reduced force recovery and development of partially- or fully- supracontracted single fibres. **Aim #2** will demonstrate that the development of contractile dysfunctions in sKATP channel muscle was due to large membrane depolarization and excessive Ca^{2+} influx into the fibres through the L-type Ca^{2+}-channels, and preventing the large Ca^{2+} influx in sKATP channel deficient muscle prevented the development of some of the contractile dysfunctions. **Aim #3** will demonstrate that the development of some contractile dysfunctions is due to greater ROS formation, which can be improved by the application of a ROS scavenger.

OBJECTIVE AND HYPOTHESIS – STUDY FOUR

Fatigue preconditioning (FPC) was defined by Bourassa (Bourassa, 2006) as a new phenomenon in which "one fatigue bout at 37°C improves, within 30 minutes, fatigue resistance while reducing the dependency of muscle on sKATP channels to protect them against functional impairment and fibre damage in subsequent fatigue bouts". Preliminary work performed by Bourassa (Bourassa, 2006) and Cifelli (Cifelli, 2006) on FPC showed that: 1. the decreases in peak tetanic $Ca^{2+}{}_i$ and force were significantly slower while the increases in unstimulated $Ca^{2+}{}_i$ and force were significantly less during a second fatigue bout (FAT2) than during a first fatigue bout (FAT1) elicited 60 min earlier; 2. The differences between FAT1 and FAT2 were especially marked when wild type FDB were exposed to glibenclamide to block KATP channels during FAT2; 3. The contractile dysfunctions observed in sKATP channel deficient muscles during FAT1 were completely abolished during FAT2. They did not attempt to determine the mechanistic pathway of FPC, but proposed a possible parallel to ischemic preconditioning (IPC) due to the similarity in metabolic demands; i.e. both occur in a situation where ATP demand exceeds ATP production. IPC, originally described by Murry in 1986, involves exposure of a tissue to several brief cycles of non-damaging ischemia which markedly reduces the extent of necrosis and functional impairment following a subsequent long and damaging ischemic period. This phenomenon was first demonstrated in cardiac muscle (Murry *et al.*, 1986), and later in many other tissues, including liver, brain and skeletal muscle.

The **overall objective and aim** of study four is to determine if the mechanism of FPC is similar to IPC.

CHAPTER 2

K_{ATP} CHANNEL DEFICIENCY IN MOUSE FLEXOR DIGITORUM BREVIS CAUSES FIBRE DAMAGE AND IMPAIRS Ca^{2+} RELEASE AND FORCE DEVELOPMENT DURING FATIGUE *IN VITRO*

By

Carlo Cifelli, François Bourassa, **Louise Gariépy**, Krystyna Banas, Maria Benkhalti and Jean-Marc Renaud

University of Ottawa, Department of Cellular and Molecular Medicine, 451 Smyth Rd., Ottawa, Ontario, Canada, K1H 8M5

The Journal of Physiology 582(2): 843-857, 2007

AUTHORS' CONTRIBUTIONS

- Gariépy: Insets of Fig. 2.2-6, Table 2.1, contributed to the writing of the revised manuscript
- Bourassa: Fig. 2.8-2.13
- Cifelli: Fig. 2.2-2.6
- Banas, Benkhalti: Fig. 2.7

ABSTRACT

Activation of the KATP channels results in faster fatigue rates as the channels depress action potential amplitude, whereas abolishing the channel activity has no effect in whole extensor digitorum longus (EDL) and soleus muscles. In this study, we examined the effects of abolished KATP channel activity during fatigue at 37°C on free intracellular Ca^{2+} (Ca^{2+}_i) and tetanic force using single muscle fibres and small muscle bundles from the flexor digitorum brevis (FDB). KATP channel deficient muscle fibres were obtained (i) pharmacologically by exposing wild type fibres to glibenclamide, and (ii) genetically using null mice for the Kir6.2 gene ($Kir6.2^{-/-}$ mice). Fatigue was elicited using 200 ms tetanic contractions every second for 3 min. This study demonstrated for the first time that abolishing KATP channel activity at 37°C resulted in faster fatigue rates, where decreases in peak Ca^{2+}_i and tetanic force were faster in KATP channel deficient fibres than in control wild type fibres. Furthermore, several contractile dysfunctions were also observed in KATP channel deficient muscle fibres. They included partially or completely supercontracted single muscle fibres, greater increases in unstimulated Ca^{2+}_i and unstimulated force, and lower force recovery. We propose that the observed faster rate of fatigue in KATP channel deficient fibres is because the decreases in peak Ca^{2+}_i and force caused by contractile dysfunctions prevail over the expected slower decreases when the channels do not depress action potential amplitude.

INTRODUCTION

Muscle activity increases metabolic rate between 20- and 100-fold depending on fibre type and activity intensity (Gibbs, 1987). Skeletal muscles have mechanisms to increase ATP production necessary to meet the increased metabolic rate. However, many muscular activities eventually lead to an ATP demand that exceeds ATP production (Fitts, 1994). The resulting energy deficit then affects the work capacity of the Na^+K^+-ATPase, Ca^{2+}-ATPase, and myosin-ATPase. Ultimately, these effects reduce the capacity of muscle to generate force or do work. If the energy deficit is excessive it can then result in fibre damage and cell death. Consequently, muscles require mechanisms that prevent damaging ATP depletion. The ATP-sensitive K^+ channel (K_{ATP} channel) may be involved in such mechanisms. The channel activity is regulated by the energy state of the cell. It is activated during an energy deficit, i.e. when intracellular ATP decreases while intracellular ADP and H^+ and extracellular adenosine increase (Noma, 1983; Davies, 1990; Vivaudou *et al.*, 1991; Barrett-Jolley *et al.*, 1996).

In unfatigued muscle fibres, K_{ATP} channel openers reduce action potential amplitude (Gong *et al.*, 2003) because the increased outward K^+ current opposes the inward Na^+ depolarization current. During fatigue, K_{ATP} channel activation leads to further reductions in action potential amplitude, as well as faster decreases in Ca^{2+} release and force (Duty & Allen, 1995; Burton & Smith, 1997a; Matar *et al.*, 2000; Gong *et al.*, 2003). Thus, activation of K_{ATP} channels increases the rate of fatigue. On this basis, it was expected that blocking K_{ATP} channels would result in a slower fatigue rate.

However, abolishing K_{ATP} channel activity leads to the possible development of one or more contractile dysfunctions. In this study, we define the term 'contractile

dysfunction' as any event from the generation of action potentials to the actin–myosin interaction that is depressed in a manner not associated with the normal process of fatigue (or any metabolic stress), and that eventually incapacitate muscle from generating force. For example, during fatigue or metabolic inhibition, it is normal to observe a depolarization of the cell membrane and small increases in unstimulated force (when muscles fail to fully relax between contractions). However, in the absence of K_{ATP} channel activity the membrane depolarization (Gramolini & Renaud, 1997) and the increases in unstimulated force are much greater (Gramolini & Renaud, 1997; Gong *et al.*, 2000; Matar *et al.*, 2000). The membrane depolarization incapacitates muscle by increasing the degree of Na^+ channel inactivation; i.e. it decreases membrane excitability and eventually force development. Furthermore, compared to control conditions, K_{ATP} channel deficient muscles have lower capacity to recover force following fatigue (Light *et al.*, 1994; Gong *et al.*, 2000; Matar *et al.*, 2000; Gong *et al.*, 2003). Finally, the absence of K_{ATP} channel activity results in fibre damage in skeletal muscle during swimming and treadmill running (Kane *et al.*, 2004; Thabet *et al.*, 2005). Taken together, the final effects of no K_{ATP} channel activity on fatigue then depend on the balance between slower rates associated with slower decreases in action potential amplitude and faster rates associated with contractile dysfunctions.

It is therefore interesting that most *in vitro* studies have reported no effect on the rate of fatigue when K_{ATP} channel activity is abolished. This was observed with a pharmacological approach using the channel blocker glibenclamide (Light *et al.*, 1994; Westerblad & Allen, 1994; Duty & Allen, 1995; Van Lunteren *et al.*, 1998; Matar *et al.*, 2000), and with a genetic approach using muscles from null mice for the Kir6.2 gene

(Kir6.2$^{-/-}$ mice) (Gong *et al.*, 2000; Gong *et al.*, 2003), the gene that encodes for the subunit making the channel pore (Inagaki *et al.*, 1997). These studies bring into question whether the KATP channel affects force during fatigue.

Many of the *in vitro* studies of KATP channel function have used whole soleus and extensor digitorum longus (EDL) muscles at 37°C. At that temperature, these muscles have a significant anoxic core that cannot be ignored (Barclay, 2005). For example, blocking mitochondrial respiration with cyanide largely increases the rate of fatigue in single soleus muscle fibres, but has very little effect in whole muscle (Zhang *et al.*, 2006b). It is therefore possible that the anoxic core masks the effect of no KATP channel activity. Many investigators have attempted to resolve the problem of the large anoxic core by studying muscle fatigue at 22–25°C. However, such experimental temperatures are not physiological.

In resting mouse, the subcutaneous temperature near the flexor digitorum brevis (FDB) is 30°C (Bruton *et al.*, 1998). During exercise, core body temperature in rat increases 3–4°C. The skin temperature, which is heated by conduction from warmed blood from active muscles, increases from 30°C to 36°C (Fuller *et al.*, 1998; Gonzalez-Alonso *et al.*, 1999). It is therefore highly likely that during exercise, the temperature of active skeletal muscles, which generate a large amount of heat, reaches or exceeds 37°C. Furthermore, the effects of ions and metabolites on contractility, and their role in the aetiology of muscle fatigue, are temperature dependent (Westerblad *et al.*, 1997; Pedersen *et al.*, 2003; Debold *et al.*, 2006).

To fully understand the effects of no KATP channel activity during fatigue at 37°C, it is necessary to use smaller muscle preparations than whole EDL and soleus

muscles. The objective of this study was to determine, at 37°C, the effects of no KATP channel activity during fatigue using single fibres and small bundles from the mouse FDB muscle. We hypothesized that abolishing KATP channel activity at 37°C results in an apparent faster rate of fatigue because the contractile dysfunctions prevail over the expected slower decreases associated with smaller depression of action potential amplitude. Testing this hypothesis is important for understanding the role of KATP channels during fatigue in skeletal muscle. Most types of fatigue involve a decrease in intracellular Ca^{2+} (Ca^{2+}_i) as a major contributing factor for the decrease in force (Allen *et al.*, 1995). So, in this study, we measured the effects of no KATP channel activity on peak Ca^{2+}_i and force.

METHODS AND MATERIALS

ANIMALS, MUSCLE BUNDLE AND SINGLE FIBRE PREPARATION

Experimental approaches. Pharmacological and genetic approaches were used to abolish KATP channel activity. For the pharmacological approach, FDBs from wild type mice were exposed to 10 μM glibenclamide. For the genetic approach, FDBs from null mice for the Kir6.2 gene (Kir6.2$^{-/-}$ mice) were used (Miki *et al.*, 1998); muscle fibres from these mice have no KATP channel activity in the sarcolemma (Miki *et al.*, 2002). Two different preparations were used: single fibres and small bundles. Since mechanically dissected single fibres are resilient to the stresses of dissection and heat (Moopanar & Allen, 2006), isolated single fibres were collected by dispersing them following a collagenase treatment, which gave viable single fibres to measure $Ca^{2+}i$. Small muscle bundles were used to measure force as our single fibre preparations do not have tendons after the collagenase treatment.

Animal care. Two- to three-month-old CD1 (wild type, from Charles River, Canada) and Kir6.2$^{-/-}$ mice weighing 20–30 g were fed *ad libitum*, and housed according to the guidelines of the Canadian Council for Animal Care (CCAC). The Animal Care Committee of the University of Ottawa approved all experimental procedures used in this study. Mice were anaesthetized with a single intraperitoneal injection of 2.2 mg ketamine, 0.44 mg xylazine, and 0.22 mg acepromazine per 10 g of body mass. FDBs were excised and then mice were killed with an overdose of anaesthetics.

Isolation of muscle bundles. The FDB is made up of three major bundles that control via individual tendons the 2nd, 3rd and 4th digit of the paw (Greene, 1968). All experiments with bundles were carried out by excising the fibres controlling the 4th digit

by cutting along and very close to the lateral fascia separating the fibres of the 3rd and 4th digit; note that the cut separated fibres controlling the 3rd digit away from the fascia, leaving the fibres controlling the 4th digit intact. On average, the bundles contained 350 ± 40 fibres (mean ± standard error of the mean (S.E.M.), number of samples n = 8), weighed 2.2 ± 0.1 mg and were 8.2 ± 0.1 mm long (n = 42). Assuming a cylindrical shape and a density of 1.06 g cm^{-3}, the average radius was 0.31 ± 0.01 mm and cross-sectional area was 0.30 ± 0.01 mm^2.

Isolation of single fibres. Single fibres were obtained by incubating whole FDBs for 4 h at 37°C in a culture medium containing minimum essential medium with Earle's salts and l-glutamine (MEM, Gibco, Canada), supplemented with 10% fetal bovine serum (FBS, Gibco), 0.2% type I collagenase (Sigma, USA), 100 units ml^{-1} of penicillin and 100 μg ml^{-1} of streptomycin (Gibco). Fibres were separated by trituration with a Pasteur pipette, plated on a coverslip covered with Matrigel (VWR, Canada), and incubated overnight at 37°C in the same culture medium (without collagenase) before being used.

SOLUTIONS

Bundles and single fibres were constantly immersed in physiological saline solution containing (mM): 118.5 NaCl, 4.7 KCl, 2.4 $CaCl_2$, 3.1 $MgCl_2$, 25 $NaHCO_3$, 2 NaH_2PO_4, and 5.5 D-glucose. Solutions were continuously bubbled with 95% O_2–5% CO_2 for a pH of 7.4. Solutions containing 10 μM glibenclamide were prepared by first dissolving glibenclamide in DMSO, which was then added to the saline solution. The final DMSO concentration was 0.1% (v/v) in all solutions (including control). All experiments were conducted at 37°C.

FORCE MEASUREMENT IN FDB BUNDLES

The muscle chambers were made of Plexiglas measuring 10 mm long, 10 mm wide and 5 mm deep. Solution entered the chamber through two Teflon pieces located just behind the bundles. The total flow of solution was 15 ml min^{-1} divided equally over the upper and lower parts of the bundles. Force measurements were carried out using paired bundles, one as control and the other exposed to glibenclamide (all bundles were fatigued only once). There was thus four experimental groups: (i) control wild type, (ii) glibenclamide wild type, (iii) control Kir6.2$^{-/-}$, and (iv) glibenclamide Kir6.2$^{-/-}$. Muscle length was adjusted to give maximum tetanic force. Force was monitored with a Cambridge ergometer (model 300, USA) or a Kulite force transducer (Model BD100, Canada), and digitized at 5 kHz by a Keithley Metrabyte A-D board (model DAS50, USA). Peak tetanic force, unstimulated force and peak total force were analysed using a computer as defined in the Results section.

Ca^{2+}_i MEASUREMENT IN FDB SINGLE

Five to seven single fibres were tested from each mouse; some of the fibres under control conditions and the remaining fibres exposed to 10 μM glibenclamide. Fibres were loaded with Fura-2 by exposing them for 30 min at 37°C to 5 μM Fura-2AM (Molecular Probes, Canada) dissolved in culture medium containing 0.1% (v/v) DMSO. The coverslip containing the fibres was then transferred to a chamber (model RC-25, Warner Instruments, USA). The flow of saline solution was maintained at 2–3 ml min^{-1} while temperature was maintained at 37°C with a dual channel heater (model TC-344B, Warner Instruments, USA), one channel heating the incoming fluid and the other heating the chamber itself.

$Ca^{2+}i$ was monitored by illuminating fibres alternately at 340 and 380 nm and measuring fluorescence at 505 nm using a spectrofluorometer (IonSpec, Canada). The ratio was then calculated by dividing the fluorescence from the 340 nm excitation by the fluorescence from the 380 nm excitation. In this study, the $[Ca^{2+}]i$ was not calculated from the 340/380 fluorescence ratio as many KATP channel deficient fibres supercontracted giving ratios greater than 5, largely exceeding the expected R_{max} reported by Westerblad & Allen (1991).

STIMULATION AND FATIGUE PROTOCOL

The stimulation and fatigue protocols were as described in previous studies using mouse EDL and soleus (Gong *et al.*, 2000; Matar *et al.*, 2000). Briefly, bundles and single fibres were allowed to equilibrate for 30 min in the absence or presence of 10 μM glibenclamide. During that time, tetanic contractions were elicited with 200 ms trains of supramaximal (8 V) square waves of 0.3 ms duration every 100 s; stimulation frequencies for bundles and single fibres were, respectively, 200 and 140 Hz (some single fibres became unstable when stimulation frequencies exceeded 140 Hz). Pulses were generated with a Grass S88 stimulator and a Grass SIU5 isolation unit (Grass Instruments, USA). For bundles, the stimulating platinum wires (4 mm apart) were located on opposite sides of the bundles. For single fibres, the platinum wires (7 mm apart) were positioned on each side of the chamber.

Fatigue was elicited with one tetanic contraction every second for 3 min in the absence or presence of 10 μM glibenclamide. After fatigue, muscles were stimulated at 10, 20 and 100 s, and every 100 s thereafter to measure force or $Ca^{2+}i$ recovery. It is important to note that under control conditions single fibres could not be fatigued with

400 ms tetanic contractions because, at 37°C, it resulted in sudden contractile failure before the end of the fatigue period, as previously reported by Moopanar & Allen (2006).

FIBRE INTEGRITY

Evans blue was used as an indicator of cell membrane damage in skeletal muscle (Anderson *et al.*, 2006). Control and glibenclamide wild type, and control Kir6.2$^{-/-}$ bundles were fatigued as described above, except that 0.01% Evans blue was added to the solution 30 min prior to fatigue and remained present until bundles were frozen. Paired bundles were used with only one bundle exposed to Evans blue in order to determine (i) the autofluorescence from muscle cross-sections, and (ii) whether Evans blue itself affects the fatigue kinetics for each of the three experimental conditions. Immediately after fatigue, bundles were embedded in optimal cutting temperature compound (OCT, Tissue Tek II, USA) and frozen in isopentane precooled in liquid nitrogen. As positive control, one control Kir6.2$^{-/-}$ bundle was stretched during 12 consecutive 1 s long contractions as described by (Decrouy *et al.*, 1997). Cross-sections, 10 μm thick, were cut at −20°C using a cryostat. Cross-sections were viewed immediately using a Sony digital camera (Model DXC-950, Canada) attached to a Zeiss Axiophot fluorescent microscope and connected to a computer. Pictures were taken first with visible light illumination to see the fibres and then with excitation at 545 nm to visualize the red fluorescence from Evans blue using the Zeiss filter set 15. A fibre was identified as Evans blue positive if under visible light it appeared blue and under 545 nm excitation it fluoresced red.

STATISTICAL ANALYSIS

Data are presented as the mean ± standard error of the mean (S.E.M.) with the number of samples, *n*. Student's *t* test was used to compare the means before fatigue. ANOVA was used to determine significant differences during fatigue and recovery. Split plot designs were used since muscles were tested at all time levels. ANOVA calculations were made using the version 9.0 GLM (General Linear Model) procedures of the Statistical Analysis Software (SAS Institute Inc., USA). When a main effect or an interaction was significant, the least square difference (LSD) was used to locate the significant differences (Steel & Torrie, 1980). The word 'significant' refers only to a statistical difference ($P < 0.05$).

RESULTS

FORCE MEASUREMENTS IN FDB BUNDLES

Figure 2.1A shows a representative trace for the change in force during fatigue in a control wild type bundle. In this case, most of the decrease in peak force occurred during the first minute while the baseline increased very little. The situation was very different with K_{ATP} channel deficient bundles. As shown for a representative trace from a glibenclamide wild type bundle (Fig. 2.1B), large increases in the baseline were observed between 20 and 30 s, i.e. K_{ATP} channel deficient bundles failed to fully relax between contractions. So, to fully understand the effects of no K_{ATP} channel activity, we characterized the fatigue kinetics using three parameters. The first was the peak tetanic force defined as the maximum change in force during tetanic stimulation, and calculated as the difference between the maximum force during the contraction and the force just before the contraction was elicited as shown in Fig. 2.1B. The second was the unstimulated force, defined as the force exerted by a bundle between stimulations because it failed to completely relax between contractions. Unstimulated force was calculated by averaging the force values during the 20 ms preceding a contraction. The third parameter was the peak total force calculated as the sum of the peak tetanic force and unstimulated force.

FIGURE 2.1

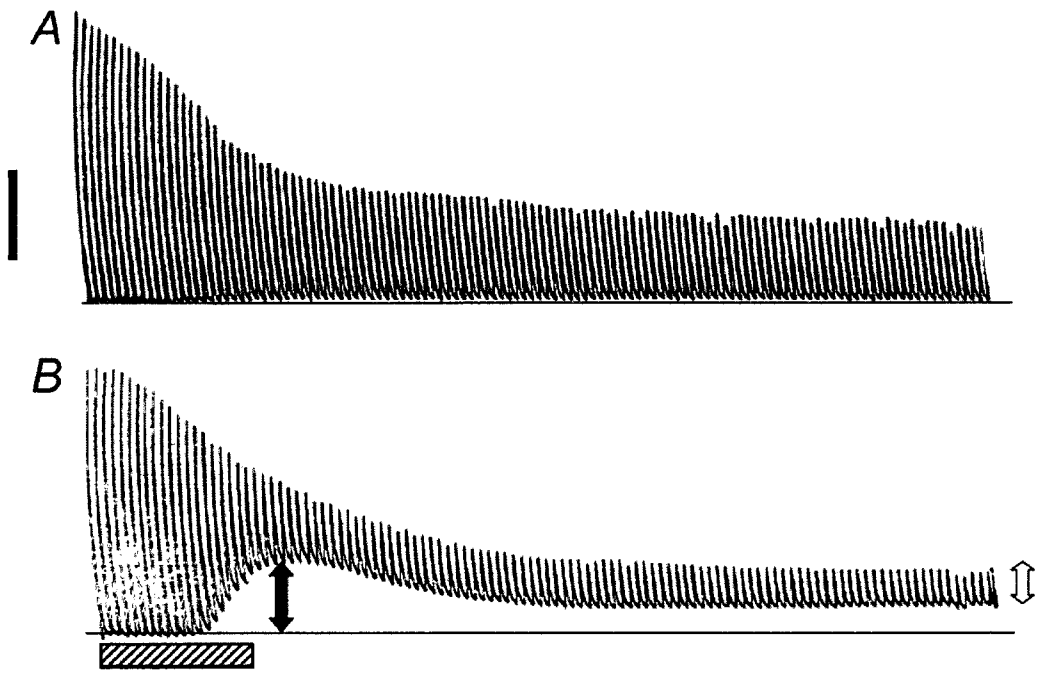

Figure 2.1. Representative traces showing the changes in unstimulated force, peak tetanic force and peak total force during fatigue in (*A*) one control wild type and (*B*) one glibenclamide wild type FDB bundle. Fatigue was elicited at 37°C with one tetanic contraction every second for 3 min. Peak tetanic force (open arrow in *B*) was calculated as the difference between the force just before contraction and the maximum force during contraction. Unstimulated force (filled arrow in *B*) was calculated from the difference in force between the baseline just before fatigue (horizontal line in *A* and *B*) and the force before contraction. Peak total force was calculated as the sum of the unstimulated force and peak tetanic force. Horizontal hatched bar represents 30 s; vertical black bar represent 15 N cm^{-2}.

Pre-fatigue peak tetanic force.

There was no unstimulated force prior to fatigue, so pre-fatigue peak tetanic force and peak total force were the same. Under control conditions, mean peak tetanic force was significantly less in Kir6.2$^{-/-}$ than wild type bundles (Table 2.1). Peak tetanic force was slightly lower in the presence of 10 μM glibenclamide than in control conditions, but the difference was not significant.

Peak tetanic force during fatigue.

On an average basis, most of the decrease in peak tetanic force during fatigue occurred during the first 60 s (Fig. 2.2A). At that time, the mean peak tetanic force of control wild type bundles was 34% of the pre-fatigue peak tetanic force. It then only decreased another 15% during the last 120 s. The decreases in peak tetanic force were significantly faster in the presence of glibenclamide. After 30 s, peak tetanic forces in the absence and presence of glibenclamide were, respectively, 70% and 40%, representing a 30% difference. Peak tetanic force of glibenclamide wild type bundles remained less than that under control conditions, albeit the differences were no longer significant after 105 s of stimulation. At 180 s, peak tetanic forces of control and glibenclamide wild type bundles were, respectively, 20% and 12% of the pre-fatigue values.

The initial decreases in peak tetanic forces were also faster in Kir6.2$^{-/-}$ than in wild type bundles under control conditions (Fig. 2.2B). After 30 s, the difference in peak tetanic force between wild type and Kir6.2$^{-/-}$ bundles was 25%, a difference similar to the one observed between control and glibenclamide wild type bundles. However, the difference between wild type and Kir6.2$^{-/-}$ fibres did not persist throughout the entire fatigue period, as the differences completely disappeared by 90 s. Exposing Kir6.2$^{-/-}$

TABLE 2.1

Experimental conditions	Peak tetanic force (N cm^{-2})	
	Wild-type bundle	Kir6.$2^{-/-}$ bundle
Control	53.8 ± 4.1	37.8 ± 5.5*
Glibenclamide (10 μM)	48.8 ± 6.0	32.0 ± 5.3*

Table 2.1. Kir6.2 $^{-/-}$ FDB bundles developed less peak tetanic force than wild type bundles. Peak tetanic forces were measured just prior to fatigue. Data are given as the mean ± S.E.M. of 5 wild type and 6 Kir6.$2^{-/-}$ bundles.

* Significantly different from wild type bundles, *t* test, $P < 0.05$.

FIGURE 2.2

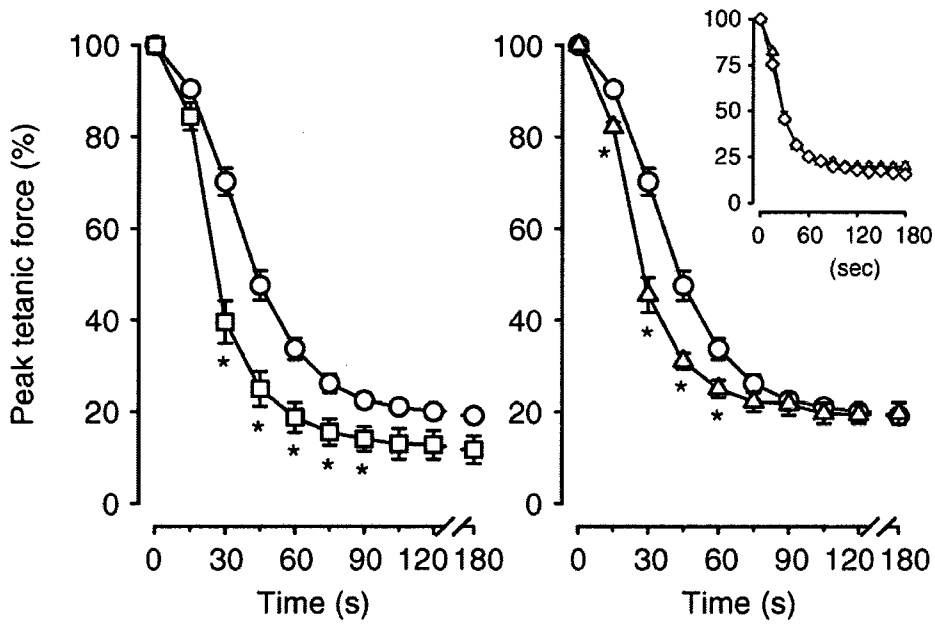

Figure 2.2. KATP channel deficient FDB bundles had faster decreases in peak tetanic force than wild type control FDBs during fatigue at 37°C. Peak tetanic force was expressed as a percentage of the pre-fatigue peak tetanic force. Symbols: O, control wild type; □, glibenclamide (10 μM) wild type; △, control Kir6.2$^{-/-}$; ◇, glibenclamide (10 μM) Kir6.2$^{-/-}$ (inset). Vertical bars represent the S.E.M. of 5 wild type and 6 Kir6.2$^{-/-}$ bundles.

* Significantly different from control wild type, ANOVA and LSD, $P < 0.05$.

bundles to 10 μM glibenclamide had no effect on the decrease in peak tetanic force when compared to control Kir6.2$^{-/-}$ bundles (Fig. 2.2B, inset).

Unstimulated force during fatigue.

Mean unstimulated force increased very little in control wild type bundles, reaching a maximum of 1% of the pre-fatigue peak tetanic force after 45 s (Fig. 2.3A). Unstimulated force of glibenclamide wild type (Fig. 2.3A) and control Kir6.2$^{-/-}$ bundles (Fig. 2.3B) increased sharply to 20% between the 15th and 30th second of stimulation. It decreased slightly thereafter, but remained at 13–15% for the rest of the fatigue period. In the presence of glibenclamide, Kir6.2$^{-/-}$ bundles generated slightly less unstimulated force compared to control conditions, but the differences were not significant (Fig. 2.3B, inset).

Peak total force during fatigue.

For the first 30 s, the decreases in mean peak total force were significantly faster in glibenclamide wild type and control Kir6.2$^{-/-}$ bundles compared to control wild type bundles (Fig. 2.4). The differences, however, were small, being less than 10% in all cases. Thereafter peak total force became significantly greater in both glibenclamide wild type and control Kir6.2$^{-/-}$ bundles compared to control wild type bundles. By the end of the fatigue period, peak total force of control wild type bundles was 19% compared to 28% and 33% for glibenclamide wild type and control Kir6.2$^{-/-}$ bundles, respectively. Glibenclamide had no significant effect on the decrease in peak total force in Kir6.2$^{-/-}$ bundles (Fig. 2.4B, inset).

FIGURE 2.3

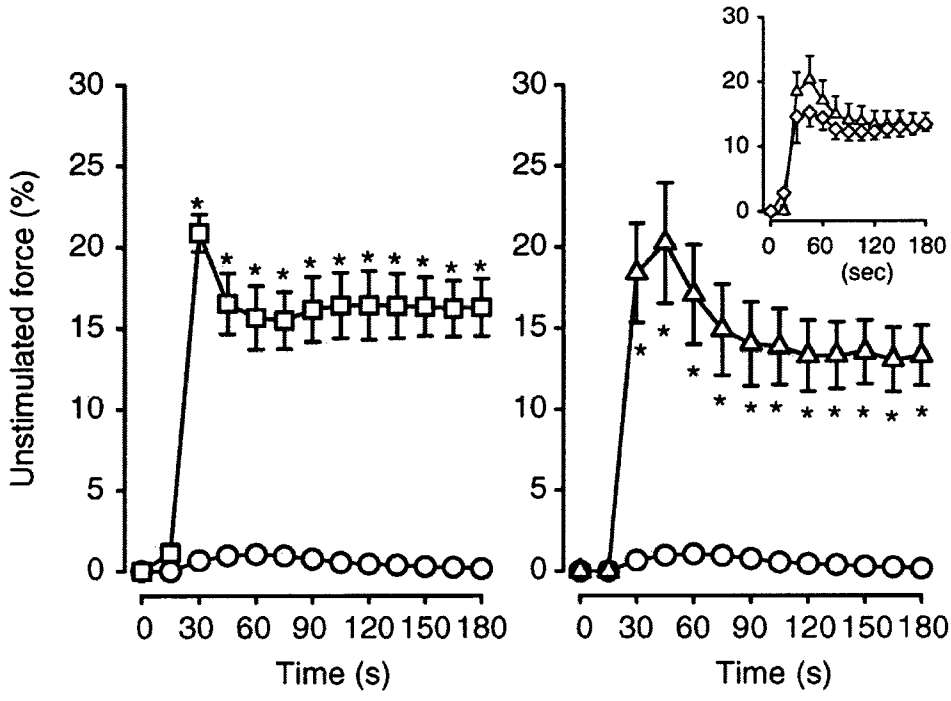

Figure 2.3. KATP channel deficient FDB bundles developed more unstimulated force than wild type control FDBs during fatigue at 37°C. Unstimulated force was expressed as a percentage of the pre-fatigue peak tetanic force. Symbols: O, control wild type; □, glibenclamide (10 μM) wild type; △, control Kir6.2$^{-/-}$; ◇, glibenclamide (10 μM) Kir6.2$^{-/-}$ (inset). Vertical bars represent the S.E.M. of 5 wild type and 6 Kir6.2$^{-/-}$ bundles.

* Significantly different from control wild type, ANOVA and LSD, $P < 0.05$.

FIGURE 2.4

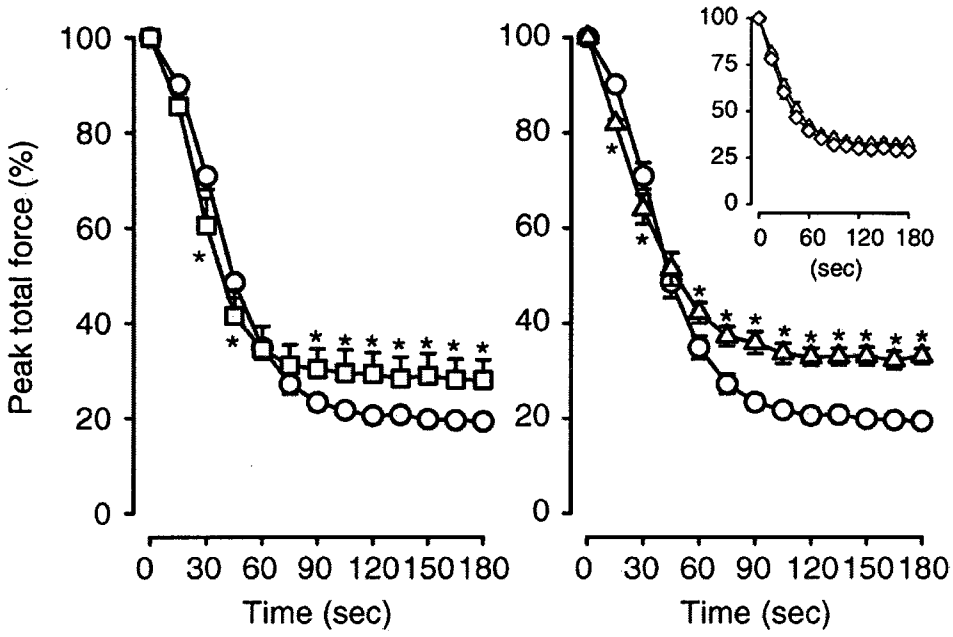

Figure 2.4. KATP channel deficient FDB bundles had smaller decreases in peak total force than wild type control FDBs during fatigue at 37°C. Peak total force was expressed as a percentage of the pre-fatigue peak total force. Symbols: O, control wild type; □, glibenclamide (10 μM) wild type; △, control Kir6.2$^{-/-}$; ◇, glibenclamide (10 μM) Kir6.2$^{-/-}$ (inset). Vertical bars represent the S.E.M. of 5 wild type and 6 Kir6.2$^{-/-}$ bundles.

* Significantly different from control wild type, ANOVA and LSD, $P < 0.05$.

Peak tetanic force during recovery.

Following fatigue, mean peak tetanic force of control wild type bundles recovered to a maximum of 91% of the pre-fatigue value within 15 min (Fig. 2.5A). The extent of peak tetanic force recovery was significantly less for KATP channel deficient bundles. After 30 min, peak tetanic forces of glibenclamide wild type and control Kir6.2$^{-/-}$ bundles were, respectively, 73% and 81% (Fig. 2.5A and B). Contrary to the situation observed during fatigue, 10 μM glibenclamide further reduced the extent of peak tetanic force recovery in Kir6.2$^{-/-}$ bundles to 65%. Of all the parameters measured in bundles, this is the only observation for which glibenclamide had an effect in Kir6.2$^{-/-}$ FDB. To better determine if the time to reach maximum force during recovery was different between the different experimental conditions, we also calculated peak tetanic force as a percentage of the force at 25 min of recovery. As shown in the inset of Fig. 2.5, the time course was the same for all four experimental conditions.

In both glibenclamide wild type and control Kir6.2$^{-/-}$ bundles, unstimulated force continuously decreased during recovery, but was still above zero after 30 min (Fig. 2.6). Glibenclamide had no effect on the recovery of unstimulated force in Kir6.2$^{-/-}$ bundles. So, compared to wild type control bundle, fatigue rates were faster, unstimulated force greater, and force recovery less when the KATP channel activity was abolished pharmacologically using glibenclamide or genetically using Kir6.2$^{-/-}$ muscles.

FIGURE 2.5

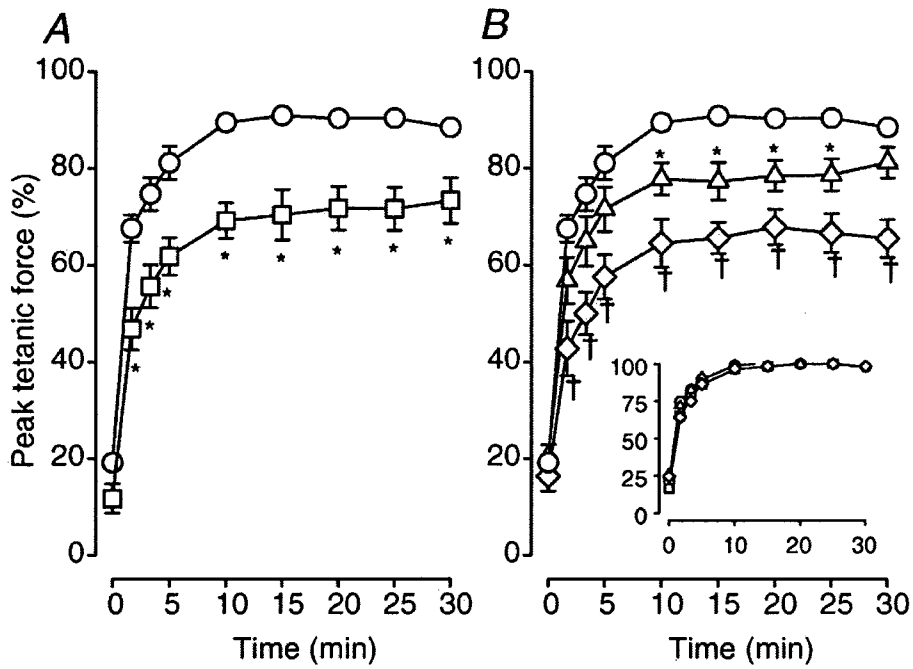

Figure 2.5. KATP channel deficient FDB bundles recovered less force following fatigue at 37°C than wild type control FDBs. *A–B*, peak tetanic force was expressed as a percent of the pre-fatigue force; inset: peak tetanic force was expressed as a percentage of the force at 25 min of recovery. Symbols: O, control wild type; □, glibenclamide (10 μM) wild type; △, control Kir6.2$^{-/-}$; ◇, glibenclamide (10 μM) Kir6.2$^{-/-}$ (inset). Vertical bars represent the S.E.M. of 5 wild type and 6 Kir6.2$^{-/-}$ bundles.

* Significantly different from control wild type, ANOVA and LSD, $P < 0.05$.

† Significantly different from control Kir6.2$^{-/-}$, ANOVA and LSD, $P < 0.05$.

FIGURE 2.6

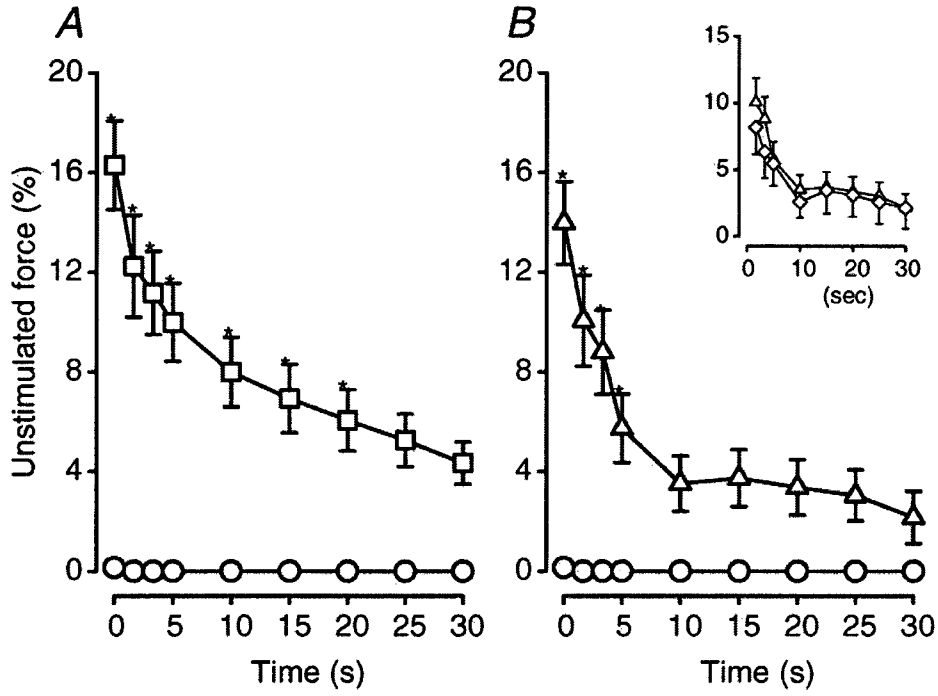

Figure 2.6. Unstimulated force in KATP channel deficient FDB bundles decreased during the recovery period at 37°C but did not completely disappear. *A–B*, wild type and Kir6.2$^{-/-}$ muscle bundles. Unstimulated force was expressed as a percentage of the pre-fatigue force. Symbols: O, control wild type; □, glibenclamide (10 μM) wild type; △, control Kir6.2$^{-/-}$; ◇, glibenclamide (10 μM) Kir6.2$^{-/-}$ (inset). Vertical bars represent the S.E.M. of 5 wild type and 6 Kir6.2$^{-/-}$ bundles.

* Significantly different from control wild type, ANOVA and LSD,$P < 0.05$.

FIBRE INTEGRITY

FDB bundles.

To determine if the reduced capacity of KATP channel deficient bundles to recover force following fatigue was due to fibre damage at the level of the cell membrane, another group of bundles were fatigued in the presence of 0.01% Evans blue, which leaks into the cytosol when the cell membrane is damaged (Anderson *et al.*, 2006). The changes in peak tetanic force and unstimulated force during fatigue in the presence of Evans blue were similar to those shown in Figs 2.2 and 2.3, respectively. A fibre was identified as Evans blue positive if under visible light it appeared blue and under 545 nm excitation it fluoresced red. There was no observed stained or fluorescent fibre in cross-sections from bundles (n = 12) that were not exposed to Evans blue during fatigue, as shown for one cross-section in Fig. 2.7D and E. Less than three fibres (< 1%) per bundle were stained when control wild type bundles (n = 4) were fatigued in the presence of Evans blue as shown for one bundle in Fig. 2.7A. The same was observed for glibenclamide wild type (n = 4) and control Kir6.2$^{-/-}$ bundles (n = 4) as shown for a representative from each group in Fig. 2.7B and C.

Eccentric contractions, elicited by stretching muscle fibres during contraction, are known to cause cell membrane damage (Decrouy *et al.*, 1997). So, as a positive control, one control Kir6.2$^{-/-}$ bundle was stretched during 12 consecutive 1 s long contractions. As shown in Fig. 2.7F, 43 fibres (25%) were Evans blue positive. So, the lack of a significant number of Evans blue positive fibres following fatigue would indicate that the cell membrane was still intact after fatigue.

FIGURE 2.7

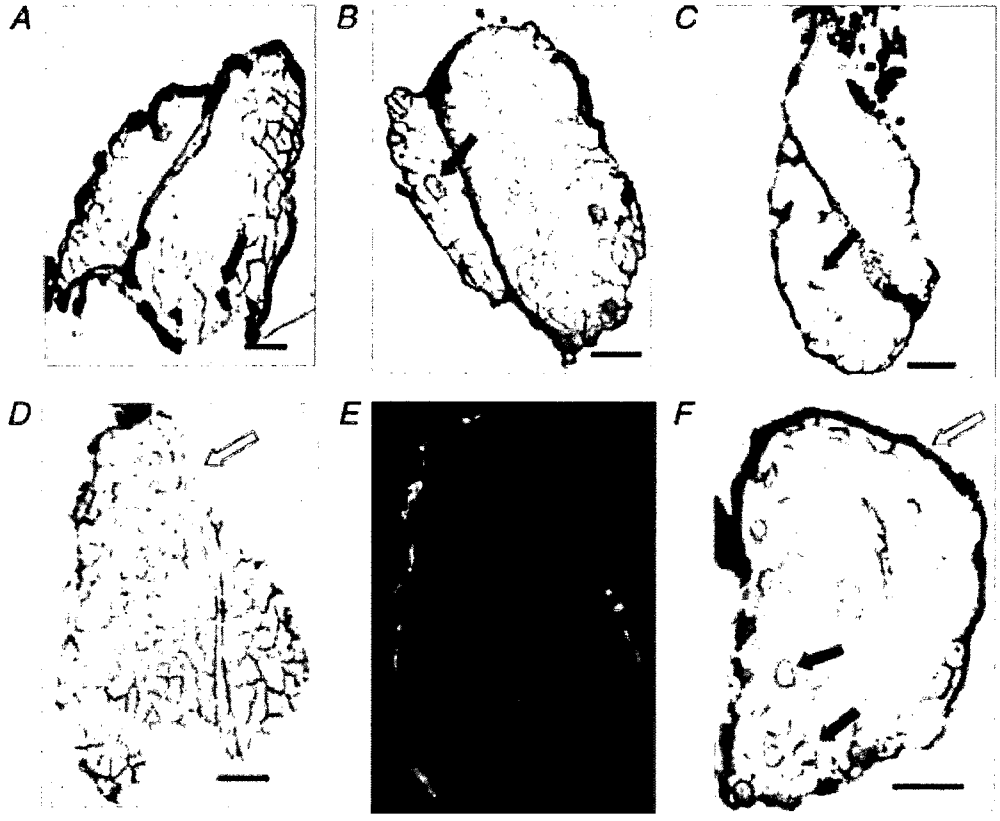

Figure 2.7. Evans blue did not stain FDB fibres during fatigue at 37°C. Bundles were fatigued in the presence of 0.01% Evans blue and cross-section visualized under visible light. *A–C*, representative from control wild type (*A*); glibenclamide wild type (*B*); control Kir6.2$^{-/-}$ (*C*). *D* and *E*, negative control: control wild type bundle fatigued in the absence of Evans blue and cross-section visualized under visible light (*D*) or excited at 545 nm for red fluorescence (*E*). *F*, positive control: one control Kir6.2$^{-/-}$ bundle after 12 eccentric contractions. Open arrows show the facia (*D*) that stained dark in the presence of Evans blue (*F*). Filled arrows show examples of fibres stained with Evans blue. Horizontal bars represent 100 μm.

Single fibres.

Single fibres were used to monitor Ca^{2+}_i. Prior to any measurements, almost all (> 95%) fibres contracted vigorously and had visible A and I bands. For 13 fibres (from 9 wild type mice), the A and I bands remained clearly visible after fatigue under control conditions as shown for one fibre in Fig. 2.8A. Nineteen fibres (from 9 wild type mice) were fatigued in the presence of 10 μM glibenclamide. Four fibres (21%) kept their pre-fatigue appearance throughout the fatigue period. The remaining 15 glibenclamide fibres either had one end supercontracted with visible A and I bands in the intact portion (11 fibres or 58%, Fig. 2.8B) or the entire fibre was supercontracted (4 fibres or 21%, Fig. 2.8C). Eleven fibres from seven Kir6.2$^{-/-}$ mice were tested under control conditions; five (45%) fibres remained intact and six (55%) partially supercontracted. Ten others fibres (from 7 Kir6.2$^{-/-}$ mice) were exposed to 10 μM glibenclamide and under those conditions 70% of the fibres supercontracted (4 partially and 3 completely).

To further test whether the supercontractions were associated with cell membrane damage we examined the fura-2 fluorescence intensities while fibres were at rest and illuminated at 380 nm. The expectation was that if the membrane was damaged and in the process became leaky, then there would be a rapid loss of fura-2 and thus fluorescence. On average, the fluorescence intensities decreased during the first minute in all KATP channel deficient fibres (Fig. 2.9). Thereafter, the fluorescence intensities increased back toward pre-fatigue levels. There was no sudden loss of fluorescence whether the fibres were partially or fully supercontracted.

FIGURE 2.8

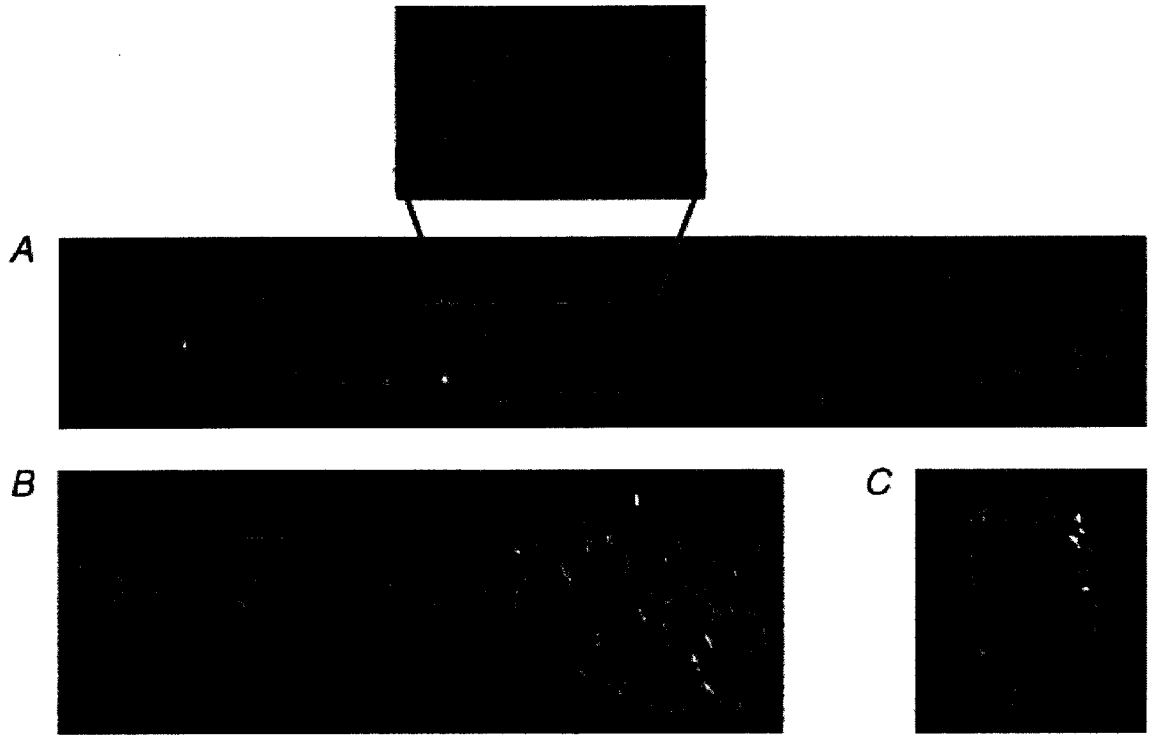

Figure 2.8. Examples of wild type single FDB fibres after fatigue: under control conditions (*A*), in the presence of 10 μM glibenclamide with one end supercontracted (*B*), and fully supercontracted (*C*). Fibre appearance of a non-fatigue single fibre is not shown as they are similar in appearance to that in *A*. Each picture is from a different fibre. Note the appearance of A and I bands in *A*.

FIGURE 2.9

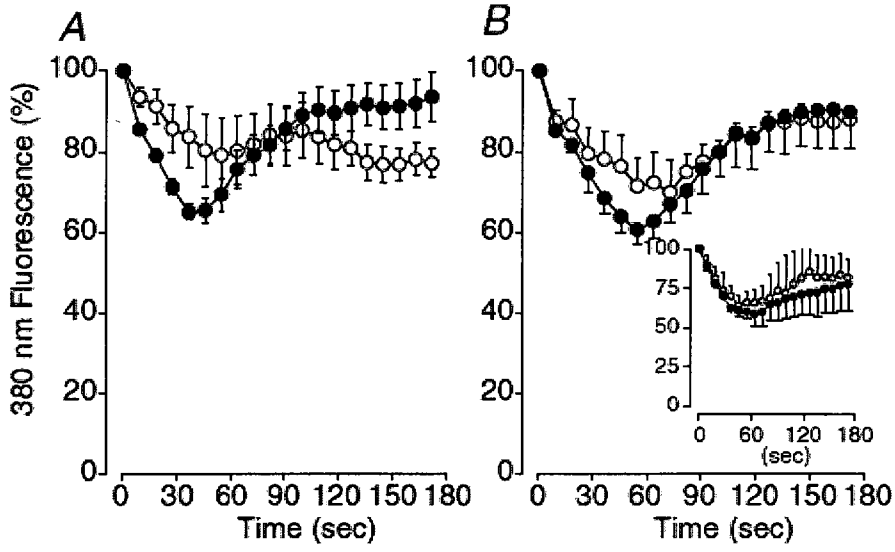

Figure 2.9. KATP channel deficient FDB fibres had no sudden loss of Fura-2. *A*, wild type fibres exposed to 10 μM glibenclamide; *B*, Kir6.2$^{-/-}$ fibres under control conditions; inset: Kir6.2$^{-/-}$ fibres exposed to 10 μM glibenclamide. Fluorescence at 505 nm from an excitation of 380 nm was averaged over the 100 ms preceding each contraction during the fatigue period, and was expressed as a percentage of the fluorescence of the pre-fatigue value. Symbols: O, fibres that did not supercontract; ●, fibres that partially or fully supercontracted. Vertical bars represent the S.E.M. (the number of fibres are given in Results).

Unstimulated and Peak $Ca^{2+}i$

To be consistent with the force parameters, unstimulated $Ca^{2+}i$ was defined as the $Ca^{2+}i$ level in the absence of stimulation and was calculated by averaging the fura-2 340/380 fluorescence ratios during the 100 ms period just preceding a contraction. Peak $Ca^{2+}i$ was defined as the maximum Ca^{2+} level during a contraction and was calculated by averaging the fura-2 340/380 fluorescent ratio of the $Ca^{2+}i$ plateau phase. When fatigued under control conditions, wild type fibres contracted throughout the entire fatigue period (Fig. 2.10A). In one representative trace, peak $Ca^{2+}i$ initially increased for about 20 s and then decreased until the 90th second; thereafter it remained relatively constant until the end of the fatigue period. For these fibres, unstimulated $Ca^{2+}i$ increased only slightly.

When wild type fibres were exposed to 10 μM glibenclamide, the changes in $Ca^{2+}i$ varied according to the final fibre appearance. For the fibres that did not supercontract (n = 4), contractions stopped within 120 s of stimulation, as shown for one fibre in Fig. 2.10B. For these fibres, the increase in unstimulated $Ca^{2+}i$ was also small. Fibres, that partially supercontracted (n = 11) at one end, had larger increases in unstimulated $Ca^{2+}i$ until they stopped contracting upon stimulation within 60 s. Thereafter, unstimulated $Ca^{2+}i$ decreased rapidly. For 3 of the 11 fibres, some contractions could be observed later in the fatigue period as shown for one fibre in Fig. 2.10C. However, for most fibres (8 out of 11), no other contractions were observed. The increase in unstimulated $Ca^{2+}i$ was the largest in the four fibres that fully supercontracted, as shown for one fibre in Fig. 2.10D. The changes in unstimulated and peak $Ca^{2+}i$ during fatigue in control and glibenclamide Kir6.2$^{-/-}$ fibres were similar to those observed for glibenclamide wild type fibres (i.e. as shown in Fig. 2.10B–D).

FIGURE 2.10

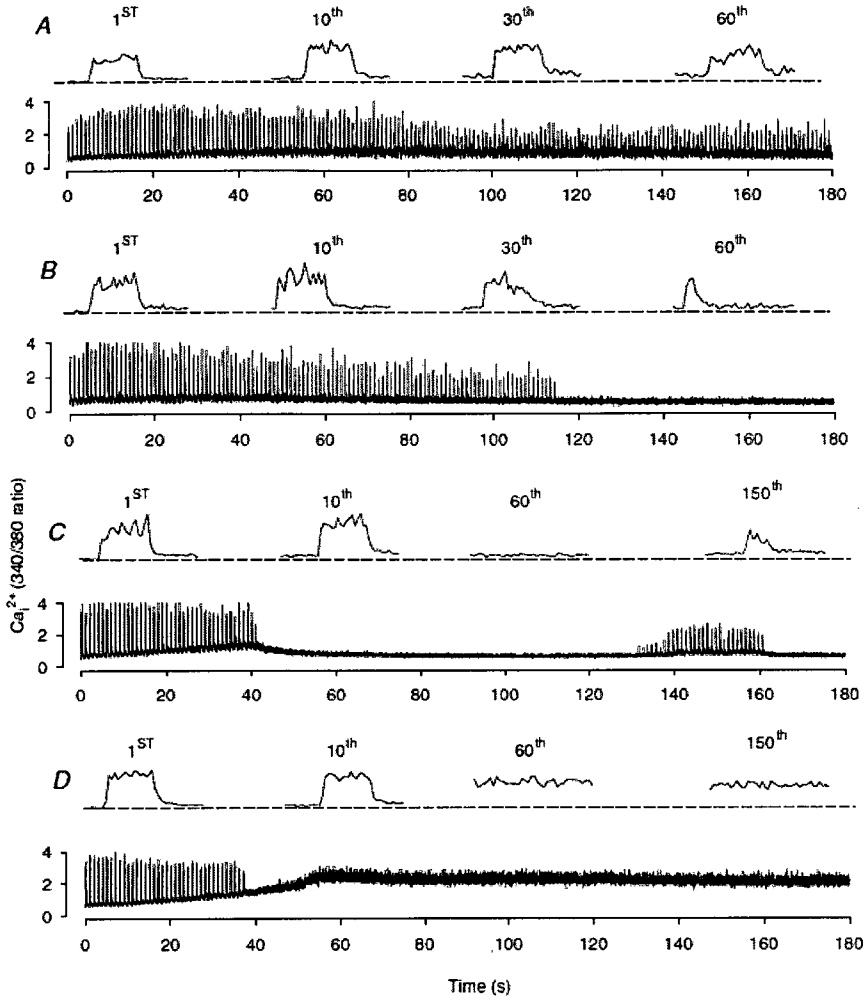

Figure 2.10. Lack of KATP channel activity impaired intracellular Ca^{2+} regulation during fatigue in FDB single fibres at 37°C. Representative Ca^{2+} traces from one control wild type fibre (*A*), and fibres that remained intact but stop contracting (*B*), that partially supercontracted (*C*), and that fully supercontracted in the presence of 10 μM glibenclamide (*D*). Bottom traces show the entire Ca^{2+}_i trace, top traces show individual Ca^{2+} transient at the indicated contraction number with the dashed lines representing the unstimulated Ca^{2+}_i before fatigue.

The initial peak 340/380 fluorescent ratios were also not different before fatigue between control (2.32) and glibenclamide wild type fibres (2.37). During the first 10–15 s of the fatigue period, peak ratios increased to a maximum of 2.83 in control fibres, which was not significantly different from the maximum value of 2.87 in glibenclamide fibres. However, the peak ratios remained significantly above the pre-fatigue peak ratios for much longer in control conditions (up to 30 s) compared to glibenclamide fibres (only 19 s). Another significant difference between the two groups of fibres was the faster decrease in peak ratios in glibenclamide fibres compared to those in control conditions.

To better understand how the lack of KATP channel activity affected the changes in force in bundles, we calculated average unstimulated and peak $Ca^{2+}i$ from all fibres for each experimental condition. The mean pre-fatigue unstimulated 340/380 fluorescence ratios were not different between control and glibenclamide wild type fibres (0.49 *versus* 0.47; Fig. 2.11). During the first minute of fatigue the mean unstimulated ratio increased to a maximum of 1.01 in control fibres and to 1.24 in the presence of glibenclamide. Thereafter, the unstimulated ratios decreased slowly.

Finally, for the last minute of the fatigue period, the peak ratios in control fibres were between 1.64 and 1.67, which was significantly different from those in glibenclamide muscle for which the ratios were between 1.10 and 1.20. Furthermore, for the last 90 s of the fatigue period, the unstimulated and peak ratios in glibenclamide fibres were not different as many fibres had stopped contracting.

FIGURE 2.11

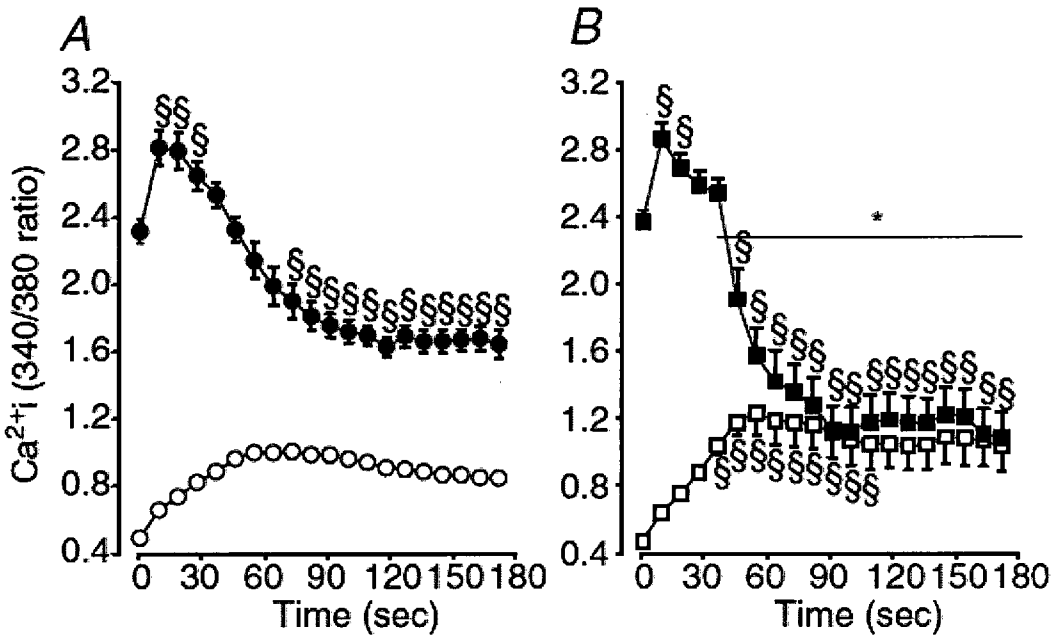

Figure 2.11. The increase in unstimulated Ca^{2+}_i and the decrease in peak Ca^{2+}_i were smaller and slower in control conditions than in the presence of glibenclamide. Mean changes in unstimulated and peak Ca^{2+}_i during fatigue at 37°C in control (*A*) and glibenclamide (10 μM) wild type FDB single fibres (*B*). Symbols: ○, ●, control wild type unstimulated and peak Ca^{2+}_i, respectively; □, ■, glibenclamide (10 μM) wild type unstimulated and peak Ca^{2+}_i, respectively. Vertical bars represent the S.E.M. of 13 control and 19 glibenclamide fibres from 9 wild type mice.

* Time (with horizontal line) when peak Ca^{2+}_i of glibenclamide fibres was significantly different from control fibres, ANOVA and LSD, $P < 0.05$.

§ Mean unstimulated or peak Ca^{2+}_i significantly different from mean value at time 0, ANOVA and LSD, $P < 0.05$.

The changes in unstimulated and peak $Ca^{2+}i$ in control Kir6.2$^{-/-}$ fibres (Fig. 2.12A) were quite similar to those observed for glibenclamide wild type fibres (Fig. 2.11B). That is, there was a rapid increase in unstimulated $Ca^{2+}i$ during the first minute and a rapid decrease in peak $Ca^{2+}i$ between the 60th and 90th seconds. There were also two major differences between the two groups. Firstly, the decreases in unstimulated $Ca^{2+}i$ during the last 2 min were greater in control Kir6.2$^{-/-}$ fibres than in glibenclamide wild type fibres. Secondly, unstimulated and peak $Ca^{2+}i$ became the same when fibres stopped contracting at 90 s in glibenclamide wild type fibres compared to 110 s for control Kir6.2$^{-/-}$ fibres. The changes in unstimulated and peak $Ca^{2+}i$ in Kir6.2$^{-/-}$ fibres were similar between control (Fig. 2.12A) and glibenclamide conditions (Fig. 2.12B). Comparing ratios between the two experimental conditions did not give rise to any significant difference.

Following fatigue, the unstimulated and peak $Ca^{2+}i$ ratios rapidly returned within 100 s to their pre-fatigue levels. This was observed for all 13 wild type fibres under control conditions, and for all KATP channel deficient fibres that did not supercontract; i.e. the four glibenclamide wild type fibres and the five control Kir6.2$^{-/-}$ fibres (Fig. 2.13). None of the supercontracted fibres recovered as unstimulated $Ca^{2+}i$ remained high. Among the fibres that partially supercontracted, only three glibenclamide wild type fibres partially recovered unstimulated and peak $Ca^{2+}i$ Fig. 2.13, inset). The three fibres were the same fibres that also contracted during fatigue (Fig. 2.10C).

FIGURE 2.12

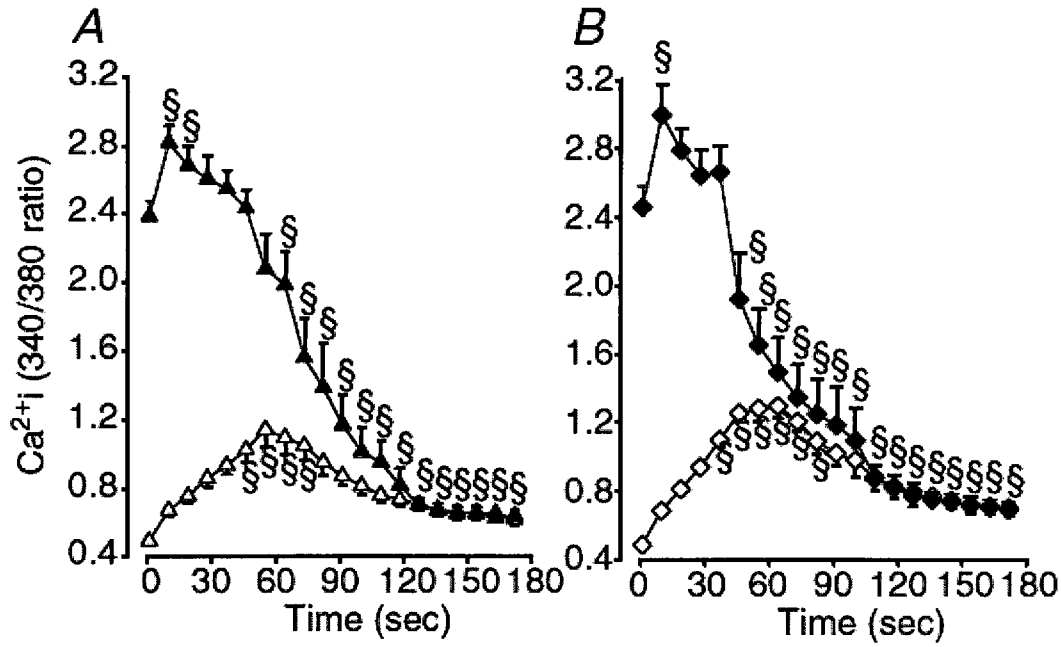

Figure 2.12. In Kir6.2$^{-/-}$ FDB fibres, the increase in unstimulated $Ca^{2+}i$ and the decrease in peak $Ca^{2+}i$ during fatigue at 37°C were also extensive while glibenclamide had no effect. Mean changes in unstimulated and peak $Ca^{2+}i$ in control (*A*) and glibenclamide (10 μM) Kir6.2$^{-/-}$ FDB fibres (*B*). Symbols: △, ▲, control Kir6.2$^{-/-}$ unstimulated and peak $Ca^{2+}i$, respectively; ◇, ◆, glibenclamide Kir6.2$^{-/-}$ unstimulated and peak $Ca^{2+}i$, respectively. Vertical bars represent the S.E.M. of 11 control and 10 glibenclamide fibres from 6 Kir6.2$^{-/-}$ mice.

§ Mean unstimulated and peak $Ca^{2+}i$ significantly different from mean value at time 0, ANOVA and LSD. $P < 0.05$.

FIGURE 2.13

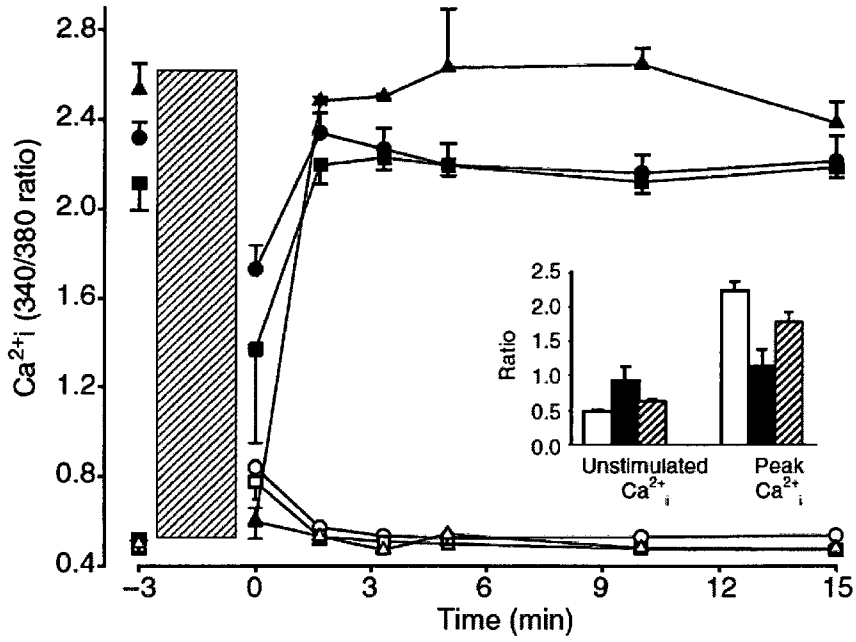

Figure 2.13. FDB fibres that did not supercontract during fatigue fully recovered unstimulated and peak $Ca^{2+}i$ after fatigue. Symbols: ○, □, △, unstimulated $Ca^{2+}i$; ●, ■, ▲, peak $Ca^{2+}i$; ○, ●, control wild type (n = 13); □, ■, glibenclamide wild type (n = 4); △, ▲, control Kir6.2$^{-/-}$ fibres (n = 5). Vertical hatched bar represents the 3 min fatigue period with time −3 min being the pre-fatigue values. Inset: recovery of unstimulated and peak $Ca^{2+}i$ only from the glibenclamide wild type fibres (n = 3) that partially supercontracted during fatigue (all other similar fibres had no recovery of peak $Ca^{2+}i$). Symbols: □, pre-fatigue value; ■, after fatigue; hatched square, after 15 min of recovery.

DISCUSSION

This study shows for the first time that abolishing KATP channel activity in FDBs during fatigue at 37°C causes faster and greater decreases in peak $Ca^{2+}i$ and peak tetanic force. Supercontraction of single fibres, greater increases in unstimulated $Ca^{2+}i$ and force during fatigue, and lower force recovery following fatigue were also observed in KATP channel deficient FDBs.

FDB MUSCLE BUNDLES AND SINGLE FIBRES TO STUDY KATP CHANNELS

The observation that KATP channel deficient fibres have faster decreases in peak $Ca^{2+}i$ and peak tetanic force is not in agreement with previous studies that have reported no effect (Weselcouch *et al.*, 1993; Light *et al.*, 1994; Duty & Allen, 1995; Van Lunteren *et al.*, 1998; Gong *et al.*, 2000; Matar *et al.*, 2000). In some of these studies, experiments were carried out at non-physiological temperatures of 20–25°C. For the studies using 37°C, a large anoxic core may have masked the effects of no KATP channel activity (see Introduction). In this study, we employed a test temperature of 37°C, but used smaller muscle preparations.

Wild type FDB single fibres, dispersed after a collagenase treatment to reduce the stress of mechanical dissection (Moopanar & Allen, 2006), contracted upon stimulation throughout the entire 3 min fatigue period under control conditions. Peak $Ca^{2+}i$ initially increased and then decreased to below pre-fatigue levels as previously reported for mechanically dissected single fibres (Westerblad & Allen, 1991). Several KATP channel deficient fibres supercontracted during fatigue, an effect not observed at lower temperatures (Duty & Allen, 1995). More importantly, the cause of the supercontraction

may also be a cause for fibre damage (see next section), i.e. our preparation may help in explaining the observation made *in vivo (Thabet et al., 2005)* that KATP channel deficient muscle fibres become damaged during muscle activity.

Peak tetanic force cannot be measured in fibres after a collagenase treatment because of the lack of tendon. Instead, we used small FDB bundles, which, on average, were 8 mm long and 2 mg in weight compared to 8 mm and 10 mg for both soleus and EDL muscles (Barclay, 2005). From the model of Barclay (2005) on O_2 diffusion in isolated muscle, an anoxic core is not expected at rest for these muscles. During fatigue with a contraction duty cycle of 0.2, the radius of the anoxic core is expected to be 0.4 mm in EDL and soleus and only 0.1 mm in FDB bundles. Despite the slight anoxic core, the FDB bundle still represents a better preparation. Firstly, peak tetanic force recovery was 92% in control wild type FDB compared to 40% in EDL and 70% in soleus (Gong *et al.*, 2000; Gong *et al.*, 2003). Secondly, a decrease in peak $Ca^{2+}i$ is a major factor contributing to the decrease in force during fatigue (Allen *et al.*, 1995). Compared to control wild type, KATP channel deficient bundles had faster decreases in peak tetanic force as expected from the faster decrease in peak $Ca^{2+}i$ in single fibres. Thus, FDB bundles and single fibres are better than whole EDL and soleus to study KATP channel function at 37°C.

EFFECT OF NO KATP CHANNEL ACTIVITY DURING FATIGUE

Fibre damage.

The occurrence of fibre damage during exercise in skeletal muscle lacking KATP channel activity was first reported *in vivo* following swimming (Kane *et al.*, 2004) and treadmill running (Thabet *et al.*, 2005) using null mice for the Kir6.2 gene. In those

studies, it was not possible to determine whether the damage was related to the lack of KATP channel activity in skeletal muscle fibres, or to a failure of the heart (Zingman *et al.*, 2002) resulting in insufficient blood flow to active muscles.

In our study, 79% of glibenclamide wild type single fibres and 55% of control Kir6.2$^{-/-}$ fibres supercontracted during fatigue and never recovered their pre-fatigue appearance. The supercontractions in single fibres are primarily due to the lack of constraint as there is no tendon to maintain constant length. Consequently, the supercontractions themselves are not fully comparable with fibre damage. However, the supercontractions were associated with large increases in unstimulated $Ca^{2+}i$, a known cause of fibre damage (Jackson *et al.*, 1984). Our results therefore provide evidence that the lack of KATP channel activity can lead to fibre damage during fatigue. More importantly, the supercontractions were observed in fibres that were superfused over most of their surface area. Thus, our results strongly support the conclusions of Thabet *et al.* (2005) that, in skeletal muscle, the KATP channels are active during exercise and fatigue and critical in preventing fibre damage, and that the damage during treadmill running was not due to insufficient blood flow.

Treadmill running only affects type IIB fibres of Kir6.2$^{-/-}$ hindlimb muscles and all fibre types in diaphragm (Thabet *et al.*, 2005). FDB is primarily composed of type IIA and IIX fibres (less than 5% are I and IIB fibres (Raymackers *et al.*, 2000)). This suggests that the role of KATP channels in preventing fibre damage is not limited to type IIB fibres in hindlimb muscles. It is possible that the metabolic stress on hindlimb type IIA and IIX fibres during treadmill running is less than in our *in vitro* model.

Cell membranes are usually impermeable to Evans blue, unless they become damaged and leaky. Contrary to the effects of eccentric contractions (Decrouy *et al.*, 1997), Evans blue stained very few fibres during fatigue. More importantly, no difference was observed between control, glibenclamide wild type, and control Kir6.2$^{-/-}$ bundles. Furthermore, KATP channel deficient single fibres, which partially or fully supercontracted, had no sudden and large decreases in fura-2 fluorescence intensities (from the 380 nm excitation) as expected if the membrane had become damaged and leaky (a decrease in fluorescence was observed during the first min of fatigue and was most likely because of the increase in $Ca^{2+}i$). Thus, the damage in KATP channel deficient fibres does not seem to involve the outer surface cell membrane. This does not, however, eliminate the possibility of damage in t-tubules, the sarcoplasmic reticulum or sarcomeres.

CONTRACTILE DYSFUNCTIONS

In the Introduction, we define 'contractile dysfunction' as any event from the generation of action potentials to the actin–myosin interaction that is depressed in a manner not associated with the normal process of fatigue (or any metabolic stress) and that eventually incapacitate muscle to generate force.

Pre-fatigued force.

The maximum force generated in unfatigued FDB bundles of 2- to 3-month-old-mice were on average 30% less in Kir6.2$^{-/-}$ than wild type bundles. Kir6.2$^{-/-}$ EDL of 1-year-old mice generates 21% less force than wild type EDL while Kir6.2$^{-/-}$ soleus generates 11% less force (Gong *et al.*, 2000). However, no differences in force were observed between wild type and Kir6.2$^{-/-}$ EDL and soleus of 2- to 3-month-old-mice.

Thus, the chronic lack of KATP channel activity reduces the capacity of muscles to generate force, but the extent of the decrease is time and muscle dependent. The nature of the contractile dysfunction causing the force loss and the difference between muscles cannot, however, be explained from our data.

Unstimulated force.

We found that KATP channel deficient bundles generate more unstimulated force than control bundles. The FDB bundles generated twice as much unstimulated force as EDL (Gong *et al.*, 2000; Matar *et al.*, 2000; Gong *et al.*, 2003), suggesting that the greater generation of unstimulated force in KATP channel deficient muscles is not linked to the anoxic core, which is the smallest in FDBs (see section above). The factor contributing to unstimulated force is most likely an uncontrolled increase in unstimulated Ca^{2+}_i causing excessive shortening in single fibres and unstimulated force in bundles kept at constant length.

Unstimulated force constitutes a minute portion of peak total force in control wild type fibres (Fig. 2.14A), yet it represented 50% or more of the peak total force in KATP channel deficient bundles for most of the fatigue period (Fig. 2.14B). Such large unstimulated force is expected to lower muscle performance *in vivo*. Firstly, when unstimulated force develops, antagonist muscles must then do more work to overcome the extra opposing force, and consequently fatigue faster. Lower cardiac performance has been shown to be a factor that reduces fatigue resistance in Kir6.2$^{-/-}$ mice (Zingman *et al.*, 2002; Kane *et al.*, 2004). We now suggest that the generation of unstimulated force is another factor. Secondly, eccentric contractions will occur in muscles generating unstimulated force when antagonist muscles contracts.

FIGURE 2.14

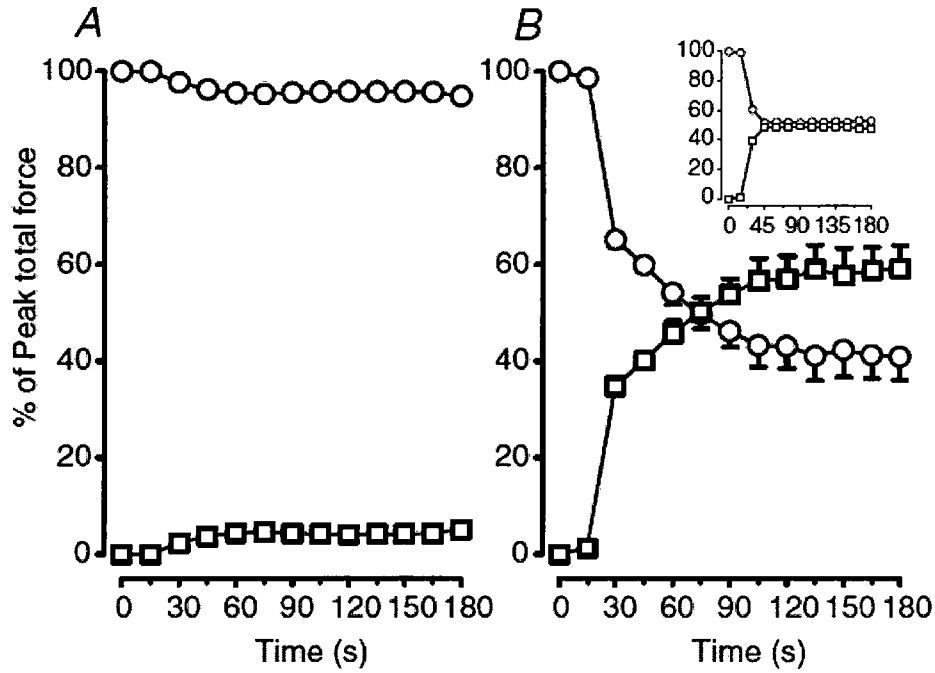

Figure 2.14. During fatigue unstimulated force contributed 50–60% of the peak total force in KATP channel deficient FDBs. *A*, control wild type; *B*, glibenclamide wild type (10 μM). Inset: control Kir6.2$^{-/-}$. For each time period, peak tetanic force (O) and unstimulated force (□) were calculated as a percentage of peak total force.

Eccentric contraction is a known factor for fibre damage (Decrouy *et al.*, 1997), and consequently unstimulated force is most likely a factor contributing to the fibre damage reported during swimming and treadmill running in Kir6.2$^{-/-}$ mice (Zingman *et al.*, 2002; Thabet *et al.*, 2005). Thus, the large unstimulated $Ca^{2+}i$ and resulting unstimulated force in Kir6.2$^{-/-}$ muscles should be considered as contractile dysfunctions because (i) they were not observed in control wild type muscles and (ii) they can depress force generation.

Force recovery.

KATP channel deficient FDBs recovered about 20% less peak tetanic force than control wild type FDBs (Fig. 2.5) compared to 10–15% difference for EDL and none for soleus (Gong *et al.*, 2000; Matar *et al.*, 2000; Gong *et al.*, 2003). The dependency of force recovery on KATP channel activity is thus in the order of FDB > EDL > soleus. Interestingly, the importance of KATP channels in preventing fibre damage is in the same order (as determined in this study for FDB, in Thabet *et al.* (2005) for EDL and soleus). Furthermore, the recovery of unstimulated and peak $Ca^{2+}i$ in KATP channel deficient single fibres that supercontracted during fatigue was (i) incomplete and (ii) in only a small number of fibres (20% for glibenclamide wild type fibres and 0% for control Kir6.2$^{-/-}$ fibres). Fibre damage is thus the most likely explanation for the lower force recovery in KATP channel deficient bundles.

Abolishing KATP channel activity using a pharmacological approach in wild type muscles (i.e. glibenclamide) or a genetic approach using Kir6.2$^{-/-}$ muscles has always given similar results in terms of peak $Ca^{2+}i$ and force, unstimulated $Ca^{2+}i$ and force, during both fatigue and recovery (this study for FDB, Gong *et al.* (2000) for EDL and soleus). Glibenclamide also had no significant effect on the decrease in peak $Ca^{2+}i$ and

force, as well as the increase in unstimulated $Ca^{2+}i$ and force in Kir6.2$^{-/-}$ muscles. We now, for the first time, report that glibenclamide reduced peak tetanic force recovery in Kir6.2$^{-/-}$ bundles.

The possibility that glibenclamide has a non-specific effect cannot be eliminated using the data reported in this study. Glibenclamide can inhibit mitochondrial KATP channels (Garlid *et al.*, 1997). Furthermore, Matar *et al.* (2000) have reported that before and during fatigue, KATP channel modulators affect ATP levels in the oxidative soleus, but not in the glycolytic EDL; they suggested that the effects in soleus were most likely due to a modulation of mitochondrial KATP channel activity. Since FDB muscles are also oxidative (type IIA and IIX fibres, (Raymackers *et al.*, 2000)), it is then possible that the lower peak tetanic force recovery in glibenclamide-exposed Kir6.2$^{-/-}$ bundles (compared to Kir6.2$^{-/-}$ control) is because of an impairment in ATP production by mitochondria.

Rate of Fatigue.

During the initial 60 s of the fatigue period, the decreases in peak $Ca^{2+}i$ and peak tetanic force were significantly faster in KATP channel deficient than in control wild type single fibres and bundles. The decreases in peak total force were also faster in KATP channel deficient bundles, but the differences with control wild type bundles were significant only at 30 and 45 s and much smaller compared to the differences for peak $Ca^{2+}i$ and peak tetanic force. Overall, the changes in peak $Ca^{2+}i$, peak tetanic force and peak total force suggest that during most of the first 60 s fatigue rate was faster in KATP channel deficient bundles and single fibres.

During the last 2 min of the fatigue period, the difference in peak tetanic force between normal and KATP channel deficient bundles eventually disappeared, but never

became greater in KATP channel deficient bundles. Peak total force, on the other hand, became greater in KATP channel deficient bundles. In most studies using isometric contractions, the rate of fatigue is determined from the decrease in peak total force; unstimulated force is ignored because it contributes very little to peak total force as we also report here for control wild type bundles (Fig. 2.14A). However, in KATP channel deficient bundles, the unstimulated force is considerable, reaching more than 20% of pre-fatigue peak total force (Fig. 2.3). More importantly, it contributed 50–60% of the peak total force during fatigue (Fig. 2.14B), and may come from fibres which supercontracted while being unexcitable as observed in single fibres. Consequently, using just peak total force as an index of fatigue can be misleading.

Several studies (e.g. (Allen *et al.*, 1995)) have shown that decreases in peak $Ca^{2+}{}_i$ is a major cause for the decrease in force during fatigue in normal muscles. If the data from peak total force are to be taken as evidence for slower fatigue rate, then peak $Ca^{2+}{}_i$ should also be greater in KATP channel deficient fibres during that time. This was clearly not the case as peak $Ca^{2+}{}_i$ remained much lower in KATP channel deficient than in control wild type fibres until the end of the fatigue period. We therefore suggest that the major impact of abolishing KATP channel activity, by either pharmacological or genetic means, is faster fatigue rate.

This result was unexpected because KATP channel openers increase the rate of fatigue (Weselcouch *et al.*, 1993; Matar *et al.*, 2000). For the openers, the mechanism of action starts with a depression of action potential amplitude as the KATP channels provide an outward K^+ current that reduces the extent of the Na^+ depolarizing current (Gong *et*

al., 2003). In the case of no KATP channel activity, a different mechanism must cause the faster fatigue rate.

If fibre damage is one mechanism, then it must occur during the fatigue period. If they had occurred during recovery, one would expect slower recovery in KATP channel deficient bundles. However, KATP channel deficient single fibres that did not supercontract during fatigue not only fully recovered their unstimulated and peak $Ca^{2+}i$, but did so with a time course similar to control wild type fibres. Furthermore, force recovery in bundles had similar time courses whether the KATP channel activity was normal or abolished. All supercontractions in KATP channel deficient single fibres occurred during the first 60 s of fatigue. Finally, the sudden rise in unstimulated force that occurred between the 15th and 30th second corresponded to the time when decreases in peak tetanic force and peak total force in KATP channel deficient bundles became faster. We therefore propose that most of the fibre damage occurred during the first 60 s of fatigue, disabling fibres from contracting correctly upon stimulation increasing the rate at which force decreases in bundles.

Fibre damage, however, cannot be the only reason for the faster decreases in force in bundles. This is because there was a group of KATP channel deficient single fibres that had a faster decrease in peak $Ca^{2+}i$ and eventually completely stopped contracting even though they did not supercontract, had very low unstimulated $Ca^{2+}i$, and completely recovered peak $Ca^{2+}i$. In cardiac and skeletal muscle, membrane depolarization during metabolic inhibition is much greater in the presence than in the absence of glibenclamide; in skeletal muscles, the depolarization can be as large as 30 mV (Gramolini & Renaud, 1997; Baczko *et al.*, 2004). Membrane potentials were not measured in this study, but

large depolarizations are likely to occur in KATP channel deficient fibres because of a lower K^+ conductance. If so, the depolarization would increase the degree of Na^+ channel inactivation resulting in lower action potential amplitude, and consequently lower Ca^{2+} release and force. Thus, large membrane depolarization constitutes another possible contractile dysfunction that increases the rate of fatigue in the absence of KATP channel activity.

In conclusion, our study shows that most of the time the absence of KATP channel activity gives rise to faster fatigue rates because the decrease in force associated with fibre damage and contractile dysfunctions prevails over the slower decreases that are expected as the channels no longer diminish action potential amplitude. We also observed that many KATP channel deficient fibres supercontracted, and had large increases in unstimulated $Ca^{2+}i$ and unstimulated force, and a lower capacity to recover force following fatigue.

ADDENDUM TO CHAPTER 2

In this study, it was observed that the rate of fatigue in sKATP channel deficient muscle was due to a balance between: 1. the greater AP amplitude (Gong *et al.*, 2003), which occurs during a contraction as K^+ conductance is decreased, causing a slower rate of fatigue; and 2. the development of contractile dysfunctions; causing a faster rate of fatigue. These contractile dysfunctions included supercontraction of single fibres, and greater increases in unstimulated $Ca^{2+}i$ and force during fatigue. The result of the two factors resulted in an apparent faster rate of fatigue when sKATP channel activity was abolished.

A comment was put forth regarding the unstimulated force during the recovery period regarding the fact that it drops to below 0% of pre-fatigue tetanic force (Figure 2.6). A mechanism for this effect cannot be explained from the results presented in this thesis. When the maximum muscle length was adjusted at the beginning of the experiment, there was always a small amount of resting tension as the elastic components were stretched. Perhaps, during fatigue and recovery, the resting force-length relationship was modified in which the eleastic components become more compliant

Another comment was raised regarding some possible discrepancy between Figure 2.4 and Figure 2.11. Specifically, why would peak total force for sKATP channel deficient muscle be greater than that in wild type from 120 – 180 s, when peak tetanic $Ca^{2+}i$ in sKATP channel deficient single fibers was less than that in wild type? The main reason for this is that in Figure 2.4, the peak total force is the measurement of unstimulated and tetanic force. Since sKATP channel deficient muscle only develop slightly less tetanic force during this time period (Figure 2.2), but develop a large amount

of unstimulated force (Figure 2.3), the result is a greater total force. Furthermore, as shown in Figure 2.8, 2.10 and 2.11, many sKATP channel deficient fibers supercontracted during the fatigue period, which would also result in generation of force.

CHAPTER 3

CONTRACTILE DYSFUNCTIONS IN K_{ATP} CHANNEL DEFICIENT MOUSE FDB MUSCLE DURING FATIGUE INVOLVE EXCESSIVE DEPOLARIZATION AND Ca^{2+} INFLUX THROUGH L-TYPE Ca^{2+} CHANNELS

By

Carlo Cifelli, **Louise Boudreault**, Bing Gong, Jean-Philippe Bercier, and Jean-Marc Renaud

University of Ottawa, Department of Cellular and Molecular Medicine, 451 Smyth Rd., Ottawa, Ontario, Canada, K1H 8M5

Experimental Physiology 93: 1126-1138, 2008.

Footnote: Carlo Cifelli and Louise Boudreault have done the same amount of work for this study.

AUTHORS' CONTRIBUTIONS

- Boudreault: most of Table 3.1 and Fig. 3.1, part of Fig. 3.3-3.5, Fig. 3.6-3.10, 3.12, major writing of manuscript
- Cifelli: part of Fig. 3.3-3.5
- Bercier: part of table 3.1 and Fig. 3.1
- Gong: Fig. 3.11

ABSTRACT

KATP channel deficient muscles develop contractile dysfunctions during fatigue that may explain their apparently faster rate of fatigue compared to wild type muscles. The objectives of this study were to determine i) whether the contractile dysfunctions, namely unstimulated force and depressed force recovery, are due to excessive membrane depolarization and Ca^{2+} influx through L-type Ca^{2+} channels and ii) whether reducing the magnitude of these two contractile dysfunctions reduces the rate of fatigue in KATP channel deficient muscles. To reduce Ca^{2+} influx, we lowered the extracellular Ca^{2+} concentration ($[Ca^{2+}]_e$) from 2.4 to 0.6 mM or added 1 μM verapamil, a L-type Ca^{2+} channel blocker. KATP channel deficient flexor digitorum brevis (FDB) were obtained by exposing wild type muscles to 10 μM glibenclamide or by using FDB from Kir6.2$^{-/-}$ mice. Fatigue was elicited with one contraction per s for 3 min at 37°C. In wild type FDB, lowered $[Ca^{2+}]_e$ and verapamil did not affect the decrease in peak tetanic force and unstimulated force during fatigue and force recovery following fatigue. In KATP channel deficient FDB, lowered $[Ca^{2+}]_e$ and verapamil slowed down the decrease in peak tetanic force and reduced unstimulated force during fatigue, and improved force recovery. In Kir6.2$^{-/-}$ FDB, the rate of fatigue actually became slower than in wild type FDB in the presence of verapamil. The cell membrane depolarized from -83 to -57 mV in normal wild type FDB. The depolarizations in some glibenclamide-exposed fibres were similar to those of normal FDB while in other fibres the cell membrane depolarized to -31 mV in 80 sec, which was also the time when these fibres supercontracted. It is concluded that 1) KATP channels are crucial in preventing excessive membrane depolarization and Ca^{2+}

influx through L-type Ca^{2+} channels and 2) that they contribute to the decrease in force during fatigue.

INTRODUCTION

The ATP-sensitive K^+ channel (K_{ATP} channel) derives its name from the fact that ATP binding on the cytosolic side results in the closure of the channel (Noma, 1983). The K_{ATP} channel is essential in preventing contractile dysfunctions. These are defined as events, from the generation of action potentials to the actin-myosin interaction, that are depressed in a manner not associated with the normal process of fatigue, and will eventually incapacitate muscle from generating force (Cifelli *et al.*, 2007). Contractile dysfunctions can include fibre damage, large membrane depolarizations, large increases in unstimulated intracellular Ca^{2+} concentration ($[Ca^{2+}]_i$) and force, and a reduced capacity to recover force after the metabolic stress (Gramolini & Renaud, 1997; Gong *et al.*, 2000; Matar *et al.*, 2000; Gong *et al.*, 2003; Baczko *et al.*, 2004; Baczko *et al.*, 2005; Cifelli *et al.*, 2007). The K_{ATP} channel is important not only during pathological conditions such as ischemia (Baczko *et al.*, 2004; Baczko *et al.*, 2005) or hypertension (Kane *et al.*, 2006), but also during normal physiological stress such as swimming and treadmill running (Zingman *et al.*, 2002; Kane *et al.*, 2004; Thabet *et al.*, 2005).

It has been shown, using verapamil, that fibre damage in cardiac muscles can involve a Ca^{2+} influx through L-type Ca^{2+} channels (Zingman *et al.*, 2002; Baczko *et al.*, 2005) that are probably activated by excessive membrane depolarization when there is no K_{ATP} channel activity (Baczko *et al.*, 2004). Contrary to cardiac muscles, in skeletal muscles, Ca^{2+} influx is not necessary to activate Ca^{2+} release due to depolarization since the L-type Ca^{2+} channels interact directly with the sarcoplasmic reticulum Ca^{2+} release channels (Tanabe *et al.*, 1990a). Furthermore, Ca^{2+} influx through L-type Ca^{2+} channels is much less in skeletal than in cardiac muscle (Tanabe *et al.*, 1990a). Thus, it remains to

be determined whether the contractile dysfunctions in KATP channel deficient skeletal muscle are related to a Ca^{2+} influx through L-type Ca^{2+} channels. Considering that: i) the large unstimulated force correlates well with the large increase in $[Ca^{2+}]_i$ during fatigue in Kir6.2$^{-/-}$ FDB; and ii) a large increase in $[Ca^{2+}]_i$ is a known cause of fibre damage (leading to lower force recovery) (Jackson *et al.*, 1984; Cifelli *et al.*, 2007), the first objective of this study was to test the hypothesis that the unstimulated force during fatigue and reduced force recovery in KATP channel deficient muscles is due to excessive membrane depolarization and Ca^{2+} influx through L-type Ca^{2+} channels.

In skeletal muscle, opening of the KATP channel reduces action potential amplitude (Gong *et al.*, 2003), which results in less Ca^{2+} released by the sarcoplasmic reticulum and force production by the sarcomeres (Weselcouch *et al.*, 1993; Burton & Smith, 1997a; Matar *et al.*, 2000; Gong *et al.*, 2003). It can then be suggested that the channel contributes to the decrease in force during fatigue. Although slower rates of fatigue are expected when KATP channel activity is abolished, many studies using pharmacological and genetic approaches reported either no effect (Weselcouch *et al.*, 1993; Light *et al.*, 1994; Gong *et al.*, 2000; Matar *et al.*, 2000; Gong *et al.*, 2003) or a faster rate of fatigue (Gramolini & Renaud, 1997; Cifelli *et al.*, 2007).

Cifelli et al. (2007) suggested that the apparent faster fatigue rate in KATP channel deficient muscles was due to contractile dysfunctions, which accelerated the decrease in force to such an extent that it prevailed over the expected slower decreases in rate. So, the second objective of this study was to test the hypothesis that reducing the extent of contractile dysfunctions in KATP channel deficient muscles results in slower fatigue rate. To test the two hypotheses, we determined the effects of lowering extracellular Ca^{2+}

concentration ($[Ca^{2+}]_e$) and of partially blocking L-type Ca^{2+} channels with verapamil on unstimulated force during fatigue and peak tetanic force during recovery (hypothesis 1) and fatigue rate (hypothesis 2).

METHODS AND MATERIALS

ANIMALS AND FDB MUSCLE BUNDLE PREPARATION

Animal care and muscle preparations. FDB muscles from CD-1 mice were used as wild type muscles. K_{ATP} channel deficient FDB muscles were obtained by either exposing wild type FDB to glibenclamide, a channel blocker, or by using Kir6.2$^{-/-}$ mice (Miki *et al.*, 2002). All mice were two to three month old mice and weighed 20-25 g. They were fed *ad libitum*, and housed according to the guidelines of the Canadian Council for Animal Care (CCAC). The Animal Care Committee of the University of Ottawa approved all experimental procedures used in this study. Small muscle bundles (force measurement) and single fibres (resting membrane potential (resting Em) measurement) were obtained from the FDB as described by Cifelli *et al.* (2007). Briefly, mice were anesthetized with a single intraperitoneal injection of 2.2 mg ketamine, 0.44 mg xylazine, and 0.22 mg acepromazine per 10 g of body mass. After excision of the FDB, the fibre bundle controlling the 4th digit was separated from the rest of the muscle. Single fibres were dispersed after a collagenase treatment of the entire FDB muscle. All mice were then euthanized with an overdose of anaesthetics.

SOLUTIONS

FDB bundles were constantly immersed in physiological saline solution. The control solution contained (in mM): 118.5 NaCl, 4.7 KCl, 2.4 $CaCl_2$, 3.1 $MgCl_2$, 25 $NaHCO_3$, 2 NaH_2PO_4, and 5.5 D-glucose. All solutions were continuously bubbled with 95% O_2-5% CO_2 and had a pH of 7.4. For the low calcium solution (0.6 mM Ca^{2+}), $CaCl_2$ was reduced appropriately and $MgCl_2$ increased to 4.9 mM to maintain osmolarity and ionic strength. For the high calcium solution (4.8 mM Ca^{2+}), the appropriate amount of

$CaCl_2$ was added while the concentration of Mg^{2+} was reduced to 0.7 mM. Glibenclamide-containing solutions (10 μM) were prepared by first dissolving it in DMSO before it was added to the physiological solution with a final DMSO concentration of 0.1% (v/v). Verapamil was directly dissolved in the physiological solution without any vehicle. All experiments were carried out at 37°C.

FORCE MEASUREMENT

Force measurements were carried out as described by Cifelli *et al.* (2007). Briefly, muscle length was adjusted to give maximum tetanic force. Force was monitored with a Cambridge ergometer (model 300, USA) or a Kulite force transducer (Model BD100, Canada), and digitized at 5 kHz by a Keithley Metrabyte A-D board (model DAS50, USA). From the force traces, four parameters were analysed: i) peak tetanic force, defined as the maximum force generated during a tetanic stimulation (Fig. 3.2); ii) unstimulated force, defined as the remaining force between contractions when it failed to completely relax; iii) peak total force, calculated as the sum of the peak tetanic force and unstimulated force; and, iv) fade, defined as the decline in force after reaching its maximum while the muscle was still stimulated, and was calculated as a ratio of the force at 200 ms (the time the last stimulation was applied) over the peak tetanic force.

STIMULATION AND FATIGUE PROTOCOL

FDB bundles were allowed 30 min equilibrium in the presence of either 0.6, 2.4 (control), 4.8 mM Ca^{2+}, 10 μM glibenclamide or 1 μM verapamil (except for the verapamil dose-response curve measurements). Unless specified otherwise, tetanic contractions were elicited with 200 ms trains of supramaximal square waves (10 V) of 0.3 ms duration at 200 Hz. Pulses were generated with a Grass S88 stimulator and a Grass SIU5 isolation unit (Grass Instruments, USA). The stimulating platinum wires (4

mm apart) were positioned on opposite sides of the bundles. Contractions were elicited every 100 s in experiments involving unfatigued muscles and prior to fatigue. Fatigue was elicited by reducing the interval between contractions to one second for 180 s. After fatigue, muscles were stimulated every 100 s to measure force recovery. For all fatigue experiments, FDB were used in pairs and fatigued only once: one muscle was exposed to control conditions (2.4 mM Ca^{2+}), while the other was exposed to either 0.6 or 4.8 mM Ca^{2+} or 1 μM verapamil.

RESTING Em MEASUREMENT

Fibres were penetrated with two microelectrodes (tip resistance 20-30 MΩ) in the centre of a fibre where movement was minimal during contraction. One microelectrode was used to inject 100-200 nA of current to elicit action potentials at 100 Hz for 200 ms (smaller fibres requiring less current than larger ones). The other microelectrode was used to measured resting and action potentials. Microelectrodes were connected to a Warner Amplifier (Model 501A, U.S.A) and data were acquired at 10 kHz using an Axon digitizer (Model 1440, USA) and pClamp (Axon Instruments, Version 10).

STATISTICAL ANALYSIS

Unless otherwise specified, split plot ANOVA designs were used to determine significant differences with the treatment 'mouse' in the whole plot and the treatments 'time' or voltage' in the split plot, as muscles were tested at all time periods or voltage levels. ANOVA calculations were made using Version 9.0 GLM (General Linear Model) procedures of the Statistical Analysis Software (SAS Institute Inc., USA). When a main effect or interaction was significant, the least significant difference (L.S.D.) was used to

locate the significant differences (Steel & Torrie, 1980). The word "significant" refers only to a statistical difference of $P<0.05$.

RESULTS

EFFECTS OF $[Ca^{2+}]_e$

We first tested the effects of reducing the Ca^{2+} concentration gradient 4-fold by lowering $[Ca^{2+}]_e$ from 2.4 to 0.6 mM to determine whether: i) the contractile dysfunctions (i.e. large unstimulated force during fatigue and depressed force recovery after fatigue) are dependent on excessive Ca^{2+} influx in Kir6.2$^{-/-}$ FDB; and ii) whether reducing the extent of the contractile dysfunctions results in a slower fatigue rate.

Peak tetanic force-stimulus strength relationship in unfatigued FDB

Unfatigued FDB did not develop unstimulated force; so, under that condition, peak total force and peak tetanic force were the same. As previously reported by Cifelli *et al.* (2007), the maximum peak tetanic force of Kir6.2$^{-/-}$ FDB, was significantly less than the force of wild type FDB (Fig. 3.1A, inset). In wild type FDB, lowering $[Ca^{2+}]_e$ from 2.4 to 0.6 mM had no effect on the peak tetanic force-stimulus strength (Fig. 3.1A and Table 3.1), including the maximum force developed at supramaximal strength (data not shown). The maximum force was also unaffected by $[Ca^{2+}]_e$ in Kir6.2$^{-/-}$ FDB, but the peak tetanic force-stimulus strength relationship was significantly shifted toward higher voltages with a 9% increase in threshold and a 25% increase in the voltage required to obtain half maximum force (Fig. 3.1B and Table 3.1). In all subsequent experiments, the stimulus strength was therefore set to a supramaximal level of 10 V.

TABLE 3.1

PARAMETER	WILD TYPE			Kir6.2$^{-/-}$		
	2.4 mM Ca^{2+}	0.6 mM Ca^{2+}	Difference	2.4 mM Ca^{2+}	0.6 mM Ca^{2+}	Difference
V_{THR} (V)	2.65 ± 0.23	2.73 ± 0.30	0.08 ± 0.30	2.50 ± 0.13	2.73 ± 0.19	0.23 ± 0.07*
$V_{50\%}$ (V)	3.73 ± 0.24	3.66 ± 0.32	-0.07 ± 0.46	3.26 ± 0.11	4.07 ± 0.12	0.81 ± 0.17*
V_{max} (V)	7.40 ± 0.47	6.95 ± 0.29	-0.45 ± 0.53	7.19 ± 0.54	7.54 ± 0.40	0.35 ± 0.32

Table 3.1. Effect of lowered $[Ca^{2+}]_e$ on the peak tetanic force-stimulus strength relationship in wild type and Kir6.2$^{-/-}$ FDB. All FDB were tested in the presence of 2.4 (control) and 0.6 mM Ca^{2+}. Voltage stimulus strengths for threshold (V_{THR}), 50% of maximum peak tetanic force ($V_{50\%}$) and maximum peak tetanic force (V_{max}) were calculated from each individual muscle and are given as mean ± S.E. for 7 wild type and 5 Kir6.2$^{-/-}$ FDB.

* Significantly different from 2.4 mM Ca^{2+}, paired t-test $P < 0.05$.

FIGURE 3.1

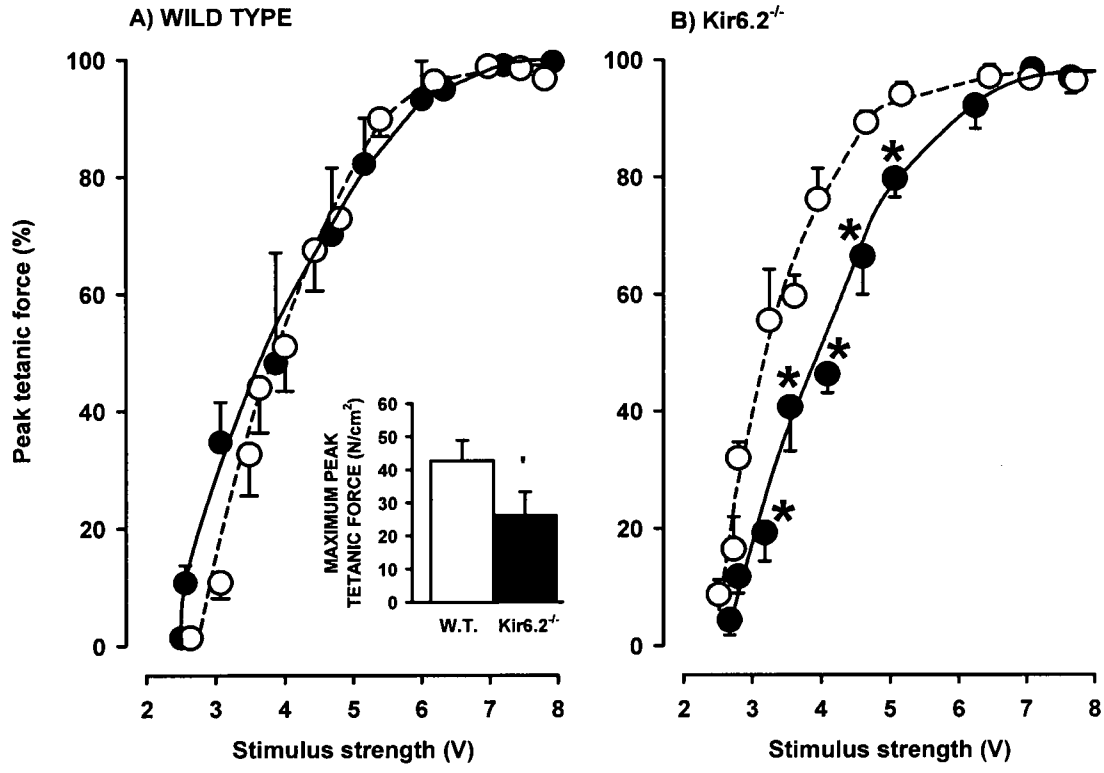

Figure 3.1. Lowering $[Ca^{2+}]_e$ significantly shifted the peak tetanic force-stimulus strength relationship toward higher voltages in Kir6.2$^{-/-}$ FDB (B) but not in wild type FDB (A). Tetanic contractions were elicited at 37°C with 200 ms train of 0.3 ms pulses at 200 Hz. Inset: peak tetanic force at 7 V representing the maximum force. Symbols: ○, 2.4 mM Ca^{2+}; ●, 0.6 mM Ca^{2+}. Vertical bars represent the S.E. of 7 wild type and 5 Kir6.2$^{-/-}$ FDB.

' Maximum peak tetanic force significantly different from wild type, t-test $P < 0.05$.

* Significantly different from 2.4 mM Ca^{2+}, ANOVA and L.S.D. $P<0.05$.

Rate of fatigue

As discussed by Cifelli *et al.* (2007), the fatigue rate cannot be determined by only measuring the decline in peak total force because of the large contribution of unstimulated force in Kir6.2$^{-/-}$ FDB (Fig. 3.2). So, in this study, we report the changes in peak tetanic force, peak total force and unstimulated force as defined in Fig. 3.2B. As previously reported (Cifelli *et al.*, 2007), the decreases in peak tetanic force during fatigue were faster in Kir6.2$^{-/-}$ than in wild type FDB. For example, at 30 s, mean peak tetanic force was 38% of the pre-fatigue force in Kir6.2$^{-/-}$ FDB compared to 67% in wild type FDB, representing a 29% difference (Fig. 3.3). Lowered $[Ca^{2+}]_e$ had no effect on the decreases in peak tetanic force in wild type FDB (Fig. 3.3A). In Kir6.2$^{-/-}$ FDB, the decreases in peak tetanic force were significantly slower at 0.6 mM than at 2.4 mM Ca^{2+} (Fig. 3.3B). The largest difference between the two conditions was 18% at 30 s. The significant differences persisted until the end of the fatigue period when peak tetanic force was still 6% higher at 0.6 mM compared to 2.4 mM Ca^{2+}.

Unstimulated force and peak total force during fatigue.

As previously reported (Cifelli *et al.*, 2007), wild type FDB generated very little unstimulated force while Kir6.2$^{-/-}$ FDB generated large amounts because they failed to fully relax between contractions during fatigue (Fig. 3.2A, B). At 2.4 mM Ca^{2+}, wild type FDB generated on average 1% of unstimulated force at 60 s and lowering $[Ca^{2+}]_e$ to 0.6 mM slightly reduced unstimulated force (Fig. 3.4A). At 2.4 mM Ca^{2+} (control), unstimulated force of Kir6.2$^{-/-}$ FDB reached a mean value of 26% of pre-fatigue peak tetanic force by 30 s, and then decreased to 16% by 90 s (Fig. 3.4B). Lowering $[Ca^{2+}]_e$ to

FIGURE 3.2

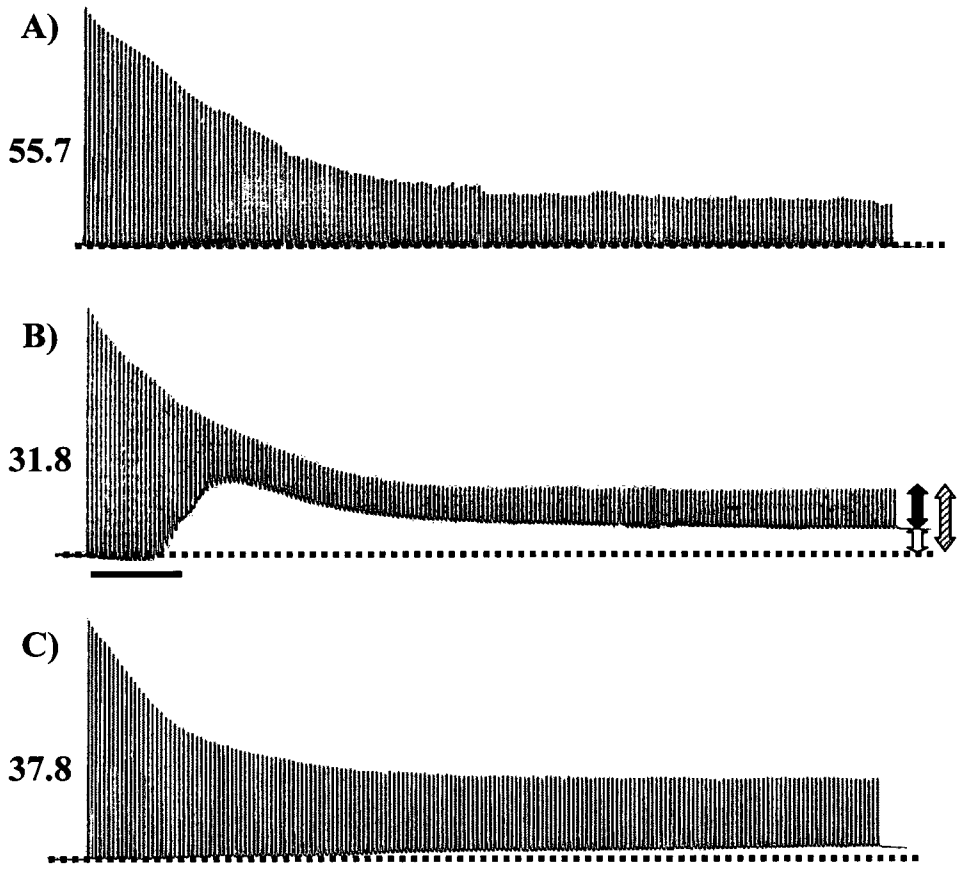

Figure 3.2. Representative traces for the changes in force during fatigue in A) normal wild type FDB, B) Kir6.2$^{-/-}$ FDB and C) Kir6.2$^{-/-}$ FDB exposed to 1 μM verapamil. Fatigue was elicited at 37°C with one tetanic contraction every s for 180 s. The heights of the first contraction were adjusted to be the same for all three traces to view the changes on a relative scale. Numbers on the left are the pre-fatigue peak tetanic force in N/cm^2. Symbols: dashed line represents the baseline; double white arrow, unstimulated force; double black arrow, peak tetanic force; double hatched arrow, peak total force. Horizontal line below trace B represents 20 s.

FIGURE 3.3

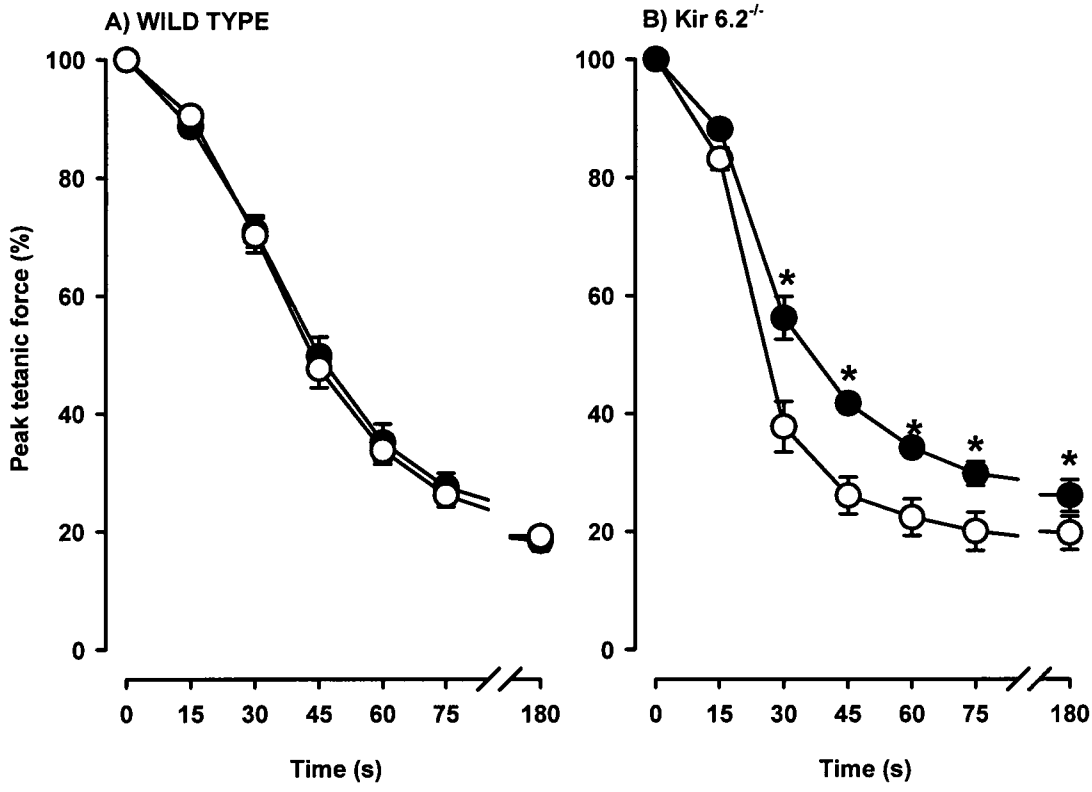

Figure 3.3. Lowering $[Ca^{2+}]_e$ to 0.6 mM reduced the rate at which peak tetanic force decreased during fatigue in Kir6.2$^{-/-}$ (B) but not in wild type FDB (A). Peak tetanic force was expressed as a percent of the pre-fatigue force. Symbols: ○, 2.4 mM Ca^{2+}; ●, 0.6 mM Ca^{2+}. Vertical bars represent the S.E. of 5 muscles.

* Mean value at 0.6 mM Ca^{2+} significantly different from mean value at 2.4 mM Ca^{2+}, ANOVA and L.S.D. $P < 0.05$.

FIGURE 3.4

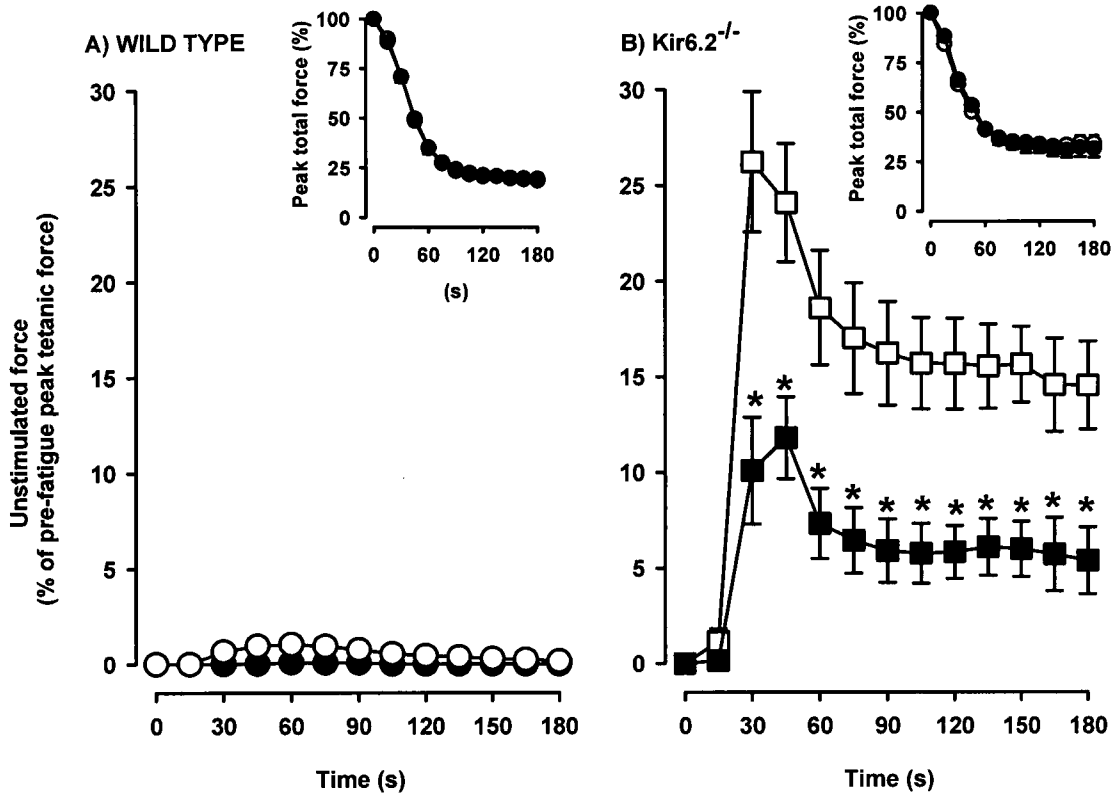

Figure 3.4. Less unstimulated force was generated at 0.6 mM Ca^{2+} than at 2.4 mM Ca^{2+} in wild type (A) and especially in Kir6.2$^{-/-}$ FDB (B). Unstimulated force was expressed as a percent of the pre-fatigue peak tetanic force. Inset: peak total force expressed as a percent of the pre-fatigue peak total force. Symbols: ○, □, 2.4 mM Ca^{2+}; ●, ■, 0.6 mM Ca^{2+}. Vertical bars represent the S.E. of 5 FDB.

* Mean value at 0.6 mM Ca^{2+} significantly different from mean value at 2.4 mM Ca^{2+}, ANOVA and L.S.D. $P < 0.05$.

0.6 mM significantly reduced unstimulated force by at least two-fold throughout the entire fatigue period in Kir6.2$^{-/-}$ FDB.

In wild type FDB, lowering $[Ca^{2+}]_e$ had no effect on the decreases in peak total force (inset of Fig. 3.4A); this result was not surprising because peak total force is the sum of the peak tetanic force and unstimulated force and neither of them was affected by $[Ca^{2+}]_e$. However, changes in $[Ca^{2+}]_e$ also failed to affect peak total force of Kir6.2$^{-/-}$ FDB (inset of Fig. 3.4B), which suggests that the decrease in unstimulated force at 0.6 mM Ca^{2+} occurred with an equivalent increase in peak tetanic force.

Peak tetanic force and unstimulated force recovery.

Following fatigue at 2.4 mM Ca^{2+}, wild type FDB recovered 91% of their pre-fatigue peak tetanic force by 15 min whereas Kir6.2$^{-/-}$ FDB only recovered 69% after 30 min (Fig. 3.5); these results are in agreement with a previous study (Cifelli *et al.*, 2007). The capacity of wild type FDB to recover peak tetanic force after fatigue was not affected by lowering $[Ca^{2+}]_e$ (Fig. 3.5A). In Kir6.2$^{-/-}$ FDB, peak tetanic force recovered significantly better at 0.6 mM Ca^{2+} reaching a maximum value of 98% by 25 min; i.e., force recovery at 0.6 mM Ca^{2+} was 29% better than at 2.4 mM (Fig. 3.5B). During the 30 min recovery, unstimulated force at 2.4 mM Ca^{2+} decreased from 15% to 6% while at 0.6 mM the unstimulated force completely disappeared (inset of Fig. 3.5B). The resulting peak total force from the sum of peak tetanic force and unstimulated force was 75% after 30 min of recovery at 2.4 mM in Kir6.2$^{-/-}$ FDB. This peak total force was still less than the peak force of wild type FDB at both Ca^{2+} levels and of Kir6.2$^{-/-}$ FDB at 0.6 mM Ca^{2+}.

FIGURE 3.5

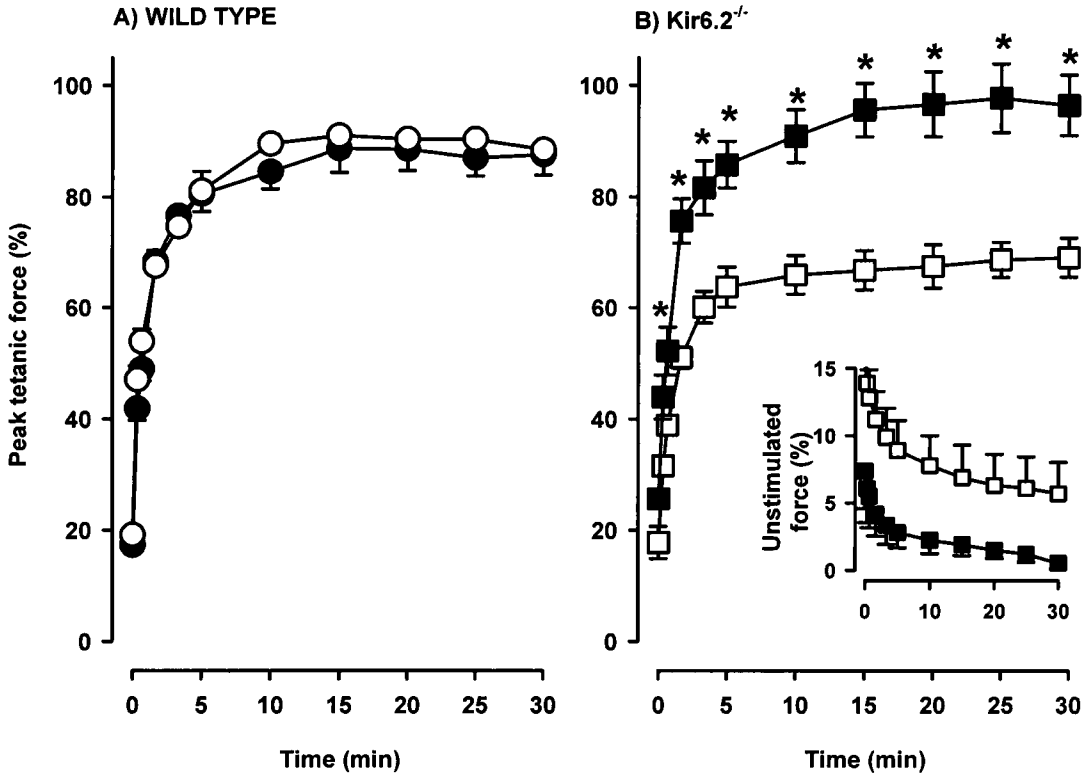

Figure 3.5. Peak tetanic force recovery after fatigue was improved at 0.6 mM Ca^{2+} in Kir6.2$^{-/-}$ FDB (B) but not in wild type FDB bundles (A). Peak tetanic force is expressed as a percent of the pre-fatigue tetanic force. Inset: recovery of unstimulated force in Kir6.2$^{-/-}$ FDB (not shown for wild type FDB as unstimulated force was zero at the end of fatigue). Symbols: ○, □, 2.4 mM Ca^{2+}; ●, ■, 0.6 mM Ca^{2+}. Vertical bars represent the S.E. of 5 FDB.

* Mean value at 0.6 mM Ca^{2+} significantly different from mean value at 2.4 mM Ca^{2+}, ANOVA and L.S.D. $P < 0.05$.

Effect of increasing $[Ca^{2+}]_e$.

We also tested whether an increase in $[Ca^{2+}]_e$ worsened the contractile dysfunctions in Kir6.2$^{-/-}$ FDB. In Kir6.2$^{-/-}$ FDB bundles, increasing $[Ca^{2+}]_e$ from 2.4 mM to 4.8 mM had no effect on unstimulated force during fatigue, force recovery following fatigue and rate of fatigue (data not shown). Considering the lack of effect in Kir6.2$^{-/-}$ FDB, wild type FDB were not tested at 4.8 mM Ca^{2+}.

EFFECTS OF BLOCKING L-TYPE Ca^{2+} CHANNELS

Next, we tested the effects of verapamil, a known Ca^{2+} channel blocker (Gallant & Goettl, 1985), to determine if the fatigue rate, unstimulated force and force recovery are altered by Ca^{2+} influx through L-type Ca^{2+} channels in K_{ATP} channel deficient FDB.

Dose-response curve of verapamil in unfatigued FDB.

Addition of 1 μM verapamil had little effect in one unfatigued wild type and Kir6.2$^{-/-}$ FDB, while peak tetanic force decreased and fade increased at 5 μM verapamil (Fig. 3.6A, B). These effects of 5 μM verapamil were also greater in Kir6.2$^{-/-}$ than in wild type FDB. At 50 μM verapamil, the contraction resembled a twitch contraction in both wild type and Kir6.2$^{-/-}$ FDB. On average, the decreases in peak tetanic force between 1 and 10 μM verapamil were significantly greater in Kir6.2$^{-/-}$ than in wild type FDB, with the largest difference being 19% at 5 μM verapamil (Fig. 3.6C). However, as concentrations exceeded 50 μM, the relative decreases became less in Kir6.2$^{-/-}$ FDB. Fade became significantly different at 5 μM verapamil and was greater in Kir6.2$^{-/-}$ FDB, where the force at 200 ms was only 48% of the peak tetanic force compared to 80% for wild type FDB (Fig. 3.6D). At concentrations greater than 10 μM, fade was very large (>80%) and did not differ between wild type and Kir6.2$^{-/-}$ FDB.

FIGURE 3.6

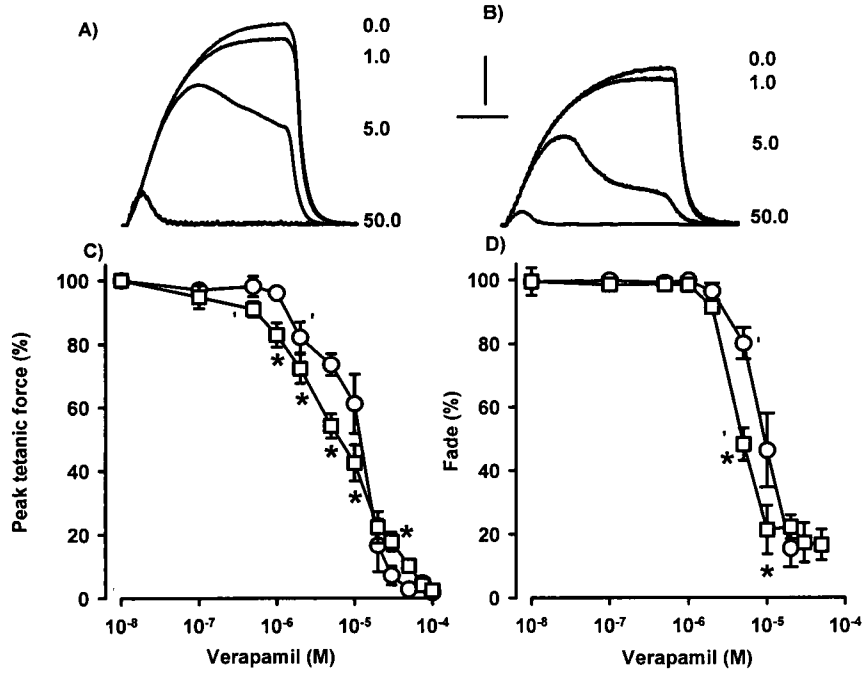

Figure 3.6. Unfatigued Kir6.2$^{-/-}$ FDB are more sensitive to verapamil than wild type FDB. Representative traces of tetanic contractions from A) wild type and B) Kir6.2$^{-/-}$ FDB. All traces were obtained after 30 min exposure to verapamil at the concentration in μM indicated by the numbers beside the force traces. Vertical bar: 10 N/cm^2; horizontal bars: 50 ms. C) Dose-response curve for peak tetanic force expressed as a percent of the force in the absence of verapamil. D) Dose-response curve for fade, being the force at 200 ms expressed as a percent of peak tetanic force during the same contraction. Symbols: ○, wild type; □, Kir6.2$^{-/-}$; vertical bars represent the S.E. of 6 muscles.

' Indicates the verapamil concentration at which peak tetanic force or fade became significantly different from control (no verapamil).

* Significantly different from wild type FDB, ANOVA and L.S.D. $P < 0.05$.

We further tested how acutely blocking KATP channels in wild type FDB affected the verapamil sensitivity. In the presence of 5 μM verapamil, the decreases in peak tetanic force were 18 ± 5% (n=5) in control wild type FDB compared to 17 ± 5% (n=5) in the presence of 10 μM glibenclamide. Fade was also not significantly different between the two groups of FDB, being 87 ± 7% and 93 ± 3% for control and glibenclamide-exposed muscles, respectively. Thus, an increase in verapamil sensitivity was observed only when KATP channel activity was chronically abolished.

Verapamil effects during fatigue and recovery

For these experiments, three experimental groups were used: 1) wild FDB as control, 2) wild type FDB exposed to 10 μM glibenclamide to test the effect of acutely blocking KATP channels and 3) Kir6.2$^{-/-}$ FDB which represented a chronic loss of KATP channel activity. For each group, muscles were divided in i) no verapamil and ii) verapamil-exposed muscles. Considering that KATP channel activity is largely controlled by the energy state of the muscle, it was important that during fatigue the verapamil be at a concentration causing little or no decrease in peak tetanic force prior to fatigue. We therefore exposed FDB to 1 μM verapamil during fatigue.

Verapamil had no effect on the decrease in peak tetanic force in wild type FDB (Fig. 3.7A). In glibenclamide-exposed wild type FDB, verapamil caused a faster decrease in peak tetanic force during the first 15 sec (Fig. 3.7B). Thereafter, the peak tetanic forces were not different between non-verapamil and verapamil-exposed FDB. Verapamil significantly slowed down the initial decrease in peak tetanic force in Kir6.2$^{-/-}$ FDB (Fig. 3.7C). However, verapamil did not significantly reduce the final extent of fatigue, as peak

FIGURE 3.7

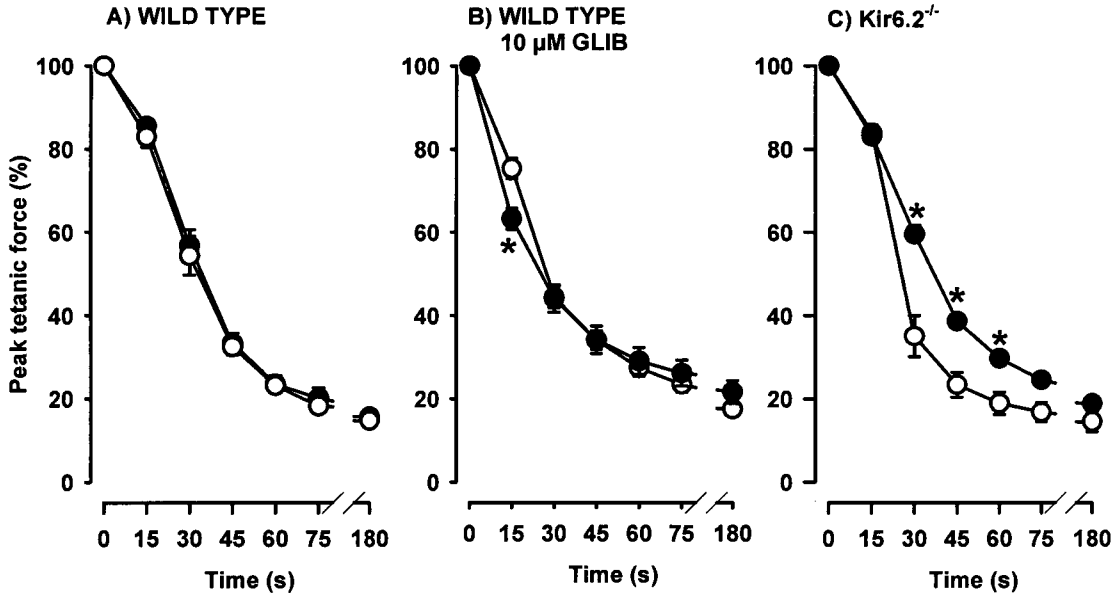

Figure 3.7. Verapamil (1 µM) significantly reduced the rate at which peak tetanic force decreased during fatigue only in Kir6.2$^{-/-}$ FDB. Peak tetanic force was expressed as a percent of the pre-fatigue forces. A) wild type FDB; B) wild type FDB exposed to 10 µM glibenclamide; C) Kir6.2$^{-/-}$ FDB. Symbols: ○, no verapamil; ●, 1 µM verapamil. Vertical bars represent the S.E. of 5 FDB bundles.

* Significantly different from no verapamil, ANOVA and L.S.D. $P < 0.05$

tetanic force of control and verapamil-exposed muscles at 180 s were 14% and 19% respectively. In wild type FDB, verapamil had no effect on unstimulated force (Fig. 3.8A). In glibenclamide-exposed wild type FDB, verapamil largely reduced unstimulated force (Fig. 3.8B) while in Kir6.2$^{-/-}$ FDB it almost abolished the increase in unstimulated force (Fig. 3.2C, 3.8C).

While verapamil had no effect on the decrease in peak total force in wild type FDB, it increased the rate at which peak total force decreased during fatigue in Kir6.2$^{-/-}$ and glibenclamide-exposed wild type FDB (Fig. 3.9). The verapamil effects were significant during the first 30 sec of the fatigue period for glibenclamide-exposed wild type FDB, while in Kir6.2$^{-/-}$ FDB the effects was observed after 45 sec until the end of the fatigue period. At 180 s, the final extent of the decrease was 8% less in the presence than in the absence of verapamil. Thus, unlike the effects of lowered $[Ca^{2+}]_e$, verapamil reduced unstimulated force to a greater extent that it allowed an increased in peak tetanic force.

Verapamil also improved peak tetanic force recovery in Kir6.2$^{-/-}$ and glibenclamide-exposed wild type FDB but not in wild type FDB (Fig. 3.10). In glibenclamide-exposed wild type FDB, the verapamil effects were significant during the first 10 min of recovery while they were not for the final extent of force recovery. In Kir6.2$^{-/-}$ FDB, the peak tetanic force recovery was improved by 10 to 14% in the presence of verapamil. After 30 min of recovery in the absence of verapamil, unstimulated force in K_{ATP} channel deficient FDB had not fully returned to zero especially for Kir6.2$^{-/-}$ FDB (insets of Fig. 3.10B, C). In the presence of verapamil, unstimulated force returned to zero within 10 min for both Kir6.2$^{-/-}$ and glibenclamide-exposed FDB.

FIGURE 3.8

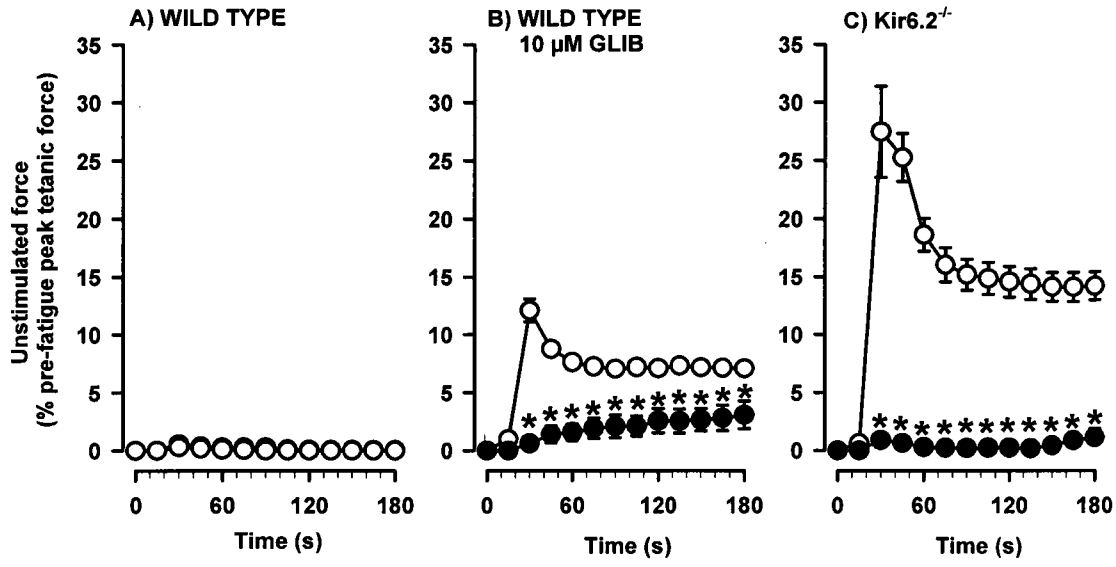

Figure 3.8. Verapamil significantly reduced unstimulated force in KATP channel deficient FDB during fatigue. A) wild type FDB; B) wild type FDB exposed to 10 µM glibenclamide; C) Kir6.2$^{-/-}$ FDB. Symbols: ○, no verapamil; ●, 1 µM verapamil. Vertical bars represent the S.E. of 5 FDB.

* Significantly different from no verapamil, ANOVA and L.S.D. $P < 0.05$.

FIGURE 3.9

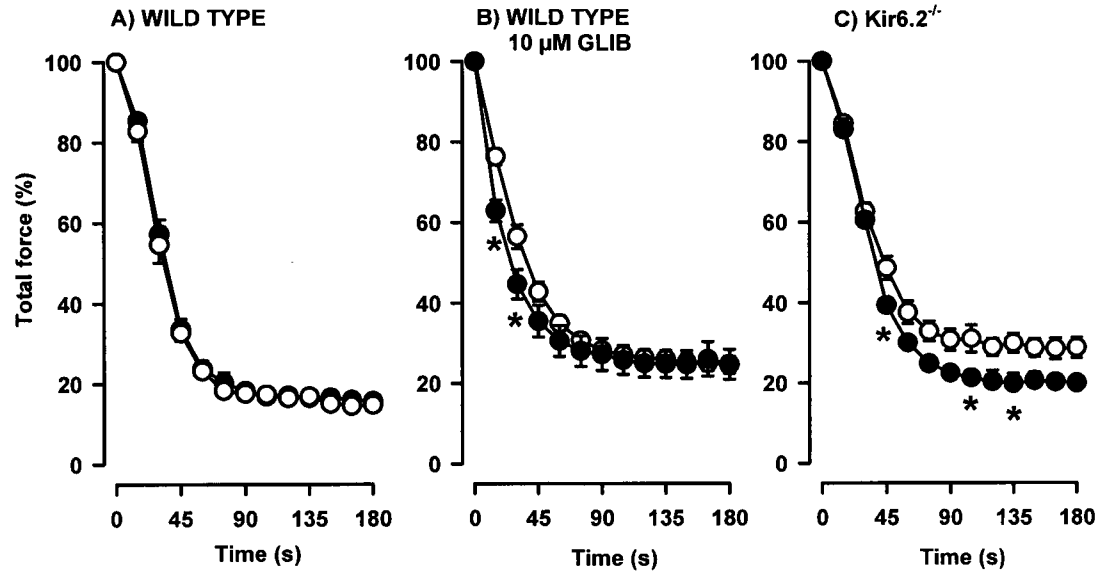

Figure 3.9. Verapamil significantly increased the rate at which peak total force decreased during fatigue in KATP channel deficient FDB during fatigue. A) wild type FDB; B) wild type FDB exposed to 10 µM glibenclamide; C) Kir6.2$^{-/-}$ FDB. Symbols: ○, no verapamil; ●, 1 µM verapamil. Vertical bars represent the S.E. of 5 FDB.

* Significantly different from no verapamil, ANOVA and L.S.D. $P < 0.05$.

FIGURE 3.10

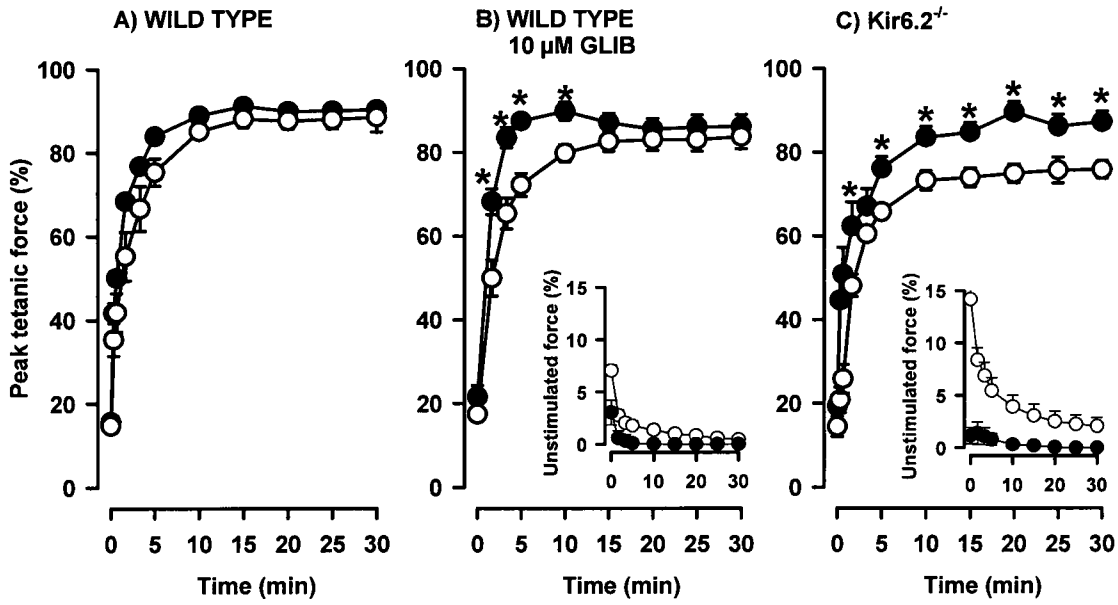

Figure 3.10. Verapamil improved the recovery of peak tetanic force in K_{ATP} channel deficient FDB. A) wild type FDB; B) wild type FDB exposed to 10 µM glibenclamide; C) Kir6.2$^{-/-}$ FDB. Inset: recovery of unstimulated force (not shown for wild type FDB because it was already at zero by the end of fatigue). Symbols: ○, no verapamil; ●, 1 µM verapamil. Vertical bars represent the S.E. of 5 FDB.

* Significantly different from control values (i.e., no verapamil), ANOVA and L.S.D. $P < 0.05$.

EFFECT OF GLIBENCLAMIDE AND VERAPAMIL ON RESTING Em

In normal wild type FDB single fibres, resting Em was -83 mV prior to fatigue (Fig. 3.11). During the first 60 sec of fatigue, the resting Em depolarized to -67 mV. Thereafter, it depolarized another 10 mV, being -57 mV at 180 sec. As reported by Cifelli et al. (2007), some but not all fibres supercontracted during fatigue in the presence of 10 μM glibenclamide. For the fibres that did not supercontract, the changes in resting Em were similar to what was observed with control fibres, except for the first 20 sec when the depolarization was significantly greater in the presence of glibenclamide. For the fibres that supercontracted, resting Em depolarized to a much greater extent from -80 mV to -31 mV in 80 sec (after which measurements were no longer possible because of the supercontraction). In the presence of 10 μM glibenclamide and 1 μM verapamil, fibres could be divided into two groups. One group had small depolarizations that were significantly greater than those of normal FDB. The other group had very large depolarizations from -80 mV to -36 mV in 80 sec. At that time, these fibres stopped contracting upon stimulation and did not supercontract. At 180 sec, these fibres had a resting Em of -26 mV.

FIGURE 3.11

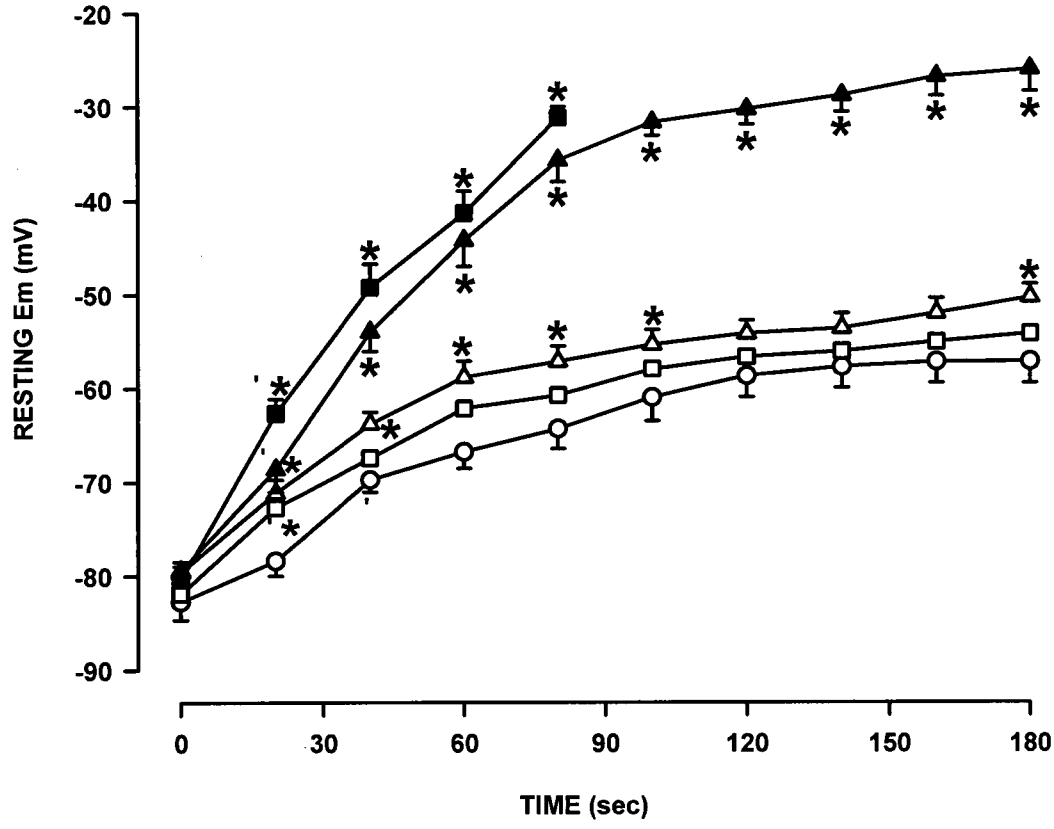

Figure 3.11. Glibenclamide caused large membrane depolarization in some but not all wild type FDB fibres during fatigue. Resting Em in the presence of glibenclamide were divided into two groups. Symbols: ○: control (no drugs); □, 10 μM glibenclamide and fibres that did not supercontract; ■, 10 μM glibenclamide in fibres that supercontracted; △, 10 μM glibenclamide and 1 μM verapamil in fibres with small membrane depolarization; ▲, 10 μM glibenclamide and 1 μM verapamil and fibres with large membrane depolarization. Vertical bars are the S.E. of 8-10 fibres

' Indicates when resting Em became significantly different from Time 0 sec.

* Significantly different from control, ANOVA and L.S.D. $P < 0.05$.

DISCUSSION

The major findings of this study were: reducing $[Ca^{2+}]_e$ from 2.4 to 0.6 mM i) shifted the peak tetanic force-stimulus strength relationship of unfatigued Kir6.2$^{-/-}$ FDB to higher voltages; ii) reduced unstimulated force by 50% during fatigue; and iii) improved force recovery. iv) The verapamil dose-response curves for peak tetanic force and fade were shifted toward lower concentrations in unfatigued Kir6.2$^{-/-}$ FDB, but not in glibenclamide-exposed wild type FDB; v) verapamil dramatically reduced unstimulated force; and vi) improved force recovery in Kir6.2$^{-/-}$ and glibenclamide-exposed wild type FDB. Finally, in Kir6.2$^{-/-}$ FDB, the rate of fatigue was significantly slower at 0.6 mM Ca^{2+} or 1 μM verapamil than in control conditions (2.4 mM Ca^{2+} and no verapamil).

THE IMPORTANCE OF K_{ATP} CHANNEL IN PREVENTING EXCESSIVE Ca^{2+} INFLUX THROUGH L-TYPE Ca^{2+} CHANNELS

As discussed in the Introduction, K_{ATP} channels are critical during metabolic stress and fatigue in preventing development of contractile dysfunctions in skeletal muscles (Light *et al.*, 1994; Comtois *et al.*, 1995; Gramolini & Renaud, 1997; Gong *et al.*, 2000; Matar *et al.*, 2000; Gong *et al.*, 2003; Thabet *et al.*, 2005; Cifelli *et al.*, 2007). One objective of this study was to determine if two contractile dysfunctions, unstimulated force and reduced force recovery, are due to excessive membrane depolarization and Ca^{2+} influx through L-type Ca^{2+} channels.

Unfatigued muscle

In wild type FDB, lowering $[Ca^{2+}]_e$ had no effect on the maximal peak tetanic force and peak tetanic force-stimulus strength, which is in agreement with previous studies (Dulhunty & Gage, 1988; Cairns *et al.*, 1998). The depression of peak tetanic

force and increased fade in the presence of verapamil was also similar to the effects reported in mouse EDL and soleus (Gallant & Goettl, 1985). In Kir6.2$^{-/-}$ FDB, lowering $[Ca^{2+}]_e$ had no effect on maximal peak tetanic force, but, contrary to the lack of effect in wild type FDB, it significantly shifted the force- stimulus strength toward higher voltages. Furthermore, 0.5 to 10 μM verapamil increased fade and reduced peak tetanic force to a greater extent in Kir6.2$^{-/-}$ than in wild type FDB.

It is well established that in skeletal muscle the initial trigger for Ca^{2+} release does not require a Ca^{2+} influx (Miledi *et al.*, 1977; McCleskey, 1985) because the L-type Ca^{2+} channels physically interact with the sarcoplasmic reticulum Ca^{2+} release channels (Tanabe *et al.*, 1990a). There is evidence, however, that reducing the Ca^{2+} influx through L-type Ca^{2+} channels reduces the generation of force during a prolonged depolarization and maintenance of the plateau during tetanic contractions (Miledi *et al.*, 1977; Gallant & Goettl, 1985; Ildefonse *et al.*, 1985; Lamb, 1986; Oz & Frank, 1991). The reduced force is because of either a decreased t-tubular contribution to the rise in $[Ca^{2+}]_i$ (Ildefonse *et al.*, 1985) or more likely to increases in L-type Ca^{2+} channel inactivation (Brum *et al.*, 1988; Garcia *et al.*, 1989; Rios & Pizarro, 1991). Regardless of the mechanism, the increased sensitivity to $[Ca^{2+}]_e$ and verapamil of unfatigued Kir6.2$^{-/-}$ FDB suggest that they have a greater dependency on Ca^{2+} influx through L-type Ca^{2+} channels to generate and especially maintain tetanic force compared to wild type FDB.

K_{ATP} channels are inactive in unfatigued muscles tested *in vitro* at 25°C (Allard *et al.*, 1995; Barrett-Jolley & McPherson, 1998). The channels have been found active at 37°C in resting skeletal muscle *in situ* (Lindinger *et al.*, 2001; Nielsen *et al.*, 2003) possibly because of an activation by exogenous factors, such as insulin (Tricarico *et al.*,

1999a). So far, there is no evidence that the channels are active in resting muscles kept at 37°C *in vitro*. For example, under similar stimulation conditions to this study, the resting membrane potential and the membrane depolarization during a 200 Hz train of action potentials were the same between unfatigued wild type and Kir6.2$^{-/-}$ EDL and soleus (Gong *et al.*, 2003). The fact that an increased verapamil sensitivity was not observed when KATP channels of wild type FDB were acutely blocked with glibenclamide further supports the notion that the channels are inactive *in vitro* at 37°C. It also suggests that the increased Ca^{2+} and verapamil sensitivity of Kir6.2$^{-/-}$ FDB is due to a chronic loss of KATP channel activity as opposed to an acute loss.

This chronic effect may be related to the fact that the disruption of a gene for knockout experiments often alters the expression of several other genes altering either the function of the protein they encode for or the function of other proteins (Porter *et al.*, 2004). Finally, although we cannot fully explain how a chronic lack of KATP channel affects the L-type Ca^{2+} channels, it is interesting to point out that patients suffering of hypokalemic period paralysis (HOPP) due to the R528H mutation in the α-subunit of L-type Ca^{2+} channels also have impaired KATP channel activity (Tricarico *et al.*, 1999a; Tricarico *et al.*, 1999b). It would appear that an interaction exists between these two channels where a chronic modification of one channel eventually affects the characteristics of the other.

Fatigued muscle

The most striking effects of lowering $[Ca^{2+}]_e$ or adding verapamil were observed during fatigue. Cifelli et al. (2007) reported a large development of unstimulated force during fatigue in small KATP channel deficient FDB bundles, reaching on average 25% of

the pre-fatigue peak tetanic force. They also showed that the unstimulated force corresponded well with large increases in unstimulated $[Ca^{2+}]_i$. This study now shows that lowering $[Ca^{2+}]_e$ from 2.4 to 0.6 mM reduced unstimulated force by ~50% while 1 μM verapamil almost abolished it. More importantly, the verapamil effects on unstimulated force were observed whether the loss of K_{ATP} channel activity was acute (glibenclamide-exposed wild type FDB) or chronic ($Kir6.2^{-/-}$ FDB). Finally, while some unstimulated force was still present after 30 min of recovery in control $Kir6.2^{-/-}$ FDB, it had completely disappeared at 0.6 mM Ca^{2+} or 1 μM verapamil. We therefore suggests that the K_{ATP} channels are crucial to maintain resting Em and in their absence excessive membrane depolarization occurs during fatigue causing an activation of L-type Ca^{2+} channels and an excessive Ca^{2+} influx that is responsible for the excessive unstimulated $[Ca^{2+}]_i$ and force.

Cifelli et al. (2007) showed that the unstimulated force during fatigue was associated with an excessive increase in unstimulated $[Ca^{2+}]_i$. It is unlikely that the $Ca^{2+}{}_e$ and verapamil effects in K_{ATP} channel deficient FDB were due to a lower energy demand, allowing better control of unstimulated $[Ca^{2+}]_i$ by the Ca^{2+} ATPase pump, because the pre-fatigue peak tetanic force was the same at 0.6 and 2.4 mM $Ca^{2+}{}_e$ while 1 μM verapamil caused no fade and only small decreases in peak tetanic force. Blocking K_{ATP} channels with glibenclamide resulted in excessive membrane depolarization in some but not all wild type FDB single fibres. Greater membrane depolarizations during metabolic stress have also been reported in K_{ATP} channel deficient muscles compared to wild type cardiac and skeletal muscles (Gramolini & Renaud, 1997; Baczko *et al.*, 2004). Furthermore, the presence of two fibre groups based on small and large membrane

depolarizations is consistent with the fact that some but not all KATP channel deficient FDB fibres had excessive unstimulated $[Ca^{2+}]i$. It is very likely that fibres with large membrane depolarization are the same as those with excessive unstimulated $[Ca^{2+}]i$ because all these fibres supercontract during fatigue (this study, Cifelli et al. 2007).

The excessive increase in unstimulated $[Ca^{2+}]i$ occurs during the first 60 sec (Cifelli et al., 2007). At that time, the resting Em of fibres with large depolarization was less than -50 mV before reaching -31 mV at 80 sec. Although, the threshold for Ca^{2+} current through L-type Ca^{2+} channels is about -30 mV in mouse EDL and soleus (Lamb & Walsh, 1987; Tanabe *et al.*, 1990b), one must remember that our measurements of resting Em were from the outer surface membrane, not the t-tubular membrane, which most likely depolarizes to an even greater extent. We therefore suggests that the lack of KATP channel activity during fatigue results, in some fibres, in excessive membrane depolarization which then activates L-type Ca^{2+} channels and the resulting Ca^{2+} influx is responsible for the excessive unstimulated $[Ca^{2+}]i$ and force.

In control conditions, the capacity of Kir6.$2^{-/-}$ FDB to recover peak tetanic force after fatigue was significantly lower than that of wild type FDB; even peak total force was less in Kir6.$2^{-/-}$ than in wild type FDB after 30 min of recovery. Lowered $[Ca^{2+}]e$ and verapamil also improved peak tetanic force recovery in KATP channel deficient FDB to levels even slightly higher than those observed in control wild type FDB. The mechanism for the poorer force recovery in Kir6.$2^{-/-}$ FDB is still not understood. Cifelli et al. (2007) had suggested that it is most likely due to fibre damage because: 1) fibre damage has been reported in KATP channel deficient skeletal muscle during treadmill running (Thabet *et al.*, 2005), and 2) because elevated $[Ca^{2+}]i$ is a known cause of fibre damage (Jackson

et al., 1984). The fact that reducing Ca^{2+} influx improved force recovery further supports our hypothesis of greater Ca^{2+} influx in KATP channel deficient muscle fibres during fatigue.

KATP CHANNEL AND THE RATE OF FATIGUE

Studies, using channel openers, have shown that opening KATP channels increase the rate of fatigue by first reducing action potential amplitude, which then lowers Ca^{2+} release and force (Matar *et al.*, 2000; Gong *et al.*, 2003). Abolishing KATP channel activity, using pharmacological and genetic approaches, does not result in a slower decrease in force as expected (Weselcouch *et al.*, 1993; Light *et al.*, 1994; Gong *et al.*, 2000; Matar *et al.*, 2000; Gong *et al.*, 2003; Cifelli *et al.*, 2007). Our second objective was to test the hypothesis (first proposed by Cifelli *et al.*, 2007) that reducing the extent of the contractile dysfunctions reduces the fatigue rate. Indeed, reducing the extent of two contractile dysfunctions by lowering $[Ca^{2+}]_e$ or using verapamil was associated with a slower fatigue rate in Kir6.2$^{-/-}$ FDB even when the pre-fatigue force was similar to that of control. More importantly, when unstimulated force was completely abolished with verapamil in Kir6.2$^{-/-}$ FDB, the fatigue rate became slower than in control wild type FDB (Fig. 3.12). This study therefore provides the first evidence that KATP channels contribute to the decrease in force during fatigue.

It may be argued that the contribution to the decrease in force is negligible because the differences in peak tetanic force between control wild type and verapamil-exposed Kir6.2$^{-/-}$ FDB are quite small. However, while the membrane depolarization in some glibenclamide-exposed fibres was similar to that of normal FDB, the depolarization was excessive in other fibres, reaching an average value of -31 mV by 80 sec. Such

depolarization is large enough to inactivate Na^+ channels rendering the cell membrane completely unexcitable (Ruff, 1999). This excessive depolarization is by itself another contractile dysfunction not unaccounted for in Figure 3.12. It will therefore be interesting to determine in future studies how slower will the rate of fatigue be when this excessive depolarization is prevented in K_{ATP} channel deficient fibres.

In conclusion, this study demonstrated that the K_{ATP} channel is crucial in preventing excessive membrane depolarization and Ca^{2+} influx through L-type Ca^{2+} channels, the latter being responsible for two contractile dysfunctions, unstimulated force and lower force recovery. We also show that abolishing the increase in unstimulated force with verapamil reduces the fatigue rate such that it becomes slower than that of normal wild type FDB. The latter finding support the conclusions of Cifelli et al. (2007) that K_{ATP} channels contribute to the decrease in force during fatigue, and that a slower fatigue rate is not observed in K_{ATP} channel deficient fibres because the depression of force by contractile dysfunctions prevails over the expected slower fatigue rate.

FIGURE 3.12

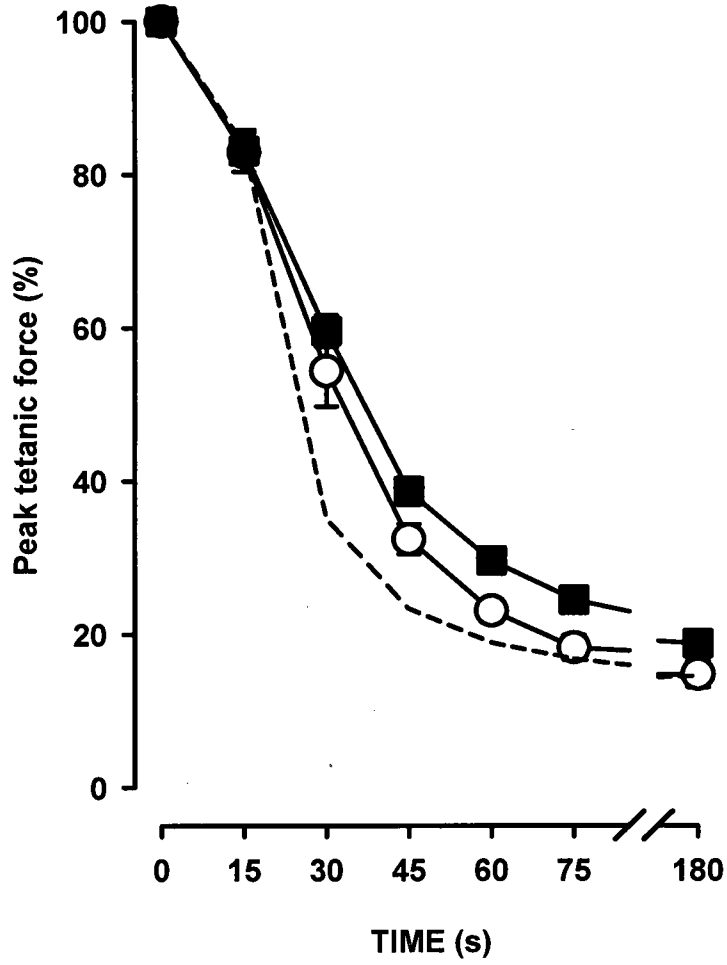

Figure 3.12. Rates of fatigue in verapamil-exposed Kir6.2$^{-/-}$ FDB are slower than in control wild type FDB. Peak tetanic forces were expressed as a percent of the pre-fatigue force. Symbols: ○, control wild type; ■, Kir6.2$^{-/-}$ exposed to 1 μM verapamil; ---, control Kir6.2$^{-/-}$.

CHAPTER 4

CONTRACTILE DYSFUNCTIONS IN sKATP CHANNEL DEFICIENT MUSCLE DURING FATIGUE INVOLVE REACTIVE OXYGEN SPECIES

By

Louise Boudreault, Jean-Philippe Bercier and Jean-Marc Renaud

University of Ottawa, Department of Cellular and Molecular Medicine, 451 Smyth Rd., Ottawa, Ontario, Canada, K1H 8M5

AUTHORS' CONTRIBUTIONS

- Boudreault: completed the experiments of Fig. 4.1-4.4, writing of manuscript
- Bercier: started experiments of Fig. 4.1-4.4 (2 samples)

ABSTRACT

Sarcolemmal ATP-sensitive K^+ (sKATP) channels are essential in preventing the development of contractile dysfunctions during fatigue by preventing excessive membrane depolarization and Ca^{2+} influx through L-type Ca^{2+} channels. Since large increases in $[Ca^{2+}]i$ can lead to deleterious ROS production, the objective of this study was to determine if the application of an ROS scavenger would reduce the extent of the contractile dysfunctions in sKATP channel deficient muscle. FDB muscles from wild type and sKATP channel deficient Kir6.2$^{-/-}$ mice were exposed to the ROS scavengers N-acetyl-cysteine (NAC) (10 mM) or tiron (10 mM). Fatigue was elicited with one contraction per s for 3 min at 37°C. In wild type FDB, NAC or tiron did not affect the decrease in peak tetanic force and unstimulated force during fatigue and force recovery following fatigue. In Kir6.2$^{-/-}$ FDB, NAC and tiron slowed down the decrease in peak tetanic force recovery, reduced unstimulated force and improved the rate of force recovery. Compared to control, Kir6.2$^{-/-}$ FDB developed 30 – 60% less unstimulated force with the presence of NAC and tiron, with greater effects from NAC. It is concluded that ROS play a role in the development of the contractile dysfunctions in sKATP channel deficient muscle, and application of ROS scavengers improved force generation and reduced unstimulated force during fatigue and increased rate of force recovery.

INTRODUCTION

The sKATP channel derives it name from the fact that binding of ATP on the cytosolic side results in channel closure (Noma, 1983). The channel activity is regulated by the energy state of the cell, whereby in cases of an energy deficit and intracellular ATP decreases while intracellular ADP and H^+ and extracellular adenosine rise, the channel activates (Noma, 1983; Vivaudou *et al.*, 1991; Davies *et al.*, 1992; Barrett-Jolley *et al.*, 1996). Thus, it links the energy status of the cell to membrane excitability.

sKATP channels are essential in preventing the development of contractile dysfunctions, defined by Cifelli *et al.* (2007) as events, from the generation of action potentials to the actin-myosin interaction, that are depressed in a manner not associated with the normal process of fatigue, and will eventually incapacitate muscle from generating force (Cifelli *et al.*, 2007). In the absence of sKATP channel activity, FDB muscle fibres and bundles can develop several contractile dysfunctions including large membrane depolarization, large increases in unstimulated intracellular Ca^{2+} concentration ($[Ca^{2+}]i$) and force, faster decreases in peak tetanic $[Ca^{2+}]i$ and force, and a reduced capacity to recover force (Light *et al.*, 1994; Thabet *et al.*, 2005; Cifelli *et al.*, 2007; Cifelli *et al.*, 2008). In both cardiac and skeletal muscle, the excessive membrane depolarization is large enough to cause excessive Ca^{2+} influx through L-type Ca^{2+} channels between contractions, and that blocking the Ca^{2+} influx with verapamil abolished the development of these dysfunctions (Zingman *et al.*, 2002; Baczko *et al.*, 2004; Baczko *et al.*, 2005; Cifelli *et al.*, 2008).

With large increase in $[Ca^{2+}]i$, the activity of the mitochondrial Ca^{2+} uniporter can increase as the $[Ca^{2+}]i$, gradient between the cytosol and mitochondria is larger (Brookes

et al., 2004). Small increases in mitochondrial [Ca^{2+}] ([Ca^{2+}]$_{mito}$) are beneficial by stimulating ATP production, but large increases are deleterious as they can lead to uncoupling of the ATP production process, generating large amounts of ROS. In skeletal muscle fibres, excessive ROS production during repetitive stimulation was shown to contribute to the development of fatigue (Reid, 2001b; Smith & Reid, 2006; Bruton *et al.*, 2008; Murphy *et al.*, 2008). Superoxide, hydrogen peroxide (H_2O_2) and hydroxyl radicals (OH•), three principal ROS known to be produced in skeletal muscle, are believed to negatively alter many cellular processes, including ATP production (Jackson, 2009). In addition, superoxide or its converted form H_2O_2 can impair both SR Ca^{2+} release channels, thus reducing maximum tetanic Ca^{2+} release, and SR ATPase pump activity, reducing the rate of Ca^{2+} reuptake (Chin & Allen, 1996; Chin *et al.*, 1997; Reid, 2001a; Brookes *et al.*, 2004; Bruton *et al.*, 2008). Furthermore, H_2O_2 and its oxidized form OH• were recently shown to decrease the Ca^{2+} sensitivity of the contractile apparatus (Burton & Smith, 1997a; Murphy *et al.*, 2008), which could be partially reversed by the application of ROS scavengers tiron or N-acetylcystine (NAC), or the reducing agent dithiothreitol (Moopanar & Allen, 2005, 2006; Bruton *et al.*, 2008; Murphy *et al.*, 2008). Application of tempol, a selective superoxide scavenger, had no effect on Ca^{2+} sensitivity or release, suggesting that H_2O_2 or OH• are the main culprits and not superoxide (Murphy *et al.*, 2008). Given that in sKATP channel deficient mice there is a large increase in [Ca^{2+}]i during fatigue which could lead to increased [Ca^{2+}]$_{mito}$, combined with the increased metabolic rate from repetitive stimulation, it is possible that large amounts of ROS are being produced (Chance *et al.*, 1979; Hansford *et al.*, 1997). Therefore, application of a ROS scavenger should prevent the reduced Ca^{2+} sensitivity and impaired

Ca^{2+} handling, thus slowing the rate of fatigue in sKATP channel deficient muscle. At the same time, reduced unstimulated force during fatigue and improved force recovery should occur as the SR Ca^{2+} ATPase activity better regulates $[Ca^{2+}]i$.

To determine that elevated $[Ca^{2+}]i$ in sKATP channel deficient muscle is deleterious by increasing ROS production, we tested the hypothesis that application of two ROS scavengers, NAC and tiron, would reduce the extent of the contractile dysfunctions and thus improve the rate of fatigue and force recovery in sKATP channel deficient muscle.

METHODS AND MATERIALS

ANIMALS AND FDB MUSCLE BUNDLE PREPARATION

FDB muscles from CD-1 mice were used as wild type muscles. KATP channel deficient FDB muscles were obtained from Kir6.2$^{-/-}$ mice, which are null mice for sKATP channels (Miki *et al.*, 2002). All mice were two to three month old mice and weighed 20-25 g. They were fed *ad libitum*, and housed according to the guidelines of the Canadian Council for Animal Care (CCAC). The Animal Care Committee of the University of Ottawa approved all experimental procedures used in this study. Small muscle bundles were obtained from the FDB as described by Cifelli *et al.* (Cifelli *et al.*, 2007). Briefly, mice were anesthetized with a single intraperitoneal injection of 2.2 mg ketamine, 0.44 mg xylazine, and 0.22 mg acepromazine per 10 g of body mass. After excision of the FDB, the fibre bundle controlling the 4th digit was separated from the rest of the muscle. All mice were then euthanized with an overdose of anaesthetics.

SOLUTIONS

FDB bundles were constantly immersed in physiological saline solution. The control solution contained (in mM): 118.5 NaCl, 4.7 KCl, 2.4 $CaCl_2$, 3.1 $MgCl_2$, 25 $NaHCO_3$, 2 NaH_2PO_4, and 5.5 D-glucose. All solutions were continuously bubbled with 95% O_2-5% CO_2 and had a pH of 7.4. NAC (10 mM) and tiron (10 mM) were directly dissolved in the physiological solution without any vehicle. All experiments were carried out at 37°C.

FORCE MEASUREMENTS

Force measurements were carried out as described by Cifelli *et al.* (Cifelli *et al.*, 2007). Briefly, muscle length was adjusted to give maximum tetanic force. Force was

monitored with a Cambridge ergometer (model 300, USA) or a Gould Statham force transducer (Model UC2, USA), and digitized at 5 kHz by a Keithley Metrabyte A-D board (model DAS50, USA). From the force traces, two parameters were analysed: i) peak tetanic force, defined as the maximum force generated during a tetanic stimulation; and ii) unstimulated force, defined as the developed force between contractions when fibres failed to completely relax (Cifelli *et al.*, 2007; Cifelli *et al.*, 2008).

STIMULATION AND FATIGUE PROTOCOL

FDB bundles were allowed 30 min equilibrium in the absence or presence 10 mM tiron or 10 mM NAC. Tetanic contractions were elicited with 200 ms trains of supramaximal square waves (10 V) of 0.3 ms duration at 200 Hz. Pulses were generated with a Grass S88 stimulator and a Grass SIU5 isolation unit (Grass Instruments, USA). The stimulating platinum wires (4 mm apart) were positioned on opposite sides of the bundles. Contractions were elicited every 100 s in experiments involving unfatigued muscles and prior to fatigue. Fatigue was elicited by reducing the interval between contractions to one second for 180 s. After fatigue, muscles were stimulated every 100 s to measure force recovery.

STATISTICAL ANALYSIS

ANOVA was used to determine significant differences. Split plot designs were used because muscles were tested at all time levels. ANOVA calculations were made using the Version 9.0 GLM (General Linear Model) procedures of the Statistical Analysis Software (SAS Institute Inc., Cary, NC USA). When a main effect or an interaction was significant, the least square difference (L.S.D.) was used to locate the significant

differences (Steel & Torrie, 1980). The word "significant" refers only to a statistical difference ($P<0.05$).

RESULTS

FATIGUE KINETICS

We tested the effects of applying two ROS scavengers, NAC and tiron, during fatigue and recovery to determine if the development of the contractile dysfunctions (i.e. faster rate of fatigue, large unstimulated force during fatigue and depressed force recovery after fatigue) in sKATP channel deficient muscle is partially due to a greater ROS content.

Rate of fatigue

As per Cifelli *et al* (2007, 2008), rate of fatigue in Kir6.2$^{-/-}$ FDB muscle bundles cannot be determined from total force due to the large development in unstimulated force that developed when sKATP channel activity is abolished, a phenomenon that does not occur in wild type muscle (Fig. 4.1A and B). Therefore, rate of fatigue is based on the peak tetanic force that develops with electrical stimulation.

Neither NAC nor tiron had any effect on wild type FDB (Fig. 4.1A). In Kir6.2$^{-/-}$ FDB, the application of 10 mM tiron also had no effect on rate of fatigue, but NAC transiently reduced the rate of fatigue in both conditions at 30 s from 52% to 63% of pre-fatigue peak tetanic force, but after there was no difference (Fig. 4.2). The final force development at 180 s in Kir6.2$^{-/-}$ muscle was 20 – 25% pre-fatigue tetanic force in both the absence and presence of tiron. This final force was not different from the force produced by wild type muscle, consistent with Cifelli *et al* (2007, 2008).

FIGURE 4.1

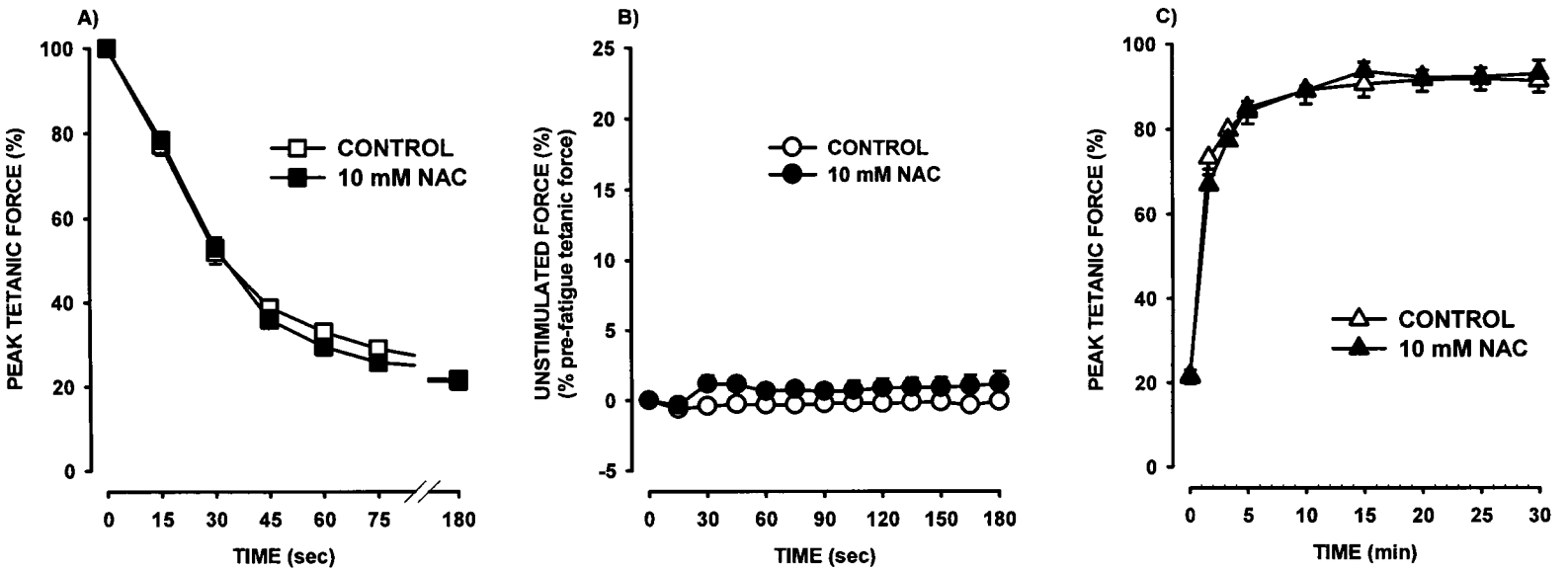

Figure 4.1. NAC had no effect on A) rate of fatigue, B) unstimulated force, or C) force recovery in wild type FDB. Fatigue was elicited with one 200 ms tetanic contraction every sec for 180 sec, and recovery every 5 min for 30 min. Peak tetanic force and unstimulated force is expressed as a percent of the pre-fatigue tetanic force. Vertical bars represent the S.E.M. of 5 FDB bundles.

FIGURE 4.2

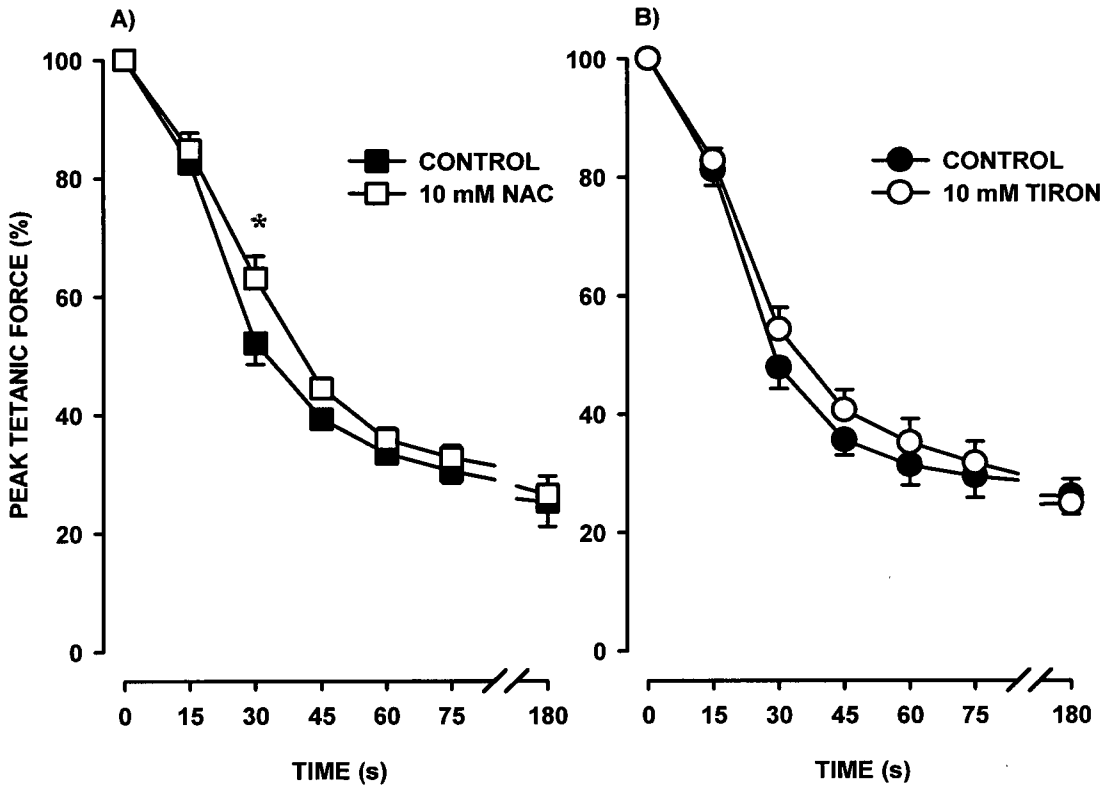

Figure 4.2. A) NAC reduced the rate of fatigue in Kir6.2$^{-/-}$ FDB bundles, while B) Tiron had no effect. Fatigue was elicited with one 200 ms tetanic contraction every sec for 3 min. Experimental temperature: 37°C. The rate of fatigue was determined from the decreases in peak tetanic force. Peak tetanic force is expressed as a percent of the pre-fatigue tetanic force. Vertical bars represent the S.E.M. of 5 FDB bundles.

* Tetanic force in the presence of NAC or Tiron was significantly different from control values, ANOVA and L.S.D. $P < 0.05$.

Unstimulated force and peak total force during fatigue.

Neither NAC nor tiron had any effect on unstimulated force in wild type FDB (Fig. 4.1B), which was not surprising since wild-type FDB develop < 1% unstimulated force (Fig. 4.1B) (Moopanar & Allen, 2005; Cifelli *et al.*, 2007; Cifelli *et al.*, 2008). However, Kir6.2$^{-/-}$ FDB generated a large amount of unstimulated force during fatigue, peaking at ~15% of pre-fatigue tetanic force at 30 s, and stabilizing from 90 – 180 s at ~8% (Fig. 4.3). This agrees with previous results published by our laboratory (Cifelli *et al.*, 2007; Cifelli *et al.*, 2008). NAC (Fig. 4.3A) prevented the large increases in unstimulated force during the fatigue bout, especially from 30 – 60 s. This effect was most prominent at 30 s, when unstimulated force was 13% lower with the presence of NAC. After 60 s, unstimulated force changed little, with the difference between the absence and presence of NAC being insignificant (~8% vs. 6% of pre-fatigue peak tetanic force, respectively). In the presence of Tiron, there was a trend of reduced unstimulated force from 30 – 60 s, however, it was not significant.

Recovery of peak tetanic force following fatigue.

The capacity of wild type FDB to recover peak tetanic force after fatigue was not affected by the presence of a ROS scavenger (Fig. 4.1C). Following fatigue, Kir6.2$^{-/-}$ FDB recovered less than 85% of their pre-fatigue peak tetanic force after 30 min (Fig. 4.4); this impaired recovery compared to wild type FDB was agreement with our previous studies (Cifelli *et al.*, 2007; Cifelli *et al.*, 2008). In bundles exposed to NAC, there was a much faster rate of force recovery for the first 20 min. In particular, within 100 s following the end of fatigue, Kir6.2$^{-/-}$ bundles exposed to NAC recovered 79% of their pre-fatigue tetanic force, compared to 66% of unexposed muscle. Until the 20 min

FIGURE 4.3

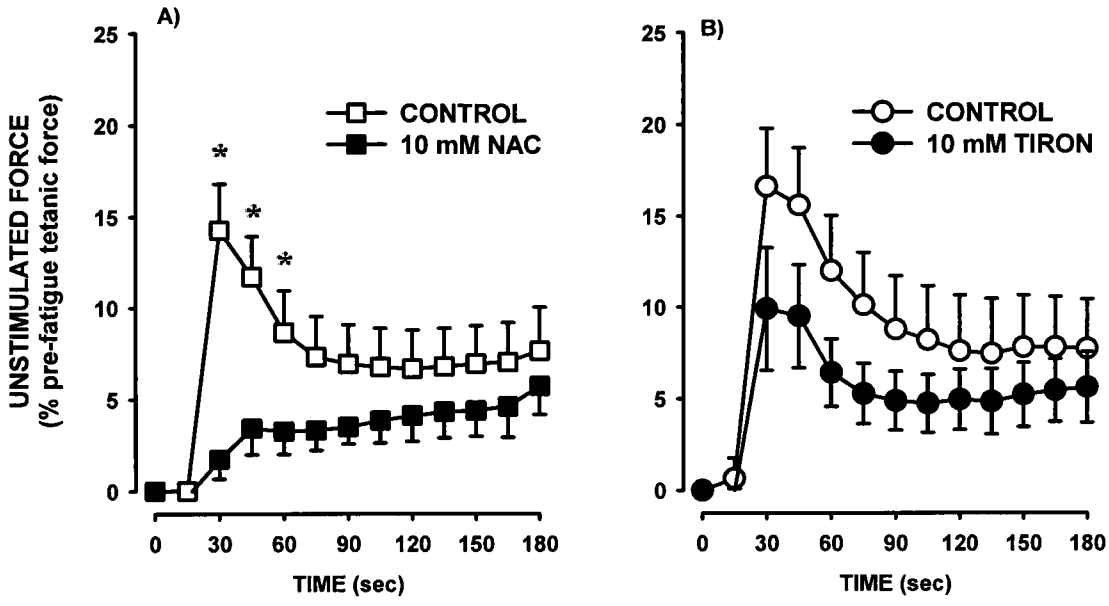

Figure 4.3. A) NAC significantly reduced unstimulated force during fatigue in Kir6.2$^{-/-}$ FDB muscle bundles, while B) Tiron had no effect. Fatigue was elicited with one 200 ms tetanic contraction every sec for 3 min. Experimental temperature: 37°C. Unstimulated force is expressed as a percent of the pre-fatigue tetanic force. Vertical bars represent the S.E.M. of 5 FDB bundles.

* Unstimulated force in the presence of NAC was significantly different from control values, ANOVA and L.S.D. $P < 0.05$.

FIGURE 4.4

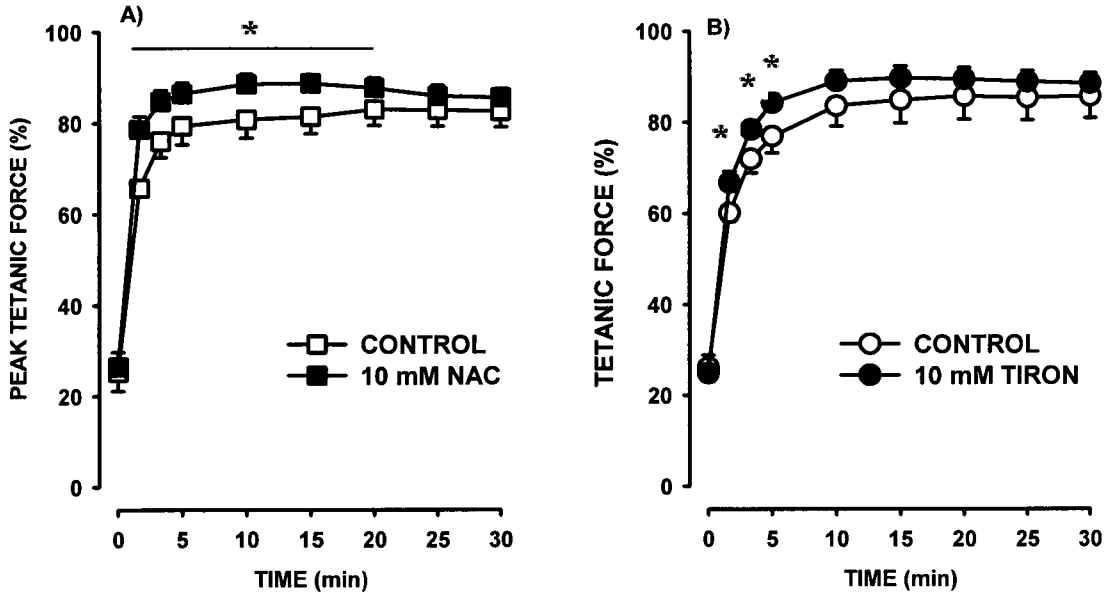

Figure 4.4. A) NAC and B) Tiron improved force recovery after fatigue in Kir6.2$^{-/-}$ FDB muscle bundles. Recovery was elicited with one 200 ms tetanic contraction every every 5 min for 30 min. Experimental temperature: 37°C. Peak tetanic force is expressed as a percent of the pre-fatigue force. Vertical bars represent the S.E.M. of 5 FDB bundles.

* Significantly different from control values, ANOVA and L.S.D. $P < 0.05$.

point, force recovery with NAC remained 5 – 9% greater, at which point the difference between Kir6.2$^{-/-}$ in the absence or presence of NAC was not different and remained stable. In the presence of tiron, force recovered significantly quicker in the first five min (6 – 8% greater). By 10 min, the difference in recovery was not significant in the absence or presence of Tiron, and did not change for the final 20 min.

DISCUSSION

Elevations in $[Ca^{2+}]_i$ is known to cause fibre damage during fatigue. As $[Ca^{2+}]_i$ increases, it can result in numerous deleterious outcomes, including a Ca^{2+} overload in the mitochondria which results in an increased generation of ROS. The major finding of this study was that the application of two nonspecific ROS scavengers, NAC and tiron, reduced the extent of the contractile dysfunctions in sKATP channel deficient FDB muscle.

Role of sKATP channels in ROS development

Wild type muscle. In wild type FDB muscle, ROS generation occurs primarily by two mechanisms. Firstly, the rise in $[Ca^{2+}]$i will create a greater $[Ca^{2+}]$ gradient between the cytosol and mitochondria, inducing Ca^{2+} uptake by the mitochondrial Ca^{2+} uniporter (MCU) (Brookes *et al.*, 2004). This, in the presence of elevated [ADP]i which occurs during fatigue, leads to an increased production of H_2O_2 by the mitochondria (Nethery *et al.*, 2000). Secondly, the rise in $[Ca^{2+}]$i can lead to oxidation of NADPH and subsequent ROS production (Martins *et al.*, 2008). In addition to the Ca^{2+}-induced rise in ROS, an increase in muscle temperature from 22°C to 37°C will result in an increased ROS production (Zuo *et al.*, 2000; van der Poel & Stephenson, 2002; Arbogast & Reid, 2004; Edwards *et al.*, 2007). The addition of an ROS scavenger to wild type muscle at 37°C *in vitro* was shown to slow the rate of fatigue with submaximal tetanic stimulation (Khawli & Reid, 1994; Bruton *et al.*, 2008) but not at maximal stimulation (Khawli & Reid, 1994; Sandstrom *et al.*, 2006; Reardon & Allen, 2009). This was confirmed by our study, suggesting that in wild type muscle, ROS levels remain below a level that is damaging to

the muscle fibres. Opposite to this, application of exogenous ROS at 37°C to muscle bundles accelerated the rate of fatigue, providing evidence for a role in of ROS in fatigue (Reardon & Allen, 2009).

KATP channel deficient muscle. Kir6.2$^{-/-}$ muscle develops numerous contractile dysfunctions when maximally stimulated with a 180 s fatigue bout (Cifelli *et al.*, 2007; Cifelli *et al.*, 2008). Recently, Cifelli *et al* (Cifelli *et al.*, 2008) demonstrated that, during fatigue, there is a large Ca^{2+} influx through L-type Ca^{2+} channels which become activated due to the excessive membrane depolarization of the t-tubular membrane. Furthermore, in single glibenclamide-exposed FDB fibres that partially supracontracted during fatigue, $[Ca^{2+}]i$ remained elevated above rest at 15 min of recovery. The increased $[Ca^{2+}]i$ during fatigue and recovery could cause an excessive ROS production, which could: 1. reduce Ca^{2+} sensitivity of the contractile components (Burton & Smith, 1997a; Murphy *et al.*, 2008); 2. impair SR Ca^{2+} release and ATPase reuptake (Chin & Allen, 1996; Chin *et al.*, 1997; Reid, 2001a; Brookes *et al.*, 2004; Bruton *et al.*, 2008); and 3. cause RYR leakiness via phosphorylation and hypernitrosylation, thus further increasing $[Ca^{2+}]i$ (Bellinger *et al.*, 2008; Bellinger *et al.*, 2009). This would explain the reduced development of contractile dysfunctions in Kir6.2$^{-/-}$ muscle (i.e. less unstimulated force during fatigue, improved force recovery) with the application of NAC and tiron. Furthermore, the improved recovery in the presence of ROS scavengers could be due to less fibres being damaged during fatigue, and therefore improved force generation. The protective effects of using a ROS scavenger to reduce the contractile dysfunctions were less than that observed when verapamil was used to prevent the rise in $[Ca^{2+}]i$ by reducing influx (Cifelli *et al.*, 2008). This suggests that elevated ROS is not the only

cause of contractile dysfunctions in sKATP channel muscle, and that the elevated $[Ca^{2+}]i$ may be having other effects.

The ability of ROS scavengers to reduce the development of unstimulated force is possibly an effect of improved SR Ca^{2+} ATPase pump activity and reduced RYR leakiness. Since there is still a large Ca^{2+} influx in sKATP channel deficient muscle, an increased activity of the ATPase pump would allow for greater reuptake of Ca^{2+}, thus reducing $[Ca^{2+}]i$ and therefore unstimulated force.

Increased ROS production from oxidative phosphorylation in Kir6.2$^{-/-}$ muscle

In addition to the increased $[Ca^{2+}]i$ in sKATP channel deficient muscle leading to ROS production, it is also possible that there is an increased ATP utilization in these muscles, which will increase ROS production. In whole bundles, a large amount of fibre damage occurs as fibres fail to contract, and thus no longer contribute to force development (Cifelli *et al.*, 2007). Therefore, increased activity of other fibres to compensate would be necessary. Furthermore, Benkhalti and Renaud (unpublished results) showed that Kir6.2$^{-/-}$ muscle had an increased possibility for greater reliance on oxidative phosphorylation for ATP production during fatigue, and if so, this could lead to a further increase in ROS production as ~0.2 – 2% of O_2 consumed by cells is turned to ROS (Chance *et al.*, 1979; Hansford *et al.*, 1997).

Altered effects of NAC and tiron in Kir6.2$^{-/-}$ muscle.

In skeletal muscle, superoxide is produced primarily within the electron transport chain. In the presence of superoxide dismutase, it is rapidly converted to H_2O_2. H_2O_2 can be further oxidized into OH•. NAC is a non-specific antioxidant, which has been shown to reduce H_2O_2, OH• and hypochlorous acid, but not superoxide (Moldeus *et al.*, 1986;

Aruoma *et al.*, 1989). Alternatively, tiron acts to scavenge both superoxide and H_2O_2, but not OH• (Greenstock & Miller, 1975; Mohanraj *et al.*, 1998). Given that tiron and NAC were shown to equally reduce the H_2O_2 and OH• effects on Ca^{2+} sensitivity of the contractile apparatus (Burton & Smith, 1997a; Murphy *et al.*, 2008), it was expected that they would have similar effects on rate of fatigue in Kir6.2$^{-/-}$ muscle. However, the ability of NAC to reduce the development of unstimulated force during fatigue greater than tiron suggests that OH• plays a large role in Ca^{2+} regulation, acting either on the SR RYR, Ca^{2+} ATPase pump, or both to alter activity.

In conclusion, this study demonstrated that ROS play a role in the development of the contractile dysfunctions in sKATP channel deficient muscle. We showed that the application of two ROS scavengers, NAC and tiron, improved force generation and reduced unstimulated force during fatigue and increased rate of force recovery.

CHAPTER 5

FATIGUE PRECONDITIONING INCREASES FATIGUE RESISTANCE AND REDUCES MUSCLE DEPENDENCY ON K_{ATP} CHANNELS TO PREVENT CONTRACTILE DYSFUNCTIONS IN MOUSE FDB

By

Louise Boudreault, Carlo Cifelli, François Bourassa, and Jean-Marc Renaud

University of Ottawa, Department of Cellular and Molecular Medicine, 451 Smyth Rd., Ottawa, Ontario, Canada, K1H 8M5

AUTHORS' CONTRIBUTIONS

- Boudreault: Tables 5.1-5.3, Fig. 5.5-5.7, writing of the manuscript
- Cifelli: Fig. 5.2-5.4
- Bourassa: Fig. 5.1

ABSTRACT

The objective of this study was to determine how at 37°C one fatigue bout affects the kinetics of a second fatigue bout in mouse flexor digitorum brevis (FDB). All fatigue bouts were elicited with one tetanic contraction every s for 3 min. The first (FAT1) and second (FAT2) fatigue bouts were elicited 60 min apart in the absence or presence of 10 μM glibenclamide, an ATP-sensitive K^+ channel (K_{ATP} channel) blocker. When FAT1 preceding FAT2 was elicited under control conditions, the decreases in peak tetanic Ca^{2+}_i and force were significantly slower while the increases in unstimulated Ca^{2+}_i and force were significantly less during FAT2 than during FAT1; the differences between the two fatigue bouts being the greatest under glibenclamide conditions for FAT2. The presence of glibenclamide during FAT1 resulted in faster decreases in peak tetanic Ca^{2+}_i and force and greater increases in unstimulated Ca^{2+}_i and force when compared to control conditions; during FAT2, glibenclamide had none of these effects. In fact, the fatigue kinetics during FAT2 were no longer different between control and glibenclamide conditions. The differences in fatigue kinetics between FAT1 and FAT2 were also observed with FDB muscles from Kir6.2$^{-/-}$ mice, which have no sarcolemmal K_{ATP} (sK_{ATP}) channel activity. It is concluded that an acute physiological process occurs following one fatigue bout resulting in an increased fatigue resistance and a decreased dependency on K_{ATP} channel for myoprotection. This novel process was termed "Fatigue Preconditioning" (FPC). Using pharmacological approaches from Ischemic Preconditioning (IPC), such as abolishing sarcolemmal or mitochondrial K_{ATP} channel activity, PKC or ROS signalling, had no effect on abolishing FPC. Therefore, the mechanism of FPC is unique from IPC.

FOOTNOTE The novel phenomenon reported here was discovered by F. Bourassa who measured intracellular Ca^{2+}. Force measurements were carried out by C. Cifelli and L. Boudreault.

INTRODUCTION

Skeletal muscles are known to respond to repetitive activity and can adapt according to physiological demands. When the capacity of muscles to generate force or do work diminishes during an acute bout of repetitive activity, the phenomenon is known as muscle fatigue. If skeletal muscles are chronically subjected to a regime of exercises, then resistance to fatigue increases. This type of adaptation involves changes in metabolic enzymes and contractile proteins that occur over several days to weeks (Pette & Vrbova, 1992; Jarvis *et al.*, 1996; Allen *et al.*, 2001). Skeletal muscles can also increase their resistance to fibre damage. For example, eccentric exercise, which involves fibre stretching during contractions, is a well known cause of fibre damage. Eccentric exercise increases resistance to further damage within 10 days (Sacco & Jones, 1992). Even a non-damaging muscular activity increases the resistance of muscle fibres against contraction-induced damage within 24 hrs (McArdle *et al.*, 2004). Finally, skeletal muscles can adapt to improve survival under pathological conditions to resist fibre damage. Short and non-damaging ischemic periods increase the resistance against fibre damage during a subsequent longer and damaging ischemic period; this phenomenon is known as Ischemic Preconditioning (IPC) (Pang & Forrest, 1995).

Opening of sarcolemmal K_{ATP} (sK_{ATP}) channels is one key mechanism for myoprotection against fibre damage and contractile dysfunctions during acute physiological stress such as exercise and fatigue (Thabet *et al.*, 2005; Cifelli *et al.*, 2007). Cifelli *et al.* (2007) defined a contractile dysfunction as any event from the generation of action potentials to the actin-myosin interaction that is depressed in a manner not associated with the normal process of fatigue (or any metabolic stress), and that

eventually incapacitates muscle from generating force. In skeletal muscle, such contractile dysfunctions include fibre supercontraction, excessive membrane depolarization, excessive increase in unstimulated $Ca^{2+}i$ and force during fatigue, and a reduced capacity to recover force after fatigue (Gramolini & Renaud, 1997; Gong *et al.*, 2003; Cifelli *et al.*, 2007).

To date, there is no report demonstrating that *in vitro* one fatigue bout results in some acute adaptive response to fatigue in skeletal muscle under physiological conditions. At 22°C two successive fatigue bouts separated by a 60 min recovery period have similar decreases in peak tetanic $Ca^{2+}i$ and force in FDB single muscle fibres (Chin & Allen, 1997). However, this was not observed 37°C. Thus, our first objective is to report the significant differences in fatigue kinetics observed *in vitro* during two fatigue bouts separated by a 60 min interval. These differences include: i) a slower fatigue rate during the second bout, and ii) sKATP channel deficient fibres no longer develop contractile dysfunctions during the second bout like they do during the first bout. These results suggest that following one fatigue bout *in vitro* important acute physiological adaptations occur that significantly increases fatigue resistance and eliminate muscle dependency on sKATP channel myoprotection. We have termed this finding "Fatigue Preconditioning" (FPC).

Ischemic preconditioning (IPC) improves resistance to fibre damage during a long and damaging ischemic period. The IPC protocol consists of one or more cycles of short and non-damaging ischemic periods elicited prior to the subsequent damaging ischemic period. The mechanisms of IPC are well characterized in several tissues, including cardiac and skeletal muscle. In brief, during an ischemic bout, paracrine factors such as

adenosine and bradykinin accumulate in the interstitium, and start the preconditioning cascade by activating G-protein coupled receptors (Oldenburg *et al.*, 2004; Gross & Gross, 2006). This activation triggers the P13K and Akt signalling pathways which ultimately lead to translocation of PKCε from the cytosol to the mitochondria, where it can phosphorylate the mitochondrial KATP (mKATP) channels, causing them to open (Cohen *et al.*, 2001; Garlid & Paucek, 2001; Costa *et al.*, 2005). The resulting K^+ influx into the mitochondrial space results in matrix alkalinization and slightly increased ROS production (Oldenburg *et al.*, 2003). The increase in ROS activates a second inner membrane PKCε which inhibits the mitochondrial permeability transition pore (MPT pore) (Costa & Garlid, 2008), the final step towards cell death via cytochrome c loss, a known activator of apoptosis. Furthermore, opening of the mKATP channels protects against Ca^{2+} overload along with mild uncoupling to prevent excessive and deleterious ROS production (Chance *et al.*, 1979; Hansford *et al.*, 1997; Holmuhamedov *et al.*, 1999; Murata *et al.*, 2001; Sato *et al.*, 2005). There is also evidence for the possible role of sKATP channels in IPC (Pang *et al.*, 1997a; Pang *et al.*, 1997b; Gurke *et al.*, 2000; Bushell *et al.*, 2002; Zheng *et al.*, 2007). Adenosine or application of an adenosine receptor agonist was shown to cause opening of sKATP channels (Forrest *et al.*, 1997; Papanastasiou *et al.*, 1999; Zheng *et al.*, 2007). In myocardial cells, this is thought to shorten the action potential duration, thus reducing Ca^{2+} influx and sparing of high-energy phosphates, the latter shown to occur in myocardial and muscle tissue (Nichols & Lederer, 1991; Nichols *et al.*, 1991; Findlay, 1994).

Therefore, our second aim was to determine if the mechanistic pathways for FPC are the same as IPC. Our results show that: i. sKATP and mKATP channels are not required

for FPC; ii. adenosine receptor agonists did not induce FPC, while PKC inhibitors and ROS scavengers did not abolish FPC; and iii. the first fatigue bout must be a minimum of 90 seconds in duration to optimize the benefits afforded by FPC, but as little as 15 seconds afforded some beneficial effects.

METHODS AND MATERIALS

ANIMALS, MUSCLE BUNDLE AND SINGLE FIBRE PREPARATION

Two to three month old CD1 mice (from Charles River, Canada) were used as wild type mice. Kir6.2$^{-/-}$ mice are null mice for the Kir6.2 gene, which encoded for the pore of the sKATP channel, and were generated as previously described (Miki *et al.*, 1998). All mice weighed 20-25 g, were fed *ad libitum*, and housed according to the guidelines of the Canadian Council for Animal Care (CCAC). The Animal Care Committee of the University of Ottawa approved all experimental procedures used in this study. Mice were anesthetized with a single intraperitoneal injection of 2.2 mg ketamine, 0.44 mg xylazine, and 0.22 mg acepromazine per 10 g of body mass. FDB muscles were excised from the hind paw and mice then euthanized with an overdose of anaesthetics.

FDB muscle bundles and single fibres were prepared as described by Cifelli et al. (2007). Briefly, the bundles of fibres controlling the 4th digit were excised by cutting along the lateral fascia separating the muscle fibres of the 3rd and 4th digits. Single fibres were dispersed by trituration after a 4 hr collagenase (0.2% type I, Sigma, USA) digestion at 37°C in culture medium containing minimum essential medium with Earle's salt and L-glutamine (MEM, Gibco, Canada) supplemented with 10% foetal bovine serum (FBS, Gibco, Canada), 100 units/ml of penicillin and 100 µg/ml of streptomycin (Gibco, Canada).

SOLUTIONS

During experiments, FDB bundles and single muscle fibres were constantly immersed in physiological saline solution. The control solution contained (in mM): 118.5 NaCl, 4.7 KCl, 2.4 $CaCl_2$, 3.1 $MgCl_2$, 25 $NaHCO_3$, 2 NaH_2PO_4, and 5.5 D-glucose. All

solutions were continuously bubbled with 95% O_2-5% CO_2 to maintain a pH of 7.4. Solutions containing glibenclamide (10 μM to block sKATP and mKATP channels), pinacidil (100 μM to open sKATP channels) and chelerythrine (1 μM to prevent PKC translocation) were prepared by first dissolving glibenclamide in DMSO, which was then added to the saline solution so that the final DMSO concentration was 0.1% (v/v) in all solutions (including control solutions). The presence of DMSO alone does not affect fatigue kinetics. Adenosine receptor agonist R-PIA (100 μM), L-type Ca^{2+} channel blocker verapamil (1 μM to partially block channels), ROS scavengers NAC (10 mM to scavenge hydroxyl radicals), Tiron (10 mM to scavenge superoxide radicals) and 2-MPG (1 mM), and mKATP channel blocker 5-HD (300 μM) were dissolved directly into the saline solution. Muscles were exposed to the drugs for 30 min prior to eliciting the fatigue bouts. All experiments were carried out at 37°C.

FORCE MEASUREMENTS

Force measurements were carried out using FDB bundles as described by Cifelli *et al.* (2007). Briefly, tetanic force was monitored with a Cambridge ergometer (model 300, USA) or a Gould Statham force transducer (Model UC2, USA), and digitized at 5 kHz by a Keithley Metrabyte A-D board (model DAS50, USA). Peak tetanic force represented the maximum change in force during tetanic stimulation and was calculated as the difference between the maximum force during the contraction and the force just before the contraction was elicited. Unstimulated force was defined as the force exerted by FDB bundles between contractions when they failed to fully relax and was calculated by averaging the force during the 5 ms immediately preceding a contraction.

$Ca^{2+}i$ MEASUREMENTS

$Ca^{2+}i$ measurements were carried out using single FDB muscle fibres as described by Cifelli *et al.* (2007). Briefly, single FDB fibres were loaded with Fura-2 by exposing them for 30 min at 37°C to 5 μM Fura-2AM (Molecular Probes, Canada). Cover slips containing FDB fibres were installed in a chamber (model RC-25, Warner Instruments, USA), and flow of saline solution was adjusted at a continuous flow of 2 ml/min. $Ca^{2+}i$ was monitored prior to fatigue, during fatigue and recovery period by illuminating the fibres alternatively between 340 and 380 nm and measuring fluorescence at 505 nm using a spectrofluorometer (IonSpec, Canada). $Ca^{2+}i$ concentration was not calculated from the 340/380 fluorescence ratio because many sK_{ATP} channel deficient fibres supercontracted and became damaged during fatigue with ratios increasing to values above 5, largely exceeding the expected R_{max} (Westerblad & Allen, 1991). Unstimulated $Ca^{2+}i$ was determined by averaging the 340/380 fluorescent ratios during the 100 ms period preceding a contraction. Peak tetanic $Ca^{2+}i$ was determined by averaging the 340/380 fluorescent ratio of the $Ca^{2+}i$ tetanic plateau phase.

STIMULATION AND FATIGUE PROTOCOL

Tetanic contractions were elicited with 200 ms train of 0.3 ms, 8 V (supramaximal voltage) pulses; stimulation frequencies for bundles and single fibres were respectively 200 and 140 Hz (FDB single fibres were unstable at stimulation frequencies exceeding 140 Hz). Pulses were generated with a Grass S88 stimulator and a Grass SIU5 isolation unit (Grass Instruments, USA). For FDB bundles, the stimulating platinum wires (4 mm apart) were located on opposite sides of the fibres. For single FDB fibres, the platinum wires (7 mm apart) were positioned on each side of the chamber. All FDB bundles and single fibres were allowed 30 min equilibrium before any fatigue bout.

During that time, tetanic contractions were elicited every 100 s. All fatigue bouts consisted of one tetanic contraction per s for 180 s, except for the FAT1 duration studies whereby muscles were randomly assigned to FAT1 durations of 0, 30, 60, 90, and 180 (control) s. Following each fatigue bout, fibres and bundles were stimulated every 100 s to measure $[Ca^{2+}]i$ or force recovery.

STATISTICAL ANALYSIS

ANOVA was used to determine significant differences. Split plot designs were used because muscles were tested at all time levels. ANOVA calculations were made using the Version 9.0 GLM (General Linear Model) procedures of the Statistical Analysis Software (SAS Institute Inc., USA). When a main effect or an interaction was significant, the least square difference (L.S.D.) was used to locate the significant differences (Steel & Torrie, 1980). The word "significant" refers only to a statistical difference ($P<0.05$).

RESULTS

UNSTIMULATED Ca^{2+}_i AND PEAK TETANIC Ca^{2+}_i

Control conditions. Unstimulated Ca^{2+}_i significantly increased during fatigue. When a first fatigue bout was elicited 30 min after an equilibrium period (FAT1-Con, Fig 5.1A), the 340/380 fura-2 fluorescence ratio increased from 0.49 to 0.89 in 80 s and thereafter slightly decreased, being 0.74 at 180 s (Fig. 5.1B). A second fatigue bout (FAT2-Con) was elicited 60 min after FAT1-Con. Prior to FAT2-Con, the unstimulated fluorescence ratio had returned to 0.54. During FAT2-Con, unstimulated Ca^{2+}_i increased again but was slightly less between the 50^{th} and 140^{th} s when compared to the increases during FAT1-Con. During FAT1-Con, the 340/380 fluorescence ratio representing peak tetanic Ca^{2+}_i increased from 2.13 to 2.64 in 16 s and then decreased to 1.86 at 127 s; thereafter, it changed very little. During the subsequent recovery period, the ratio returned to 2.05. During FAT2-Con, peak tetanic Ca^{2+}_i increased as observed during FAT1-Con whereas the subsequent decreases were significantly slower during FAT2-Con between the 70^{th} and 95^{th} s.

Glibenclamide conditions. When the first fatigue bout was elicited in the presence of 10 μM glibenclamide (FAT1-Gli), the ratio for unstimulated Ca^{2+}_i sharply rose from 0.49 to 1.25 in 50 s (Fig. 5.1C). Furthermore, 79% of the tested fibres supercontracted and failed to recover a normal unstimulated Ca^{2+}_i after fatigue as previously reported (Cifelli *et al.*, 2007). Therefore, to determine the glibenclamide effect during FAT2, fibres were first fatigued under control conditions (FAT1-Con) and then exposed to 10 μM glibenclamide after 30 min of recovery. FAT2-Gli was elicited after another 30 min (Fig. 5.1A).

FIGURE 5.1

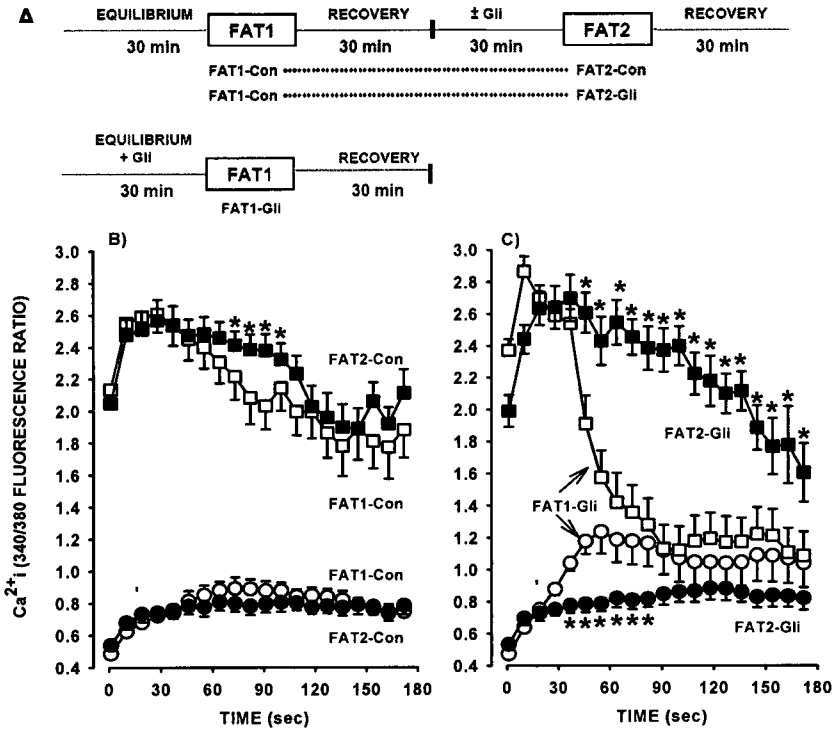

Figure 5.1. Increases in unstimulated $[Ca^{2+}]i$ and decreases in peak tetanic $[Ca^{2+}]i$ were significantly slower during a second fatigue bout (FAT2) than during a first bout (FAT1), especially in the presence of glibenclamide. A) Fatigue protocols. Equilibrium, recovery and pre-fatigue exposure to glibenclamide were all 30 min. Fatigue was elicited with one tetanic contraction every s for 3 min. FAT1 and FAT2 were elicited under B) control conditions or C) in the presence of 10 μM glibenclamide. Symbols: ○ ●, unstimulated $Ca^{2+}i$; □ ■, peak tetanic $Ca^{2+}i$. Vertical bars represent the S.E. of 11-12 fibres (not shown if smaller than symbol).

' Indicates when unstimulated $Ca^{2+}i$ became significantly different from Time 0.

* Mean values between FAT1 and FAT2 were significantly different. ANOVA, L.S.D. $P < 0.05$

The increase in unstimulated $Ca^{2+}i$ was significantly less during FAT2-Gli than during FAT1-Gli. The increases in unstimulated $Ca^{2+}i$ during FAT2-Gli were actually similar to those during FAT2-Con. Contrary to the situation during FAT1-Gli, supercontracted fibres were not observed following FAT2-Gli. During FAT1-Gli, the ratio for peak tetanic $Ca^{2+}i$ increased from 2.39 to 2.87 in 10 s and then decreased sharply to 1.08 by 90 s; the decreases being much more pronounced when compared to those during FAT1-Con. The decreases in peak tetanic $Ca^{2+}i$ were significantly slower during FAT2-Gli than during FAT1-Gli. In fact, the ratios were not different between FAT2-Con and FAT2-Gli until the final 30 s. Therefore, the increase in unstimulated $Ca^{2+}i$ and decrease in peak tetanic $Ca^{2+}i$ were slower during FAT2 elicited 60 min after FAT1, and the differences between the two fatigue bouts were strikingly evident in the presence of glibenclamide.

PEAK TETANIC FORCE

For the experiments involving FDB bundles, a third fatigue protocol was added in which the first fatigue bout was delayed a full hour (delFAT1); i.e., it was elicited at the same time as FAT2 (Fig. 5.2A) to control for possible changes in fatigue kinetics with time. The decreases in peak tetanic force during FAT1 and delFAT1 were not significantly different for both control (Fig. 5.2B, inset) and glibenclamide conditions (Fig. 5.2C, inset). Following FAT1-Con and delFAT1-Con, peak tetanic force returned back to 90% of the pre-fatigue tetanic force (Table 5.1). The recovery was significantly less following FAT1-Gli and delFAT1-Gli when compared to FAT1-Con and delFAT1-Con. So, only the FDB bundles fatigued under FAT1-Con underwent the FAT2-Con or FAT2-Gli protocol.

FIGURE 5.2

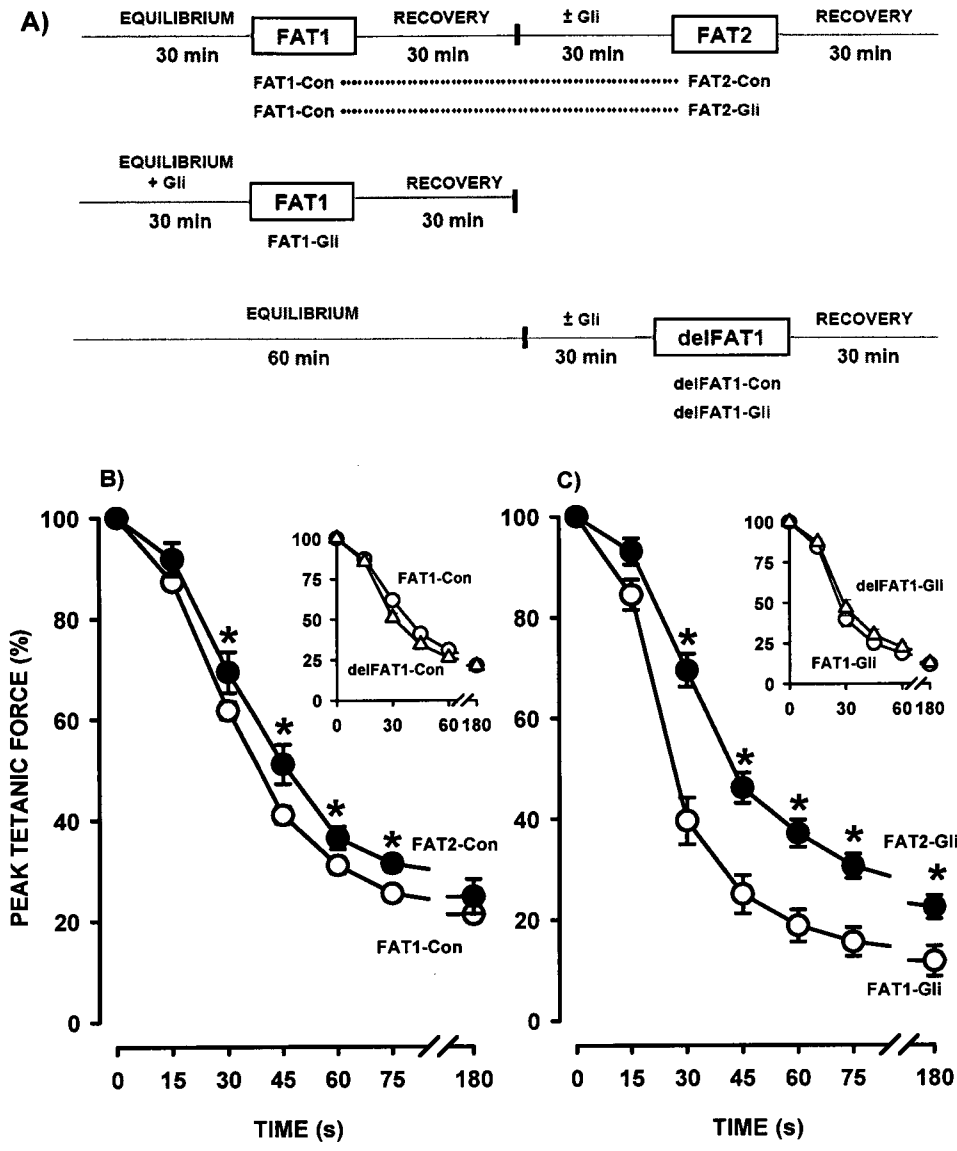

Figure 5.2. Decreases in peak tetanic force during FAT2 were slower than during FAT1 in control conditions (B) and in the presence of 10 μM glibenclamide (C). Peak tetanic force is expressed as a percent of the pre-fatigue peak tetanic force. Vertical bars represent the S.E. of 5 FDB bundles.

* Peak tetanic force significantly different from FAT1, ANOVA, L.S.D. $P < 0.05$

TABLE 5.1

A

FATIGUE CONDITIONS		% PEAK TETANIC FORCE at 30 s fatigue		% PEAK TETANIC FORCE at 60 s fatigue	
FAT1	**FAT2**	**FAT1**	**FAT2**	**FAT1**	**FAT2**
Control	Gli	58.9 ± 0.6	63.4 ± 0.8 '*	37.1 ± 0.1	35.7 ± 1.6
Gli	-	40.2 ± 4.2 '	-	15.7 ± 1.7 '	-

B

FAT1	FAT2	FAT1	FAT2	FAT1	FAT2
5-HD	Gli	-2.2 ± 11.2	0.3 ± 7.0	-3.4 ± 4.9	-2.46 ± 7.5
R-PIA	Gli	-	-35.1 ± 11.3*	-	-11.6 ± 4.1*
Chel	Gli	-5.2 ± 11.7	-8.3 ± 5.7	-10.0 ± 16.4	-9.7 ± 11.0
2-MPG	Gli	0.6 ± 4.3	-0.8 ± 4.2	-0.2 ± 7.3	-1.5 ± 3.4
NAC	Gli	1.1 ± 4.0	-0.7 ± 10.0	-3.7 ± 4.5	0.5 ± 7.9
Tiron	Gli	-1.6 ± 9.2	-4.0 ± 5.7	-1.6 ± 6.1	-4.1 ± 8.0

Table 5.1. A) Peak tetanic force at 30 and 60 s during FAT2 was greater in the presence of 10 μM glibenclamide when a prior fatigue bout was elicited under control conditions. (B) Peak tetanic force during FAT2 was unaffected when FAT1 was elicited in the presence of mKATP channel blocker 5-HD (300 μM), adenosine agonist R-PIA (1 μM), PKC inhibitor Chel (1 μM) and ROS scavengers 2-MPG (1 mM), NAC (10 mM) and Tiron (10 mM). Values are expressed as the percent of the pre-fatigue peak tetanic force (A) or the difference in % pre-fatigue peak tetanic force between paired bundles (B). FAT2 was elicited 60 min after FAT1 under the conditions indicated in table. All drugs were added 30 min prior to a fatigue bout; those added prior to FAT1 were removed 30 min after FAT1.

' Significantly different from FAT1-Con, ANOVA and LSD $P < 0.05$.

* Not significantly different from FAT1-Glib, ANOVA and LSD $P > 0.05$.

Under control conditions, the decrease in peak tetanic force during FAT1-Con occurred predominantly during the first 75 s as it reached 22% of the pre-fatigue force (Fig. 5.2B). Thereafter, peak tetanic force decreased very little, being 20% at 180 s. When FAT2-Con was elicited 60 min after FAT1-Con, the decreases in peak tetanic force were significantly slower during FAT2-Con than during FAT1-Con, especially between the 15^{th} to 75^{th} s, with a maximum force difference of 17% at 45 s (Fig. 5.2B). Similarly, peak tetanic force decreased at a significant slower rate during FAT2-Gli than during FAT1-Gli (Fig. 5.2C). As observed for peak tetanic $Ca^{2+}i$, the decreases in peak tetanic force during FAT1 and delFAT1 were faster in the presence than in the absence of glibenclamide. For example, at 30 sec, peak tetanic force was 61% during FAT1-Con compared to 40% during FAT1-Gli. Such differences, were, however, no longer observed between FAT2-Con and FAT2-Gli.

UNSTIMULATED FORCE

Unstimulated force increased during fatigue as muscles failed to fully relax between contractions. During delFAT1-Con, unstimulated force reached a maximum of 3% of the pre-fatigue peak tetanic force within 30 s, an increase of ~1% compared to the value observed during FAT1 (Fig. 5.3A, inset). Unstimulated force was lower during FAT2-Con, but only one significant difference occurred at 30 s when compared to FAT1 (Fig. 5.3A). Glibenclamide-exposed FDB generated significantly more unstimulated force, which reached 17-20% at 30 sec during both FAT1-Gli and delFAT1-Gli (Fig. 5.3B and inset). However, there was no drastic increase in unstimulated force during FAT2-Gli (Fig. 5.3B). Instead, unstimulated force progressively increased, but remained below 5% until the end of the fatigue period, compared to 16% for FAT1-Gli.

FIGURE 5.3

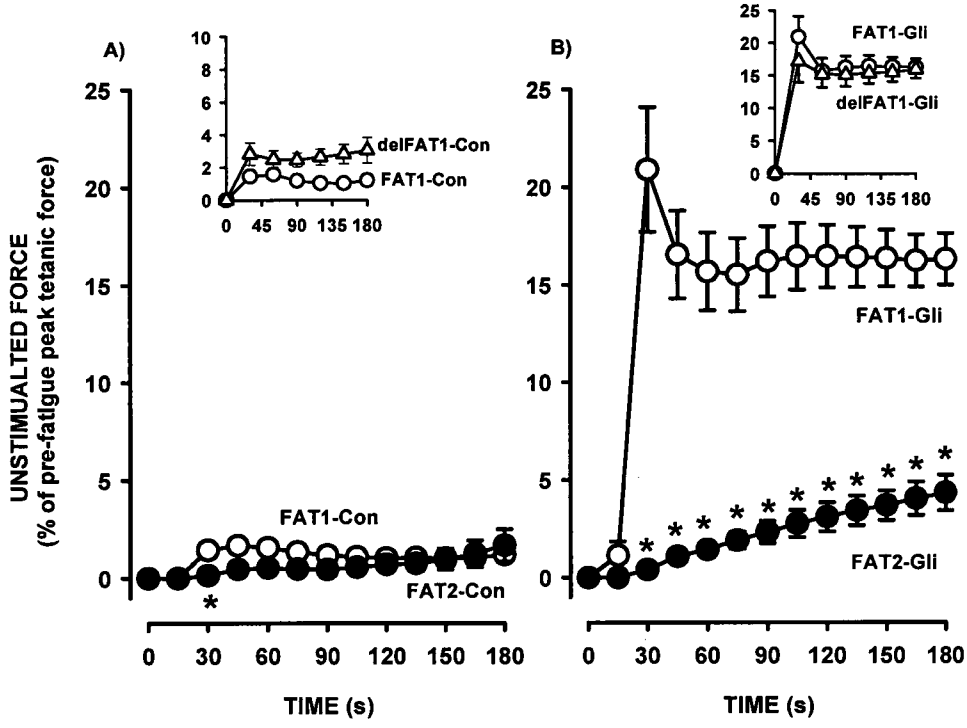

Figure 5.3. Increases in unstimulated force were less during FAT2 than during FAT1 in control conditions (A) and in the presence of 10 μM glibenclamide (B). The fatigue protocols were as illustrated in Fig. 5.2A. Unstimulated force was expressed as a percent of the pre-fatigue peak tetanic force. Vertical bars represent the S.E. of 5 FDB bundles.

* Unstimulated force significantly different from FAT1, ANOVA, L.S.D. $P < 0.05$

Thus, following a first bout of fatigue under control conditions (FAT1-Con), the decrease in peak tetanic force was slower and the increase in unstimulated force less during a second bout of fatigue (FAT2) especially in the presence of glibenclamide. This suggests an acute increase in fatigue resistance after FAT1.

RECOVERY OF PEAK TETANIC FORCE

The recovery of peak tetanic force following FAT1, delFAT1 and FAT2 under control conditions followed a similar time course (Fig. 5.4A). After 30 min of recovery, peak tetanic force was 90-94% of the pre-fatigue force. Peak tetanic forces after 30 min of recovery following FAT1 or delFAT1 in the presence of 10 μM glibenclamide were respectively 73% and 79% (inset of Fig. 5.4B), values that were significantly less than those observed in control conditions. However, force recovery following FAT2-Gli was 92% after 30 min, a value that was significantly greater than following FAT1-Gli and delFAT1-GLI while being the same as after FAT1-Con or FAT2-Con.

MECHANISM OF THE INCREASED FATGUE RESISTANCE DURING FAT2

Role of the sarcolemmal KATP (sKATP) channel. The lack of glibenclamide effects during FAT2 may either be because KATP channels are no longer necessary to prevent contractile dysfunction or because glibenclamide no longer blocks KATP channels, as previously reported during prolonged ischemia in heart (Findlay, 1993). Also, sKATP channels play important role in myoprotection during IPC in both cardiac and skeletal muscle. To test for these possibilities, the effects of two fatigue bouts in Kir6.2$^{-/-}$ FDB, which are sKATP channel deficient muscles (Miki *et al.*, 2002), was examined. As observed with glibenclamide-exposed wild type FDB, Kir6.2$^{-/-}$ FDB generate large

FIGURE 5.4

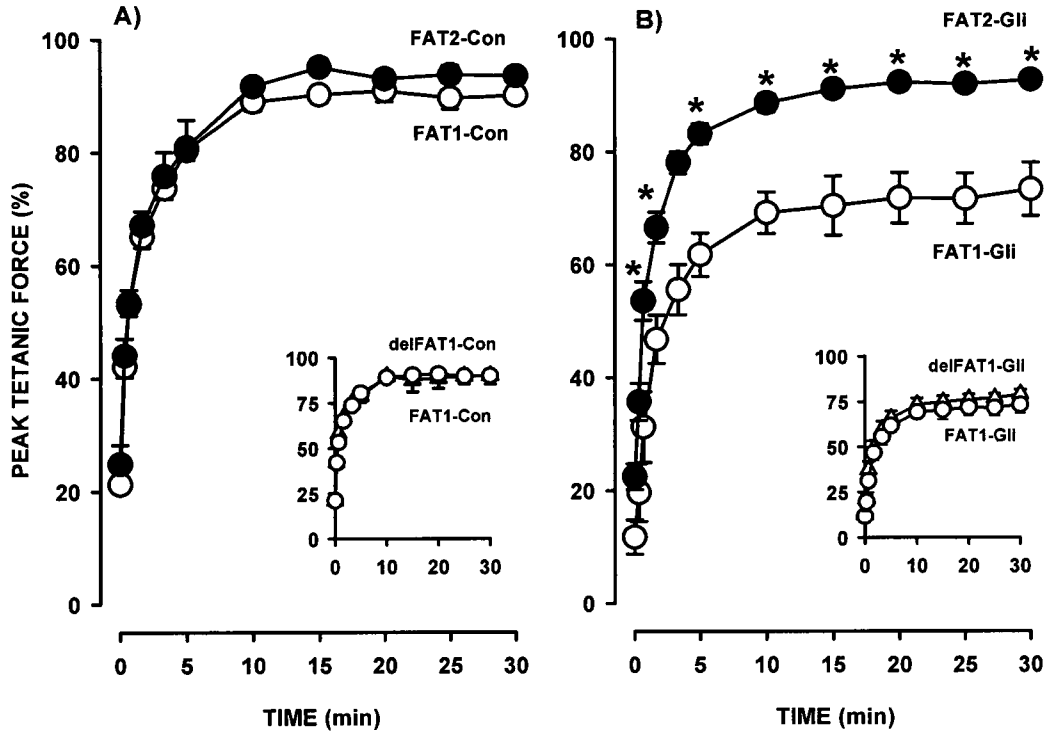

Figure 5.4. Peak tetanic force recovery was significantly faster and greater following FAT2 compared to FAT1 when FAT1 was elicited in the in the presence of 10 μM glibenclamide. A) control conditions B) 10 μM glibenclamide. The fatigue protocols were as illustrated in Fig. 5.2A. Peak tetanic force was expressed as a percent of the pre-fatigue peak tetanic force. Vertical bars represent the S.E. of 5 FDB bundles.

* Unstimulated force significantly different from FAT1, ANOVA, L.S.D. $P < 0.05$

amount of unstimulated force during fatigue and has a lower capacity to recover force following fatigue (Cifelli *et al.*, 2007). These two contractile dysfunctions are prevented when Kir6.2$^{-/-}$ FDB is fatigued in the presence of 1 μM verapamil to partially block L-type Ca^{2+} channels and thus prevent the deleterious Ca^{2+} influx between contractions (Cifelli *et al.*, 2008). So, in this study, FAT2-Con was elicited after FAT1 was carried out in the presence of verapamil (FAT1-Ver), and the results compared with those when FAT1 was elicited 30 min after an equilibrium period (FAT1-Con) or at the same time as FAT2 was elicited (delFAT1-Con, Fig. 5.5A), all in Kir6.2$^{-/-}$ muscle.

The decreases in peak tetanic force (Fig. 5.5B, inset) and the increases in unstimulated force (Fig. 5.5C, inset) were not different between FAT1-Con and delFAT1-Con. The decreases in peak tetanic force during FAT1-Con and FAT1-Ver were similar whereas they were significantly slower during FAT2-Con (Fig. 5.5B). A large increase in unstimulated force to 20% was observed in Kir6.2$^{-/-}$ FDB during both FAT1-Con and delFAT1-Con (Fig. 5.5C). The increases in unstimulated force were significantly reduced during FAT1-Ver and absent during FAT2-Con. Finally, force recovery following FAT2-Con and FAT1-Ver was significantly better than after FAT1-Con or delFAT1-Con (Table 5.1).

Muscles exposed to R-PIA, an adenosine receptor agonist, were shown to display significant myoprotection following ischemia (Jeffrey *et al.*, 2002). To further verify that the mechanistic pathway of FPC is independent of adenosine-sK$_{ATP}$ channel activity, FDB bundles to were exposed to 100 μM R-PIA for 60 min (replacing FAT1) prior to fatigue in the presence of glibenclamide. Comparison between R-PIA-Gli and FAT2-Con (Table 5.1 – 5.3) shows that R-PIA-Gli bundles generated 35% and 12% less

FIGURE 5.5

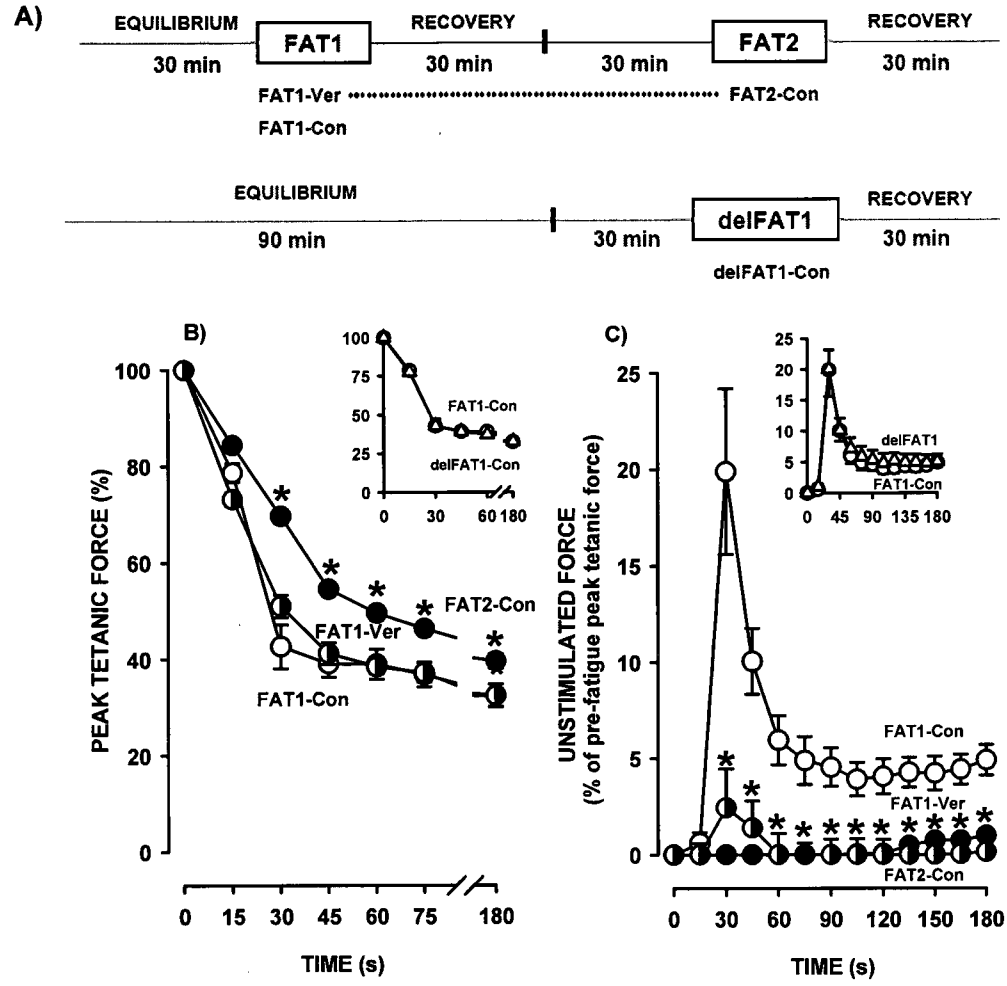

Figure 5.5. In Kir6.2$^{-/-}$ FDB, decreases in peak tetanic force (B) were slower and increases in unstimulated force (C) were less during FAT2 than during FAT1. Prior to FAT2-Con, Kir6.2$^{-/-}$ FDB was fatigued in the presence of 1 μM verapamil (FAT1-Ver). Peak tetanic force and unstimulated force were expressed as a percent of the pre-fatigue peak tetanic force. Vertical bars represent the S.E. of 5 FDB bundles.

* Peak tetanic force and unstimulated force significantly different from FAT1, ANOVA, L.S.D. $P < 0.05$

FIGURE 5.6

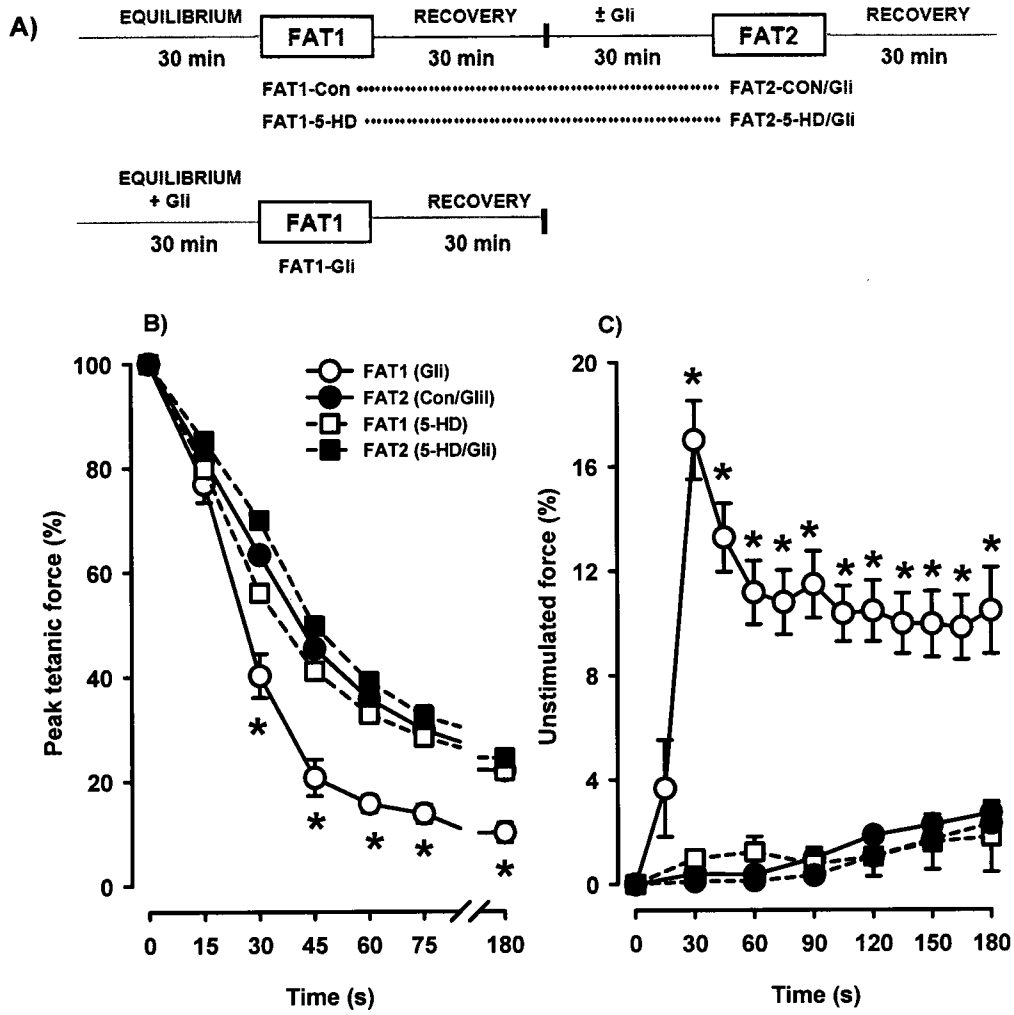

Figure 5.6. Exposing FDB to 300 μM 5-HD during FAT1 did not inhibit fatigue pre-conditioning. A) Fatigue protocols. B) Peak tetanic force and C) unstimulated force expressed as a percent of the pre-fatigue peak tetanic force. Vertical bars represent the S.E. of 5 FDB bundles.

* Peak tetanic force and unstimulated force significantly different from FAT1, ANOVA, L.S.D. $P < 0.05$.

TABLE 5.2

A

FATIGUE CONDITIONS		% PRE-FATIGUE PEAK TETANIC FORCE at 30 s		% PRE-FATIGUE PEAK TETANIC FORCE at 180 s	
FAT1	**FAT2**	**FAT1**	**FAT2**	**FAT1**	**FAT2**
Control	Gli	0.05 ± 0.33	0.40 ± 0.60*	1.35 ± 0.89	2.70 ± 0.40*
Gli	-	17.0 ± 1.5	-	10.5 ± 1.7	-

B

FATIGUE CONDITIONS		DIFFERENCE at 30 s BETWEEN PAIRED BUNDLES		DIFFERENCE at 1800 s BETWEEN PAIRED BUNDLES	
FAT1	**FAT2**	**FAT1**	**FAT2**	**FAT1**	**FAT2**
5-HD	Gli	0.48 ± 0.52	-0.12 ± 0.45	0.11 ± 1.63	0.40 ± 1.79
R-PIA	Gli		24.67 ± 10.44*		6.77 ± 2.75*
Chel	Gli	2.06 ± 3.69	0.86 ± 2.16	2.28 ± 2.09	2.87 ± 6.56
2-MPG	Gli	0.61 ± 4.25	0.77 ± 4.14	1.02 ± 5.45	-1.54 ± 3.42
NAC	Gli	1.59 ± 1.24	0.21 ± 0.75	1.26 ± 1.45	-0.26 ± 1.30
Tiron	Gli	0.35 ± 0.84	-0.27 ± 1.13	0.03 ± 0.61	0.57 ± 3.42

Table 5.2. A) Unstimulated force at 30 and 180 s during FAT2 was less in the presence of 10 μM glibenclamide when a prior fatigue bout was elicited under control conditions. (B) Unstimulated force during FAT2 was unaffected when FAT1 was elicited in the presence of mKATP channel blocker 5-HD (300 μM), adenosine agonist R-PIA (1 μM), PKC inhibitor Chel (1 μM) and ROS scavengers 2-MPG (1 mM), NAC (10 mM) and Tiron (10 mM). Values are expressed as the percent of the pre-fatigue peak tetanic force (A) or the difference in % pre-fatigue peak tetanic force between paired bundles (B). FAT2 was elicited 60 min after FAT1 under the conditions indicated in table. All drugs were added 30 min prior to a fatigue bout; those added prior to FAT1 were removed 30 min after FAT1.

' Significantly different from FAT1-Con, ANOVA and LSD $P < 0.05$.

* Not significantly different from FAT1-Glib, ANOVA and LSD $P > 0.05$.

TABLE 5.3

A

FATIGUE CONDITIONS		PEAK TETANIC FORCE AT 30 min RECOVERY (% of PRE-FATIGUE TETANIC FORCE)	
FAT1	**FAT2**	**FAT1**	**FAT2**
Control	Gli	0.05 ± 0.33	0.40 ± 0.60*
Gli	-	17.0 ± 1.5	-

B

		DIFFERENCE IN % PEAK TETANIC FORCE BETWEEN PAIRED BUNDLES AT 30 min RECOVERY	
FAT1	**FAT2**	**FAT1**	**FAT2**
5-HD	Gli	1.5 ± 14.0	0.7 ± 9.3
R-PIA	Gli	-	-10.1 ± 11.5
Chel	Gli	-3.4 ± 20.0	1.8 ± 6.9
2-MPG	Gli	0.9 ± 12.6	-0.5 ± 0.8
NAC	Gli	1.8 ± 11.0	7.1 ± 5.9
Tiron	Gli	-3.2 ± 6.3	-0.5 ± 4.3

Table 5.3. A) Recovery of peak tetanic force after 30 min following FAT2 was greater in the presence of 10 μM glibenclamide when a prior fatigue bout was elicited under control conditions. (B) Recovery of peak tetanic force following FAT2 was unaffected when FAT1 was elicited in the presence of mKATP channel blocker 5-HD (300 μM), adenosine agonist R-PIA (1 μM), PKC inhibitor Chel (1 μM) and ROS scavengers 2-MPG (1 mM), NAC (10 mM) and Tiron (10 mM). Values are expressed as the percent of the pre-fatigue peak tetanic force (A) or the difference in % pre-fatigue peak tetanic force between paired bundles (B). FAT2 was elicited 60 min after FAT1 under the conditions indicated in table. All drugs were added 30 min prior to a fatigue bout; those added prior to FAT1 were removed 30 min after FAT1.

' Significantly different from FAT1-Con, ANOVA and LSD $P < 0.05$.

* Not significantly different from FAT1-Glib, ANOVA and LSD $P > 0.05$.

tetanic force, 25% greater unstimulated force at 30 s, and recovered 10% less force following 30 min of recovery. These values were not significantly different from FAT1-Gli.

Role of the mitochondrial KATP (mKATP) channel. mKATP channels also play a major role during IPC in cardiac and skeletal muscle (Cohen *et al.*, 2001; Garlid & Paucek, 2001; Costa *et al.*, 2005). To test whether these channels are important in the increased fatigue resistance during FAT2, mKATP channels were blocked with 100 μM 5-HD during FAT1 (FAT1-5-HD) to prevent the increase in fatigue resistance during FAT2-Gli. The presence of 5-HD during FAT1 did not affect fatigue kinetics compared to FAT1-Con. As shown in Tables 5.1-5.3, the presence of 5-HD during FAT1 did not prevent the slowed decrease in peak tetanic force (difference of <1% at 30 s and 2% at 60 s), nor did it cause greater unstimulated force during FAT2-Gli (difference of <1% at 30 and 180 s) when compared to FAT2-Gli elicited after FAT1-Con. Furthermore, equal recovery from FAT2 was observed (difference of < 1%).

Role of ROS and PKC. To determine if PKC and ROS are part of the signalling process of FPC, FAT1 was elicited in the presence of PKC inhibitor Chel or ROS scavengers NAC, tiron or 2-MPG and then FAT2 in glibenclamide. Like 5-HD, the presence of these compounds did not affect the fatigue kinetics during FAT-1 when compared to FAT1-Con. Furthermore, none of these compounds blocked the protective effects of FPC on fatigue kinetics during FAT2-Gli as the decrease in peak tetanic force and increase in unstimulated force during FAT2-Gli were similar whether FAT1 was elicited in control (FAT1-CON) conditions or in the presence of a Chel or the ROS scavengers (Tables 5.1-5.3).

FAT1 DURATION

Next, it was determined how long FAT1-Con should be to observe the effects on peak tetanic force and unstimulated force during FAT2. Considering the large effects of glibenclamide on peak tetanic force and unstimulated force, the protocol here was to elicit FAT1 under control conditions with duration varying between 30 and 180 sec under control conditions and FAT2 60 min later in the presence of 10 μM glibenclamide, using a different FDB bundle for each FAT1 time period.

Mean peak tetanic force decreased to 40% of pre-fatigue force in 30 sec during delFAT1-GLI (Fig. 5.7A). If FAT2-Gli is preceded by a 30 sec bout of FAT1-Con, the reduction in peak tetanic force generation during FAT2-Gli was significantly less as the peak tetanic force averaged 45% of pre-fatigue peak tetanic force. As the duration of FAT1-Con was increased to 60, 90 and 180 s long, mean peak tetanic forces at 30 s of FAT2-Gli were respectively 60%, 56% and 70%. Similarly, peak tetanic force at 60 sec of FAT2-Gli increased from 16% to 37% as the duration of FAT1 was increased from 0 to 180 s.

Unstimulated force at 30 sec of FAT2-Gli was completely abolished when the duration of FAT1-Con was or exceeded 90 s (Fig. 5.7B). The unstimulated force at 180 s, however, was reduced when FAT1-Con duration was increased from 0 to 90 s, but it did not decrease further with a prolongation of FAT1-Con to 180 s. Recovery of peak tetanic force following FAT2-Gli was also improved as the duration of FAT1-Con increased from 0 to 180 s (Fig. 5.7C).

FIGURE 5.7

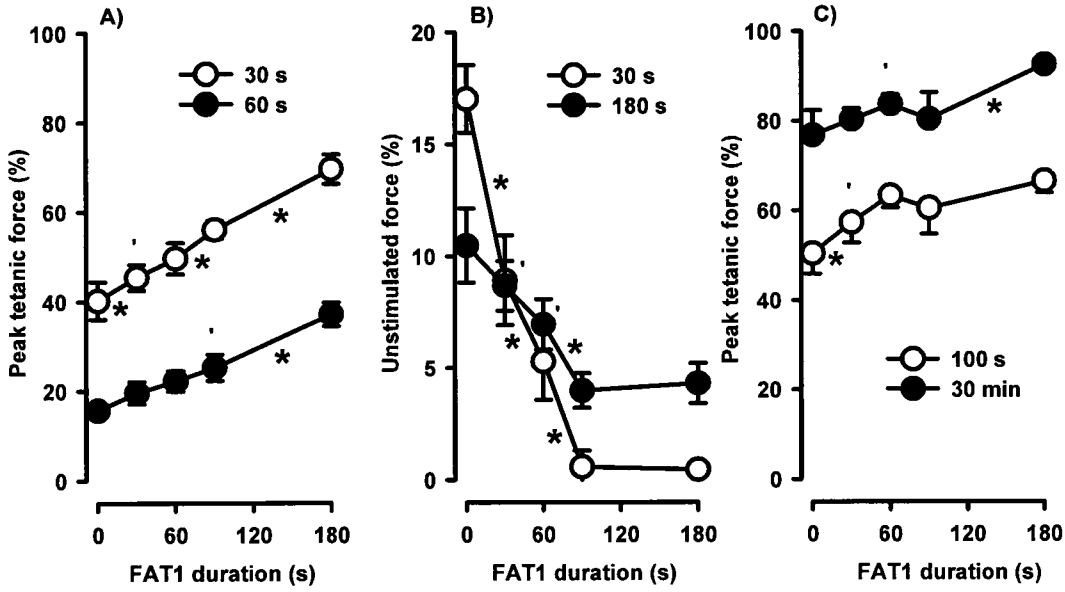

Figure 5.7 The effects of FAT1 duration on A) peak tetanic force and B) unstimulated force during FAT2 in the presence of 10 μM glibenclamide and C) peak tetanic force recovery following FAT2. FAT1 was elicited under control conditions with duration varying between 30 and 180 s while FAT2 was elicited 60 min after FAT1 in the presence of 10 μM glibenclamide added 30 min prior to FAT2. Data at Time 0, which represents no FAT1 preceding FAT2, are from delFAT1 from Fig. 5.1-5.3. Peak tetanic force and unstimulated force are expressed as a percent of the pre-fatigue peak tetanic force. A) Peak tetanic force after 30 and 60 s during FAT2. B) Unstimulated force after 30 and 180 s during FAT2. C) Peak tetanic force after 100 s and 30 min of recovery following FAT2. Vertical bars represent the S.E. of 5 muscle bundles.

' Significantly different from 0 sec, ANOVA and L.S.D. $P<0.05$.

* Significant changes, ANOVA and L.S.D. $P<0.05$.

DISCUSSION

The major findings of this study are: 1. the decreases in peak tetanic $Ca^{2+}i$ and force were significantly slower while the increases in unstimulated $Ca^{2+}i$ and force were significantly less during a second fatigue bout (FAT2) than during a first fatigue bout (FAT1) elicited 60 min earlier; 2. The differences between FAT1 and FAT2 were especially marked when wild type FDB were exposed to glibenclamide to block KATP channels during FAT2; 3. The contractile dysfunctions observed in sKATP channel deficient muscles during FAT1 were completely abolished during FAT2; 4. The mechanism of FPC is not the same as IPC. These results suggest that an acute physiological process occurs following one fatigue bout resulting in an increased fatigue resistance and a decreased dependency on sKATP channel for myoprotection. This novel phenomenon was termed "Fatigue Preconditioning" (FPC).

During the first fatigue bout (FAT1), peak tetanic $Ca^{2+}i$ and force decreased at a faster rate while the increases in unstimulated $Ca^{2+}i$ and force were greater in Kir6.2$^{-/-}$ and glibenclamide-exposed FDB than in control wild type FDB. After FAT1, peak tetanic $Ca^{2+}i$ and force recovered to a lesser extent in glibenclamide-exposed than in control muscles. These results are in agreement with those reported by Cifelli *et al.* (2007). Also, Kir6.2$^{-/-}$ FDB developed significantly less unstimulated force during FAT1 and had greater force recovery following FAT1 in the presence of 1 μM verapamil; these results are also in agreement with a previous study (Cifelli *et al.*, 2008). So, these observations will not be discussed here.

An increased fatigue resistance and a lack of dependence on KATP channel did not occur when the first fatigue bout was delayed (delFAT1) to be elicited at the same time as

FAT2 suggesting that the differences between FAT1 and FAT2 cannot be associated to a time effect. FDB muscles are primarily composed of type IIA and IIX (Raymackers *et al.*, 2000) and peak tetanic force recovery after FAT1-Con was only to 90% of the pre-fatigue level. If the permanent force loss is related to fibre damage for a particular fibre type, one can then argue that the differences in fatigue kinetics between FAT1 and FAT2 are due to differences in the composition of fibre types that can still contract during FAT2. This possibility is unlikely because all tested single fibres (n=23) fully recovered their unstimulated and peak tetanic $Ca^{2+}i$ after FAT1-Con and the increases in unstimulated $Ca^{2+}i$ were still less while the decreases in peak tetanic $Ca^{2+}i$ were slower during FAT2. Furthermore, the differences in unstimulated $Ca^{2+}i$ and peak tetanic $Ca^{2+}i$ between FAT2 and FAT1 were especially marked in the presence of glibenclamide as observed with unstimulated force and peak tetanic force. It's important to note that the lack of a glibenclamide effect during FAT2 cannot be explained by a loss of efficacy in blocking K_{ATP} channels because $Kir6.2^{-/-}$ FDB also had slower fatigue rate, did not develop any unstimulated force and recovered force better when FAT2 was elicited after FAT1 in the presence of verapamil (to prevent the development of contractile dysfunctions).

As discussed by Cifelli *et al.* (2007), an hypoxic/anoxic core during fatigue at 37°C is expected to occur in small FDB bundles according to Barclays' modelling of O_2 supply in isolated muscles (Barclay, 2005). Short bouts of ischemia are known to increase the capacity of both cardiac and skeletal muscle to survive long and damaging ischemic period, a phenomenon known as ischemic preconditioning (Pang & Forrest, 1995; Oldenburg *et al.*, 2002). It is unlikely that an hypoxic/anoxic core in FDB bundles

during FAT1 is the cause for the changes in fatigue kinetics during FAT2 because the changes were observed for unstimulated Ca^{2+}_i and peak tetanic Ca^{2+}_i in single fibres for which a hypoxic core is not expected.

MECHANISM OF FPC IS DIFFERENT FROM IPC

There is a large amount of evidence for the role of adenosine receptors and sKATP channels in IPC of cardiac and skeletal muscle (Pang *et al.*, 1997a; Pang *et al.*, 1997b; Gurke *et al.*, 2000; Cohen *et al.*, 2001; Garlid & Paucek, 2001; Bushell *et al.*, 2002; Costa *et al.*, 2005; Zheng *et al.*, 2007). Adenosine or application of an adenosine receptor agonist has been shown to cause opening of sKATP channels. It is believed that this will lead to a shortened action potential duration (Forrest *et al.*, 1997; Papanastasiou *et al.*, 1999; Zheng *et al.*, 2007), thus reducing Ca^{2+} influx and resulting in sparing of high-energy phosphates (Nichols & Lederer, 1991; Nichols *et al.*, 1991; Findlay, 1994; Halestrap *et al.*, 2007). While some researchers have shown a preservation of ATP and reduced lactate production with IPC in skeletal muscle (Pang *et al.*, 1995; Pang *et al.*, 1997a; Moses *et al.*, 2005), others have not (Gurke *et al.*, 1996; Mattei *et al.*, 2000). Furthermore, the role of adenosine and sKATP channels themselves is controversial. Activation of adenosine receptors using adenosine or R-PIA or antagonists such as 8-SPT show conflicting results, as does using glibenclamide (sKATP channel blocker), and HMR-1098 or cromakalim (sKATP channel openers) (Gurke *et al.*, 2000). Furthermore, it was shown in myocardial tissue from Kir6.2$^{-/-}$ mice that sKATP channels were required for IPC (Suzuki *et al.*, 2001; Suzuki *et al.*, 2002; Gumina *et al.*, 2003; Gumina *et al.*, 2007). However, based on our results using R-PIA there is no evidence that sKATP channels are

required for FPC; indeed, Kir6.2$^{-/-}$ FDB bundles were afforded the protective effects of FPC.

The role of PKC, mKATP channels and ROS in FPC also appears to be different than for IPC. mKATP channels have been strongly implicated in IPC (Garlid *et al.*, 1997; Cohen *et al.*, 2001; Garlid & Paucek, 2001; Garlid *et al.*, 2003; O'Rourke, 2004; Costa & Garlid, 2008). As shown in Tables 5.1-5.3, the use of selective mKATP channel antagonist 5-HD suggest that mKATP channels are not involved in FPC. However, evidence for the existence of mKATP channels is debatable. The role for mKATP channels in IPC was first proposed by Garlid *et al* (1997), and is supported based solely on pharmacological data. However, data from Kir6.2$^{-/-}$ mice and an inability to sequence mKATP channel genes suggests these channels may not exist. In fact, 5-HD has been shown to be metabolized to 5-hydroxydecanoyl Co-A, a respiratory chain intermediate substrate which will attenuate the mitochondrial metabolic inhibition afforded by IPC (Hanley *et al.*, 2002; Lim *et al.*, 2002; Hanley *et al.*, 2003; Hanley *et al.*, 2005). Furthermore, diazoxide, a selective mKATP channel opener, was shown to inhibit succinate-supported mitochondrial respiration (Hanley *et al.*, 2002; Lim *et al.*, 2002; Minners *et al.*, 2007). Therefore, it is hypothesized that these pharmaceutical approaches may be acting by reducing the deleterious ROS production.

The lack of effect of chelerytherine, a non-selective PKC inhibitor, to abolish FPC was unexpected, given the well-accepted role of PKC in the signalling cascade of IPC (Sato *et al.*, 1998; Hopper *et al.*, 2000; Inagaki *et al.*, 2003a; Inagaki *et al.*, 2003b; Costa & Garlid, 2008). Furthermore, NAC, tiron and 2-MPG, all ROS scavengers, failed to abolish the protective effects of FPC. NAC is a non-specific antioxidant, which has been

shown to reduce H_2O_2, OH• and hypochlorous acid, but not superoxide (Moldeus *et al.*, 1986; Aruoma *et al.*, 1989). Alternatively, tiron acts to scavenge both superoxide and H_2O_2, but not OH• (Greenstock & Miller, 1975; Mohanraj *et al.*, 1998). 2-MPG is a highly selective scavenger of OH•. Superoxide and OH• scavengers have repeatedly been shown to abolish IPC in skeletal muscle (Murata *et al.*, 2001; O'Rourke, 2004; Sato *et al.*, 2005; Minners *et al.*, 2007), but do not appear to affect FPC. Thus, given the strong reliance of IPC on PKC-mKATP-ROS signalling, it appears that FPC is completely unrelated to IPC.

Therefore, our results show that the mechanistic pathway of FPC is different from IPC. Interestingly, this new phenomenon is temperature dependent because it is not observed when FAT1 is performed at 22°C (Chin & Allen, 1997; Moopanar & Allen, 2005). Temperature preconditioning of the heart, which also requires PKCε activation and ROS production, was observed with a combination of repeated rewarming with hypothermia (37° and 26°C) cycles, but not with a single period of 26° (Khaliulin *et al.*, 2007). Thus, the mechanism for temperature preconditioning is not the same as FPC.

In conclusion, this study reports for the first time that FDB muscles have the capability to acutely respond to a muscular activity where the fatigue resistance increases and the dependency on KATP channel to prevent contractile dysfunction decreases within 60 min following one fatigue bout at 37°C. This novel phenomenon was termed "Fatigue Preconditioning".

CHAPTER 6 - DISCUSSION

The findings of this study are that during fatigue, abolishing sKATP channel activity at 37°C leads to several contractile dysfunctions that include: **1.** excessive membrane depolarization, which can cause **2.** Na^+ channel inactivation and reduced fibre excitability; and **3.** deleterious Ca^{2+} influx through L-type Ca^{2+} channels, which leads to **4.** a possible greater ROS formation. These contractile dysfunctions lead to the production of several contractile dysfunctions, including partially or completely supercontracted single muscle fibres, greater increases in unstimulated $Ca^{2+}{}_i$ and unstimulated force, lower force recovery, and fibre damage. As a result of these contractile dysfunctions, there is **5.** an apparent faster rate of fatigue in sKATP channel deficient muscle.

Furthermore, we discovered a physiological process that occurs following one fatigue bout whereby muscle acutely adapts to result in an increased fatigue resistance and a decreased dependency on sKATP channels for myoprotection. We termed this novel process "Fatigue Preconditioning" (FPC).

Physiological function of sKATP channels during fatigue

Prior to this thesis, work performed primarily by Gong *et al* (2000, 2003) and Matar *et al* (2000) focused on the role of opening sKATP channels during fatigue (Gong *et al.*, 2000; Matar *et al.*, 2000; Gong *et al.*, 2003). They observed that channel opening reduced AP amplitude during contractions (Fig. 6.1A) (Gong *et al.*, 2003). As a consequence of the lowered AP amplitude, the SR Ca^{2+} release is reduced (Burton & Smith, 1997a), which has two effects on ATP utilization:

FIGURE 6.1

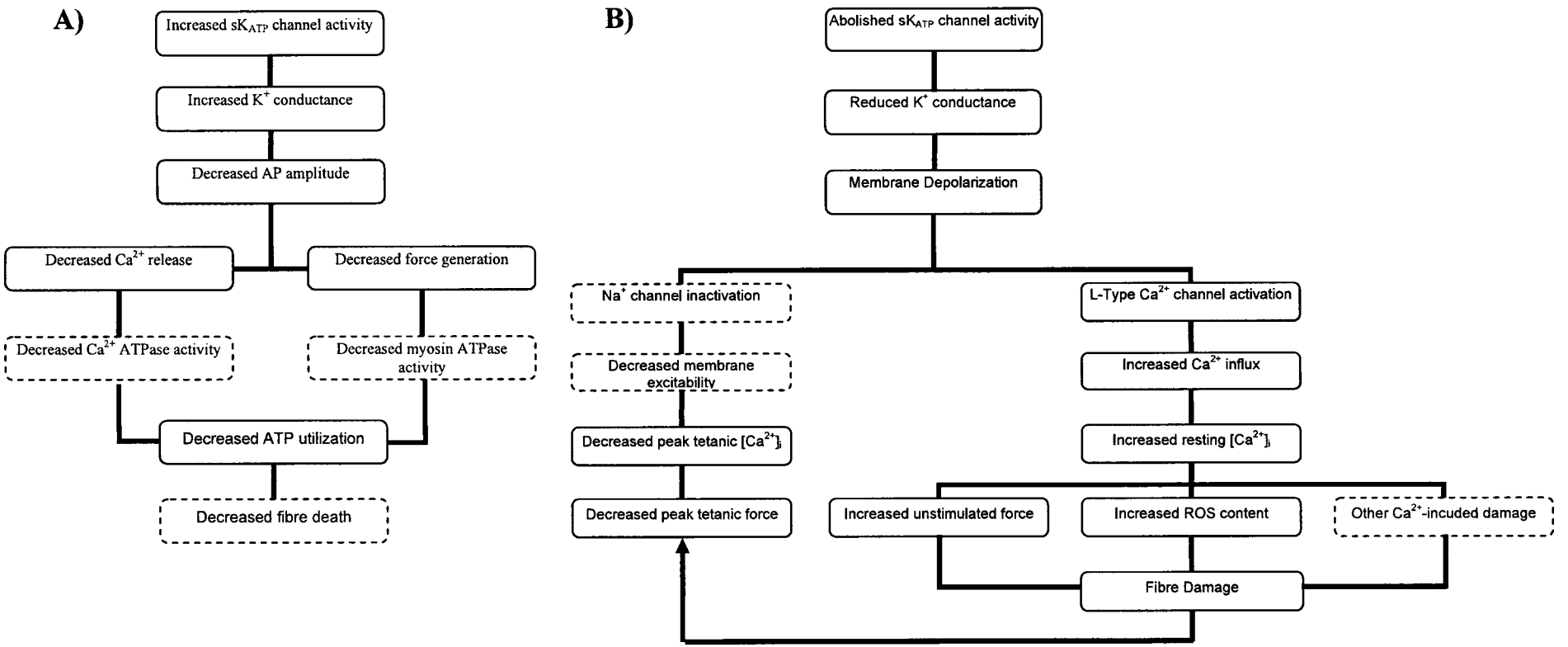

Figure 6.1. Physiological functions of the sKATP channel during fatigue in skeletal muscle. Pathways in patterned boxes are those previously demonstrated. Pathways in grey boxes indicate those determined from this research. Pathways in dashed boxes are proposed, but yet to be shown. For references, refer to text. Figure modified from (Bourassa, 2006; Cifelli, 2006).

1. decreased SR ATPase activity, and 2. decreased myosin ATPase due to less actin-myosin crossbridge formation. Matar *et al* (2000) demonstrated that the application of pinacidil, a sKATP channel opener, during fatigue led to ATP preservation in mouse soleus and FDB muscle (Matar *et al.*, 2000), and a corresponding faster rate of fatigue. Therefore, closing sKATP channels should have opposite effects on ATP. Li (M.Sc. thesis) showed greater ATP utilization and depletion in Kir6.2$^{-/-}$ FDB, but not with glibenclamide, suggesting a possible difference between acute and chronic sKATP channel activity abolishment. However, greater ATP depletion when channel activity was abolished with glibenclamide was also observed by Matar *et al* (2000) with mouse soleus muscle during fatigue (Matar *et al.*, 2000) and by Gramolini and Renaud (1997) using frog sartorius muscle during metabolic inhibition (Gramolini & Renaud, 1997).

Further observed by Matar et al (2000) and Gong et al (2000) was that abolishing sKATP channel activity using glibenclamide had no effect on rate of fatigue in EDL or soleus muscle (Gong *et al.*, 2000; Matar *et al.*, 2000). This was not due to a lack of sKATP channel activity because: a) Kir6.2$^{-/-}$ muscle showed similar results; and b) they observed a greater development of unstimulated force during fatigue and reduced force recovery in sKATP channel deficient muscle compared to wild type. Furthermore, pinacidil and glibenclamide had no effect on contractile function in Kir6.2$^{-/-}$ muscle, suggesting that the effects on unstimulated force and force recovery were due to a modulation of sKATP channel activity.

Therefore, one question is why opening channels gives a faster rate of fatigue, and yet closing channels does not show the opposite effect. For the first time, this study shows an apparent faster rate of fatigue observed in sKATP channel deficient single fibres

and muscle bundles. The next question is then how both activation and inhibition of channel activity can lead to the same result.

From these results, it appears that while sKATP channels may modulate ATP utilization by directly altering membrane excitability during contractions, reducing Ca^{2+} release and force production, it also suggests that they may play other roles in myoprotection. Gramolini and Renaud (1997) demonstrated that between contractions, blocking sKATP channels during metabolic inhibition resulted in smaller increases in K^+ conductance and large membrane depolarization to -50 mV, while in the absence of glibenclamide there was no effect (Gramolini & Renaud, 1997). This study now confirms that during fatigue, similar membrane depolarizations to -30 mV also occur with the application of glibenclamide (Figure 6.1B). This has two major effects. Firstly, Na^+ channel slow inactivation will occur, reducing membrane excitability and therefore force generation (Ruff, 1999). Evidence for this occurring during fatigue came from the single fibre experiments where undamaged fibres skipped contractions or completely stopped contracting during the fatigue period (Chapter 2). Secondly, these membrane depolarizations activate L-type Ca^{2+} channels (Lamb & Walsh, 1987; Tanabe *et al.*, 1990b), resulting in excessive Ca^{2+} influx and possible RYR activation (Chapter 3). The rise in $[Ca^{2+}]i$ then leads to an increased unstimulated force (Chapter 2, 3). It is known that a prolonged rise in $[Ca^{2+}]i$ can cause fibre damage by increasing ROS production or calpain activation. The slower rate of fatigue, reduced unstimulated force, and faster force recovery in the presence of a ROS scavenger in sKATP channel deficient muscle supports the possibility of altered activity due to greater ROS production (Chapter 4).

Therefore, while activating sKATP channels increases the rate of fatigue, blocking sKATP channels leads to the development of numerous contractile dysfunctions, and as such, also an apparent faster rate of fatigue. It is possible that if the contractile dysfunctions that occur when sKATP channel activity are eliminated, then a slower rate of fatigue may occur in sKATP channel deficient muscle. When the L-type Ca^{2+} channels were blocked using verapamil, a slower rate of fatigue, abolished unstimulated force and improved force recovery was observed in Kir6.2$^{-/-}$ muscle (Chapter 3). Therefore, many of the contractile dysfunctions that sKATP channel deficient muscle develops during fatigue were abolished. However, there is still the large membrane depolarization that occurs upstream of the abolished Ca^{2+} influx. It is possible that if the large depolarization was counteracted, a rate of fatigue even slower than that of wild type muscle would be observed.

On this basis, it is proposed that sKATP channels are crucial in preventing the development of contractile dysfunctions and fibre damage during fatigue by: 1. reducing AP amplitude during contractions to prevent ATP depletion; and 2. preventing excessive membrane depolarization and thus deleterious $[Ca^{2+}]i$ influx.

Reliance of sKATP channels for myoprotection during multiple fatigue bouts

So far, the role of sKATP channels during a single fatigue bout has been to prevent the development of numerous contractile dysfunctions. However, in Chapter 5, a novel situation is reported that when one fatigue bout (FAT1) was followed by a subsequent fatigue bout (FAT2) during which time sKATP channel activity was abolished, development of any contractile dysfunctions was not observed. This phenomenon was termed 'Fatigue Preconditioning' (FPC). In fact, fatigue kinetics and calcium handling

during the second fatigue bout were identical to that of wild type muscle under control conditions. This suggests that other mechanisms exist where muscle can protect themselves. The mechanisms of FPC appear to be dissimilar from ischemic preconditioning (IPC). This is based on the fact that pharmacological approaches that either abolish or induce protection with IPC had no effect on FPC. It is possible that one or more intracellular signalling pathways is inducing myoprotection, which could be affecting muscle excitability or energy metabolism.

Interestingly, Thabet *et al* (2005) observed that in Kir6.2$^{-/-}$ mouse exposed to a 4-week treadmill running protocol, there was evidence for a reduced reliance on sKATP channels in hindlimb muscle. The presence of centrally nucleated fibres, which is evidence for muscle regeneration, and the absence of any recent fibre damage, suggests that muscles were damaged at the onset of the four weeks, but were not repetivively damaged with continued running. . Thus, reliance on sKATP channels for myoprotection was also reduced over time *in vivo*.

Thus, it appears that sKATP channels are necessary for myoprotection during a single fatigue bout, and blocking channel activity leads to the development of contractile dysfunctions and an apparent faster rate of fatigue. However, during subsequent fatigue bouts separated by short periods of time, sKATP channels are not necessary for (not involved in) myoprotection.

REFERENCES

Aguilar-Bryan L, Nichols CG, Wechsler SW, Clement JPt, Boyd AE, 3rd, Gonzalez G, Herrera-Sosa H, Nguy K, Bryan J & Nelson DA. (1995). Cloning of the beta cell high-affinity sulfonylurea receptor: a regulator of insulin secretion. *Science (New York, NY* **268,** 423-426.

Allard B, Lazdunski M & Rougier O. (1995). Activation of ATP-dependent K^+ channels by metabolic poisoning in adult mouse skeletal muscle: role of intracellular Mg^{2+} and pH. *The Journal of physiology* **485 (Pt 2),** 283-296.

Allen DG, Kabbara AA & Westerblad H. (2002). Muscle fatigue: the role of intracellular calcium stores. *Can J Appl Physiol* **27,** 83-96.

Allen DG, Lamb GD & Westerblad H. (2008). Impaired calcium release during fatigue. *J Appl Physiol* **104,** 296-305.

Allen DG, Lannergren J & Westerblad H. (1995). Muscle cell function during prolonged activity: cellular mechanisms of fatigue. *Experimental physiology* **80,** 497-527.

Allen DG, Lee JA & Westerblad H. (1989). Intracellular calcium and tension during fatigue in isolated single muscle fibres from Xenopus laevis. *The Journal of physiology* **415,** 433-458.

Allen DG, Whitehead NP & Yeung EW. (2005). Mechanisms of stretch-induced muscle damage in normal and dystrophic muscle: role of ionic changes. *The Journal of physiology* **567,** 723-735.

Allen DL, Harrison BC, Maass A, Bell ML, Byrnes WC & Leinwand LA. (2001). Cardiac and skeletal muscle adaptations to voluntary wheel running in the mouse. *J Appl Physiol* **90,** 1900-1908.

Anderson CL, De Repentigny Y, Cifelli C, Marshall P, Renaud JM, Worton RG & Kothary R. (2006). The mouse dystrophin muscle promoter/enhancer drives expression of mini-dystrophin in transgenic mdx mice and rescues the dystrophy in these mice. *Mol Ther* **14,** 724-734.

Antcliff JF, Haider S, Proks P, Sansom MS & Ashcroft FM. (2005). Functional analysis of a structural model of the ATP-binding site of the K_{ATP} channel Kir6.2 subunit. *The EMBO journal* **24,** 229-239.

Anzai K, Ogawa K, Ozawa T & Yamamoto H. (2000). Oxidative modification of ion channel activity of ryanodine receptor. *Antioxid Redox Signal* **2,** 35-40.

Arbogast S & Reid MB. (2004). Oxidant activity in skeletal muscle fibers is influenced by temperature, CO_2 level, and muscle-derived nitric oxide. *Am J Physiol Regul Integr Comp Physiol* **287,** R698-705.

Aruoma OI, Halliwell B, Hoey BM & Butler J. (1989). The antioxidant action of N-acetylcysteine: its reaction with hydrogen peroxide, hydroxyl radical, superoxide, and hypochlorous acid. *Free Radic Biol Med* **6,** 593-597.

Ashcroft FM. (2000). *Ion channels and disease : channelopathies*. Academic Press, San Diego.

Ashcroft FM. (2006). K_{ATP} channels and insulin secretion: a key role in health and disease. *Biochemical Society transactions* **34,** 243-246.

Ashcroft FM & Gribble FM. (1998). Correlating structure and function in ATP-sensitive K^+ channels. *Trends in neurosciences* **21,** 288-294.

Ashford ML, Sturgess NC, Trout NJ, Gardner NJ & Hales CN. (1988). Adenosine-5'-triphosphate-sensitive ion channels in neonatal rat cultured central neurones. *Pflugers Arch* **412,** 297-304.

Aughey RJ, Murphy KT, Clark SA, Garnham AP, Snow RJ, Cameron-Smith D, Hawley JA & McKenna MJ. (2007). Muscle Na^+-K^+-ATPase activity and isoform adaptations to intense interval exercise and training in well-trained athletes. *J Appl Physiol* **103,** 39-47.

Baczko I, Giles WR & Light PE. (2003). Resting membrane potential regulates Na^+-Ca^{2+} exchange-mediated Ca^{2+} overload during hypoxia-reoxygenation in rat ventricular myocytes. *The Journal of physiology* **550,** 889-898.

Baczko I, Giles WR & Light PE. (2004). Pharmacological activation of plasma-membrane K_{ATP} channels reduces reoxygenation-induced Ca^{2+} overload in cardiac myocytes via modulation of the diastolic membrane potential. *British journal of pharmacology* **141,** 1059-1067.

Baczko I, Jones L, McGuigan CF, Manning Fox JE, Gandhi M, Giles WR, Clanachan AS & Light PE. (2005). Plasma membrane K_{ATP} channel-mediated cardioprotection involves posthypoxic reductions in calcium overload and contractile dysfunction: mechanistic insights into cardioplegia. *Faseb J* **19,** 980-982.

Baker AJ, Brandes R, Schendel TM, Trocha SD, Miller RG & Weiner MW. (1994). Energy use by contractile and noncontractile processes in skeletal muscle estimated by ^{31}P-NMR. *The American journal of physiology* **266,** C825-831.

Balnave CD & Allen DG. (1995). Intracellular calcium and force in single mouse muscle fibres following repeated contractions with stretch. *The Journal of physiology* **488 (Pt 1),** 25-36.

Bangsbo J, Gollnick PD, Graham TE, Juel C, Kiens B, Mizuno M & Saltin B. (1990). Anaerobic energy production and O_2 deficit-debt relationship during exhaustive exercise in humans. *The Journal of physiology* **422,** 539-559.

Barclay CJ. (2005). Modelling diffusive O_2 supply to isolated preparations of mammalian skeletal and cardiac muscle. *J Muscle Res Cell Motil* **26,** 225-235.

Barrett-Jolley R, Comtois A, Davies NW, Stanfield PR & Standen NB. (1996). Effect of adenosine and intracellular GTP on K_{ATP} channels of mammalian skeletal muscle. *The Journal of membrane biology* **152,** 111-116.

Barrett-Jolley R & McPherson GA. (1998). Characterization of K_{ATP} channels in intact mammalian skeletal muscle fibres. *British journal of pharmacology* **123,** 1103-1110.

Belcastro AN, Shewchuk LD & Raj DA. (1998). Exercise-induced muscle injury: a calpain hypothesis. *Mol Cell Biochem* **179,** 135-145.

Bellinger AM, Reiken S, Carlson C, Mongillo M, Liu X, Rothman L, Matecki S, Lacampagne A & Marks AR. (2009). Hypernitrosylated ryanodine receptor calcium release channels are leaky in dystrophic muscle. *Nat Med* **15,** 325-330.

Bellinger AM, Reiken S, Dura M, Murphy PW, Deng SX, Landry DW, Nieman D, Lehnart SE, Samaru M, LaCampagne A & Marks AR. (2008). Remodeling of ryanodine receptor complex causes "leaky" channels: a molecular mechanism for decreased exercise capacity. *Proceedings of the National Academy of Sciences of the United States of America* **105,** 2198-2202.

Bennetts B, Parker MW & Cromer BA. (2007). Inhibition of skeletal muscle CLC-1 chloride channels by low intracellular pH and ATP. *The Journal of biological chemistry* **282,** 32780-32791.

Blanchard EM & Solaro RJ. (1984). Inhibition of the activation and troponin calcium binding of dog cardiac myofibrils by acidic pH. *Circulation research* **55,** 382-391.

Bolli R & Marban E. (1999). Molecular and cellular mechanisms of myocardial stunning. *Physiological reviews* **79,** 609-634.

Bouclin R, Charbonneau E & Renaud JM. (1995). Na^+ and K^+ effect on contractility of frog sartorius muscle: implication for the mechanism of fatigue. *The American journal of physiology* **268,** C1528-1536.

Bourassa F. (2006). K_{ATP} channel deficiency causes fiber damage and impairs Ca^{2+} release during fatigue *in vitro*. In *Cellular and Molecular Medicine*. University of Ottawa, Ottawa.

Brookes PS, Yoon Y, Robotham JL, Anders MW & Sheu SS. (2004). Calcium, ATP, and ROS: a mitochondrial love-hate triangle. *American journal of physiology* **287,** C817-833.

Brum G, Rios E & Stefani E. (1988). Effects of extracellular calcium on calcium movements of excitation-contraction coupling in frog skeletal muscle fibres. *The Journal of physiology* **398,** 441-473.

Bruton JD, Lannergren J & Westerblad H. (1998). Effects of CO_2-induced acidification on the fatigue resistance of single mouse muscle fibers at 28 degrees C. *J Appl Physiol* **85,** 478-483.

Bruton JD, Place N, Yamada T, Silva JP, Andrade FH, Dahlstedt AJ, Zhang SJ, Katz A, Larsson NG & Westerblad H. (2008). Reactive oxygen species and fatigue-induced prolonged low-frequency force depression in skeletal muscle fibres of rats, mice and SOD2 overexpressing mice. *The Journal of physiology* **586,** 175-184.

Bryant SH & Morales-Aguilera A. (1971). Chloride conductance in normal and myotonic muscle fibres and the action of monocarboxylic aromatic acids. *The Journal of physiology* **219,** 367-383.

Burton FL & Smith GL. (1997a). The effect of cromakalim on intracellular [Ca^{2+}] in isolated rat skeletal muscle during fatigue and metabolic blockade. *Experimental physiology* **82,** 469-483.

Burton FL & Smith GL. (1997b). The effect of cromokalim on intracellular [Ca2+] in isolated rat skeletal muscle during fatigue and metabolic blockade. *Exp Physiol* **82,** 469-483.

Bushell AJ, Klenerman L, Davies H, Grierson I, McArdle A & Jackson MJ. (2002). Ischaemic preconditioning of skeletal muscle 2. Investigation of the potential mechanisms involved. *J Bone Joint Surg Br* **84,** 1189-1193.

Cady EB, Jones DA, Lynn J & Newham DJ. (1989). Changes in force and intracellular metabolites during fatigue of human skeletal muscle. *The Journal of physiology* **418,** 311-325.

Cairns SP, Hing WA, Slack JR, Mills RG & Loiselle DS. (1998). Role of extracellular [Ca^{2+}] in fatigue of isolated mammalian skeletal muscle. *J Appl Physiol* **84,** 1395-1406.

Chance B, Sies H & Boveris A. (1979). Hydroperoxide metabolism in mammalian organs. *Physiological reviews* **59,** 527-605.

Chase PB & Kushmerick MJ. (1988). Effects of pH on contraction of rabbit fast and slow skeletal muscle fibers. *Biophysical journal* **53,** 935-946.

Chasiotis D, Bergstrom M & Hultman E. (1987). ATP utilization and force during intermittent and continuous muscle contractions. *J Appl Physiol* **63,** 167-174.

Chin ER & Allen DG. (1996). The role of elevations in intracellular [Ca^{2+}] in the development of low frequency fatigue in mouse single muscle fibres. *The Journal of physiology* **491 (Pt 3),** 813-824.

Chin ER & Allen DG. (1997). Effects of reduced muscle glycogen concentration on force, Ca^{2+} release and contractile protein function in intact mouse skeletal muscle. *The Journal of physiology* **498 (Pt 1),** 17-29.

Chin ER, Balnave CD & Allen DG. (1997). Role of intracellular calcium and metabolites in low-frequency fatigue of mouse skeletal muscle. *The American journal of physiology* **272,** C550-559.

Chutkow WA, Samuel V, Hansen PA, Pu J, Valdivia CR, Makielski JC & Burant CF. (2001). Disruption of SUR2-containing K_{ATP} channels enhances insulin-stimulated glucose uptake in skeletal muscle. *Proceedings of the National Academy of Sciences of the United States of America* **98,** 11760-11764.

Chutkow WA, Simon MC, Le Beau MM & Burant CF. (1996). Cloning, tissue expression, and chromosomal localization of SUR2, the putative drug-binding subunit of cardiac, skeletal muscle, and vascular K_{ATP} channels. *Diabetes* **45,** 1439-1445.

Cifelli C. (2006). Impairment of force development in K_{ATP} channel deficient skeletal muscle involves calcium influx through L-type calcium channels. In *Cellular and Molecular Medicine*. University of Ottawa, Ottawa.

Cifelli C, Boudreault L, Gong B, Bercier JP & Renaud JM. (2008). Contractile dysfunctions in ATP-dependent K^+ channel-deficient mouse muscle during fatigue involve excessive depolarization and Ca^{2+} influx through L-type Ca^{2+} channels. *Experimental physiology* **93,** 1126-1138.

Cifelli C, Bourassa F, Gariepy L, Banas K, Benkhalti M & Renaud JM. (2007). K_{ATP} channel deficiency in mouse flexor digitorum brevis causes fibre damage and impairs Ca^{2+} release and force development during fatigue in vitro. *The Journal of physiology* **582,** 843-857.

Clausen T. (1996). The Na^+, K^+ pump in skeletal muscle: quantification, regulation and functional significance. *Acta physiologica Scandinavica* **156,** 227-235.

Clausen T. (2003). Na^+-K^+ pump regulation and skeletal muscle contractility. *Physiological reviews* **83,** 1269-1324.

Clausen T, Andersen SL & Flatman JA. (1993). Na^+-K^+ pump stimulation elicits recovery of contractility in K^+-paralysed rat muscle. *The Journal of physiology* **472,** 521-536.

Clement JPt, Kunjilwar K, Gonzalez G, Schwanstecher M, Panten U, Aguilar-Bryan L & Bryan J. (1997). Association and stoichiometry of K_{ATP} channel subunits. *Neuron* **18,** 827-838.

Cohen MV, Yang XM, Liu GS, Heusch G & Downey JM. (2001). Acetylcholine, bradykinin, opioids and phenylephrinie, but not adenosine, trigger preconditioning by generating free radicals and opening mitochondrial K_{ATP} channels. *Circulation research* **89,** 273-278.

Comtois A, Light P & Renaud JM. (1995). Effect of tolbutamide on the rate of fatigue and recovery in frog sartorius muscle. *J Pharmacol Exp Ther* **274,** 1061-1066.

Cook DL & Hales CN. (1984). Intracellular ATP directly blocks K^+ channels in pancreatic B-cells. *Nature* **311,** 271-273.

Costa AD & Garlid KD. (2008). Intramitochondrial signaling: interactions among mitoK_{ATP}, $PKC_{epsilon}$, ROS, and MPT. *Am J Physiol Heart Circ Physiol* **295,** H874-882.

Costa AD, Garlid KD, West IC, Lincoln TM, Downey JM, Cohen MV & Critz SD. (2005). Protein kinase G transmits the cardioprotective signal from cytosol to mitochondria. *Circulation research* **97,** 329-336.

Dahlstedt AJ, Katz A, Wieringa B & Westerblad H. (2000). Is creatine kinase responsible for fatigue? Studies of isolated skeletal muscle deficient in creatine kinase. *FASEB J* **14,** 982-990.

Davidson GA & Berman MC. (1996). Mechanism of thermal uncoupling of Ca^{2+}-ATPase of sarcoplasmic reticulum as revealed by thapsigargin stabilization. *Biochim Biophys Acta* **1289,** 187-194.

Davies NW. (1990). Modulation of ATP-sensitive K^+ channels in skeletal muscle by intracellular protons. *Nature* **343,** 375-377.

Davies NW, Standen NB & Stanfield PR. (1992). The effect of intracellular pH on ATP-dependent potassium channels of frog skeletal muscle. *The Journal of physiology* **445,** 549-568.

de Paoli FV, Overgaard K, Pedersen TH & Nielsen OB. (2007). Additive protective effects of the addition of lactic acid and adrenaline on excitability and force in isolated rat skeletal muscle depressed by elevated extracellular K^+. *The Journal of physiology* **581,** 829-839.

Debold EP, Romatowski J & Fitts RH. (2006). The depressive effect of Pi on the force-pCa relationship in skinned single muscle fibers is temperature dependent. *American journal of physiology* **290,** C1041-1050.

Decrouy A, Renaud JM, Davis HL, Lunde JA, Dickson G & Jasmin BJ. (1997). Mini-dystrophin gene transfer in mdx4cv diaphragm muscle fibers increases sarcolemmal stability. *Gene Ther* **4,** 401-408.

Duke AM & Steele DS. (2001). Interdependent effects of inorganic phosphate and creatine phosphate on sarcoplasmic reticulum Ca^{2+} regulation in mechanically skinned rat skeletal muscle. *The Journal of physiology* **531,** 729-742.

Dulhunty AF. (1979). Distribution of potassium and chloride permeability over the surface and T-tubule membranes of mammalian skeletal muscle. *The Journal of membrane biology* **45,** 293-310.

Dulhunty AF & Gage PW. (1988). Effects of extracellular calcium concentration and dihydropyridines on contraction in mammalian skeletal muscle. *The Journal of physiology* **399,** 63-80.

Duty S & Allen DG. (1995). The effects of glibenclamide on tetanic force and intracellular calcium in normal and fatigued mouse skeletal muscle. *Experimental physiology* **80,** 529-541.

Eberstein A & Sandow A. (1962). Fatigue mechanisms in muscle fibers. In *Symposium on the Effect of Use and Disuse on Neuromuscular Functions*, ed. Gutmann E & Hník P, pp. 576. Pub. House of the Czechoslovak Academy of Sciences, Czechoslovakia.

Edwards JN, Macdonald WA, van der Poel C & Stephenson DG. (2007). O_2*- production at 37 degrees C plays a critical role in depressing tetanic force of isolated rat and mouse skeletal muscle. *American journal of physiology* **293,** C650-660.

Fabiato A & Fabiato F. (1978). Effects of pH on the myofilaments and the sarcoplasmic reticulum of skinned cells from cardiace and skeletal muscles. *The Journal of physiology* **276,** 233-255.

Findlay I. (1993). Sulphonylurea drugs no longer inhibit ATP-sensitive K^+ channels during metabolic stress in cardiac muscle. *J Pharmacol Exp Ther* **266,** 456-467.

Findlay I. (1994). The ATP sensitive potassium channel of cardiac muscle and action potential shortening during metabolic stress. *Cardiovasc Res* **28,** 760-761.

Fitts RH. (1994). Cellular mechanisms of muscle fatigue. *Physiological reviews* **74,** 49-94.

Fitts RH & Balog EM. (1996). Effect of intracellular and extracellular ion changes on E-C coupling and skeletal muscle fatigue. *Acta physiologica Scandinavica* **156,** 169-181.

Forrest CR, Neligan P, Zhong A, He W, Yang RZ & Pang CY. (1997). Acute adenosine treatment is effective in augmentation of ischemic tolerance in muscle flaps in the pig. *Plast Reconstr Surg* **99,** 172-182.

Fowles JR, Green HJ, Schertzer JD & Tupling AR. (2002). Reduced activity of muscle Na^+-K^+-ATPase after prolonged running in rats. *J Appl Physiol* **93,** 1703-1708.

Fraser SF, Li JL, Carey MF, Wang XN, Sangkabutra T, Sostaric S, Selig SE, Kjeldsen K & McKenna MJ. (2002). Fatigue depresses maximal in vitro skeletal muscle Na^+-K^+-ATPase activity in untrained and trained individuals. *J Appl Physiol* **93,** 1650-1659.

Fryer MW, Owen VJ, Lamb GD & Stephenson DG. (1995). Effects of creatine phosphate and P_i on Ca^{2+} movements and tension development in rat skinned skeletal muscle fibres. *The Journal of physiology* **482 (Pt 1),** 123-140.

Fuller A, Carter RN & Mitchell D. (1998). Brain and abdominal temperatures at fatigue in rats exercising in the heat. *J Appl Physiol* **84,** 877-883.

Gallant EM & Goettl VM. (1985). Effects of calcium antagonists on mechanical responses of mammalian skeletal muscles. *Eur J Pharmacol* **117,** 259-265.

Garcia J, Amador M & Stefani E. (1989). Relationship between myoplasmic calcium transients and calcium currents in frog skeletal muscle. *The Journal of general physiology* **94,** 973-986.

Garlid KD, Dos Santos P, Xie ZJ, Costa AD & Paucek P. (2003). Mitochondrial potassium transport: the role of the mitochondrial ATP-sensitive K^+ channel in cardiac function and cardioprotection. *Biochem Biophys Acta* **1606,** 1-21.

Garlid KD & Paucek P. (2001). The mitochondrial potassium cycle. *IUBMB Life* **52,** 153-158.

Garlid KD, Paucek P, Yarov-Yarovoy V, Murray HN, Darbenzio RB, D'Alonzo AJ, Lodge NJ, Smith MA & Grover GJ. (1997). Cardioprotective effect of diazoxide and its interaction with mitochondrial ATP-sensitive K^+ channels. Possible mechanism of cardioprotection. *Circulation research* **81,** 1072-1082.

Giannesini B, Izquierdo M, Le Fur Y, Cozzone PJ & Bendahan D. (2001). In vivo reduction in ATP cost of contraction is not related to fatigue level in stimulated rat gastrocnemius muscle. *The Journal of physiology* **536,** 905-915.

Gibbs CL. (1987). Comparative muscle energetics and the cost of activation. *Proc Austr Physiol* **431,** 713-741.

Godt RE & Nosek TM. (1989). Changes of intracellular milieu with fatigue or hypoxia depress contraction of skinned rabbit skeletal and cardiac muscle. *The Journal of physiology* **412,** 155-180.

Goll DE, Thompson VF, Li H, Wei W & Cong J. (2003). The calpain system. *Physiological reviews* **83,** 731-801.

Gong B, Legault D, Miki T, Seino S & Renaud JM. (2003). K_{ATP} channels depress force by reducing action potential amplitude in mouse EDL and soleus muscle. *American journal of physiology* **285,** C1464-1474.

Gong B, Miki T, Seino S & Renaud JM. (2000). A K_{ATP} channel deficiency affects resting tension, not contractile force, during fatigue in skeletal muscle. *American journal of physiology* **279,** C1351-1358.

Gonzalez-Alonso J, Teller C, Andersen SL, Jensen FB, Hyldig T & Nielsen B. (1999). Influence of body temperature on the development of fatigue during prolonged exercise in the heat. *J Appl Physiol* **86,** 1032-1039.

Gramolini A & Renaud JM. (1997). Blocking ATP-sensitive K^+ channel during metabolic inhibition impairs muscle contractility. *The American journal of physiology* **272,** C1936-1946.

Green S, Bulow J & Saltin B. (1999). Microdialysis and the measurement of muscle interstitial K^+ during rest and exercise in humans. *J Appl Physiol* **87,** 460-464.

Green S, Langberg H, Skovgaard D, Bulow J & Kjaer M. (2000). Interstitial and arterial-venous $[K^+]$ in human calf muscle during dynamic exercise: effect of ischaemia and relation to muscle pain. *The Journal of physiology* **529 Pt 3,** 849-861.

Greene EC. (1968). *The anatomy of the rat*. Hafner Publisheing Co., New York.

Greenstock CL & Miller RW. (1975). The oxidation of tiron by superoxide anion. Kinetics of the reaction in aqueous solution in chloroplasts. *Biochim Biophys Acta* **396,** 11-16.

Gross ER & Gross GJ. (2006). Ligand triggers of classical preconditioning and postconditioning. *Cardiovasc Res* **70,** 212-221.

Gumina RJ, O'Cochlain DF, Kurtz CE, Bast P, Pucar D, Mishra P, Miki T, Seino S, Macura S & Terzic A. (2007). KATP channel knockout worsens myocardial calcium stress load in vivo and impairs recovery in stunned heart. *Am J Physiol Heart Circ Physiol* **292,** H1706-1713.

Gumina RJ, Pucar D, Bast P, Hodgson DM, Kurtz CE, Dzeja PP, Miki T, Seino S & Terzic A. (2003). Knockout of Kir6.2 negates ischemic preconditioning-induced protection of myocardial energetics. *Am J Physiol Heart Circ Physiol* **284,** H2106-2113.

Gurke L, Marx A, Sutter PM, Frentzel A, Salm T, Harder F, Seelig J & Heberer M. (1996). Ischemic preconditioning improves post-ischemic skeletal muscle function. *Am Surg* **62,** 391-394.

Gurke L, Mattei A, Chaloupka K, Marx A, Sutter PM, Stierli P, Harder F & Heberer M. (2000). Mechanisms of ischemic preconditioning in skeletal muscle. *J Surg Res* **94,** 18-27.

Halestrap AP, Clarke SJ & Khaliulin I. (2007). The role of mitochondria in protection of the heart by preconditioning. *Biochim Biophys Acta* **1767,** 1007-1031.

Hamilton SL & Reid MB. (2000). RyR1 modulation by oxidation and calmodulin. *Antioxid Redox Signal* **2,** 41-45.

Hancock CR, Brault JJ, Wiseman RW, Terjung RL & Meyer RA. (2005). ^{31}P-NMR observation of free ADP during fatiguing, repetitive contractions of murine skeletal muscle lacking AK1. *American journal of physiology* **288,** C1298-1304.

Hanley PJ, Drose S, Brandt U, Lareau RA, Banerjee AL, Srivastava DK, Banaszak LJ, Barycki JJ, Van Veldhoven PP & Daut J. (2005). 5-Hydroxydecanoate is metabolised in mitochondria and creates a rate-limiting bottleneck for beta-oxidation of fatty acids. *The Journal of physiology* **562,** 307-318.

Hanley PJ, Gopalan KV, Lareau RA, Srivastava DK, von Meltzer M & Daut J. (2003). Beta-oxidation of 5-hydroxydecanoate, a putative blocker of mitochondrial ATP-sensitive potassium channels. *The Journal of physiology* **547,** 387-393.

Hanley PJ, Mickel M, Loffler M, Brandt U & Daut J. (2002). K_{ATP} channel-independent targets of diazoxide and 5-hydroxydecanoate in the heart. *The Journal of physiology* **542,** 735-741.

Hansford RG, Hogue BA & Mildaziene V. (1997). Dependence of H_2O_2 formation by rat heart mitochondria on substrate availability and donor age. *J Bioenerg Biomembr* **29,** 89-95.

Holmuhamedov EL, Wang L & Terzic A. (1999). ATP-sensitive K^+ channel openers prevent Ca^{2+} overload in rat cardiac mitochondria. *The Journal of physiology* **519 Pt 2,** 347-360.

Hopper RA, Forrest CR, Xu H, Zhong A, He W, Rutka J, Neligan P & Pang CY. (2000). Role and mechanism of PKC in ischemic preconditioning of pig skeletal muscle against infarction. *Am J Physiol Regul Integr Comp Physiol* **279,** R666-676.

Ildefonse M, Jacquemond V, Rougier O, Renaud JF, Fosset M & Lazdunski M. (1985). Excitation contraction coupling in skeletal muscle: evidence for a role of slow Ca^{2+} channels using Ca^{2+} channel activators and inhibitors in the dihydropyridine series. *Biochem Biophys Res Commun* **129,** 904-909.

Inagaki K, Chen L, Ikeno F, Lee FH, Imahashi K, Bouley DM, Rezaee M, Yock PG, Murphy E & Mochly-Rosen D. (2003a). Inhibition of delta-protein kinase C protects against reperfusion injury of the ischemic heart in vivo. *Circulation* **108,** 2304-2307.

Inagaki K, Hahn HS, Dorn GW, 2nd & Mochly-Rosen D. (2003b). Additive protection of the ischemic heart ex vivo by combined treatment with delta-protein kinase C inhibitor and epsilon-protein kinase C activator. *Circulation* **108,** 869-875.

Inagaki N, Gonoi T & Seino S. (1997). Subunit stoichiometry of the pancreatic beta-cell ATP-sensitive K^+ channel. *FEBS letters* **409,** 232-236.

Ingalls CP, Warren GL, Williams JH, Ward CW & Armstrong RB. (1998). E-C coupling failure in mouse EDL muscle after in vivo eccentric contractions. *J Appl Physiol* **85,** 58-67.

Inoue M, Sato EF, Nishikawa M, Park AM, Kira Y, Imada I & Utsumi K. (2003). Mitochondrial generation of reactive oxygen species and its role in aerobic life. *Curr Med Chem* **10,** 2495-2505.

Jackson MJ. (2009). Redox regulation of adaptive responses in skeletal muscle to contractile activity. *Free Radic Biol Med.*

Jackson MJ, Jones DA & Edwards RH. (1984). Experimental skeletal muscle damage: the nature of the calcium-activated degenerative processes. *Eur J Clin Invest* **14,** 369-374.

Jacobs I, Bar-Or O, Karlsson J, Dotan R, Tesch P, Kaiser P & Inbar O. (1982). Changes in muscle metabolites in females with 30-s exhaustive exercise. *Medicine and science in sports and exercise* **14,** 457-460.

Jacquemond V & Allard B. (1998). Activation of Ca2+-activated K+ channels by an increase in intracellular Ca2+ induced by depolarization of mouse skeletal muscle fibres. *The Journal of physiology* **509 (Pt 1),** 93-102.

Jansson E, Dudley GA, Norman B & Tesch PA. (1987). ATP and IMP in single human muscle fibres after high intensity exercise. *Clinical physiology (Oxford, England)* **7,** 337-345.

Jarvis JC, Sutherland H, Mayne CN, Gilroy SJ & Salmons S. (1996). Induction of a fast-oxidative phenotype by chronic muscle stimulation: mechanical and biochemical studies. *The American journal of physiology* **270,** C306-312.

Jeffrey IW, Bushell M, Tilleray VJ, Morley S & Clemens MJ. (2002). Inhibition of protein synthesis in apoptosis: differential requirements by the tumor necrosis factor alpha family and a DNA-damaging agent for caspases and the double-stranded RNA-dependent protein kinase. *Cancer Res* **62,** 2272-2280.

Juel C, Pilegaard H, Nielsen JJ & Bangsbo J. (2000). Interstitial K^+ in human skeletal muscle during and after dynamic graded exercise determined by microdialysis. *Am J Physiol Regul Integr Comp Physiol* **278,** R400-406.

Jurkat-Rott K, Fauler M & Lehmann-Horn F. (2006). Ion channels and ion transporters of the transverse tubular system of skeletal muscle. *J Muscle Res Cell Motil* **27,** 275-290.

Kane GC, Behfar A, Dyer RB, O'Cochlain DF, Liu XK, Hodgson DM, Reyes S, Miki T, Seino S & Terzic A. (2006). KCNJ11 gene knockout of the Kir6.2 K_{ATP} channel causes maladaptive remodeling and heart failure in hypertension. *Hum Mol Genet* **15,** 2285-2297.

Kane GC, Behfar A, Yamada S, Perez-Terzic C, O'Cochlain F, Reyes S, Dzeja PP, Miki T, Seino S & Terzic A. (2004). ATP-sensitive K^+ channel knockout compromises the metabolic benefit of exercise training, resulting in cardiac deficits. *Diabetes* **53 Suppl 3,** S169-175.

Karatzaferi C, de Haan A, Ferguson RA, van Mechelen W & Sargeant AJ. (2001). Phosphocreatine and ATP content in human single muscle fibres before and after maximum dynamic exercise. *Pflugers Arch* **442,** 467-474.

Keung EC & Li Q. (1991). Lactate activates ATP-sensitive potassium channels in guinea pig ventricular myocytes. *J Clin Invest* **88,** 1772-1777.

Khaliulin I, Clarke SJ, Lin H, Parker J, Suleiman MS & Halestrap AP. (2007). Temperature preconditioning of isolated rat hearts--a potent cardioprotective mechanism involving a reduction in oxidative stress and inhibition of the mitochondrial permeability transition pore. *The Journal of physiology* **581,** 1147-1161.

Khawli FA & Reid MB. (1994). N-acetylcysteine depresses contractile function and inhibits fatigue of diaphragm in vitro. *J Appl Physiol* **77,** 317-324.

Kristensen M, Hansen T & Juel C. (2006). Membrane proteins involved in potassium shifts during muscle activity and fatigue. *Am J Physiol Regul Integr Comp Physiol* **290,** R766-772.

Lamb GD. (1986). Components of charge movement in rabbit skeletal muscle: the effect of tetracaine and nifedipine. *The Journal of physiology* **376,** 85-100.

Lamb GD, Recupero E & Stephenson DG. (1992). Effect of myoplasmic pH on excitation-contraction coupling in skeletal muscle fibres of the toad. *The Journal of physiology* **448,** 211-224.

Lamb GD & Walsh T. (1987). Calcium currents, charge movement and dihydropyridine binding in fast- and slow-twitch muscles of rat and rabbit. *The Journal of physiology* **393,** 595-617.

Lannergren J & Westerblad H. (1986). Force and membrane potential during and after fatiguing, continuous high-frequency stimulation of single Xenopus muscle fibres. *Acta physiologica Scandinavica* **128,** 359-368.

Lannergren J & Westerblad H. (1987). Action potential fatigue in single skeletal muscle fibres of Xenopus. *Acta physiologica Scandinavica* **129,** 311-318.

Laver DR, Lenz GK & Dulhunty AF. (2001). Phosphate ion channels in sarcoplasmic reticulum of rabbit skeletal muscle. *The Journal of physiology* **535,** 715-728.

Lee C & Okabe E. (1995). Hydroxyl radical-mediated reduction of Ca(2+)-ATPase activity of masseter muscle sarcoplasmic reticulum. *Jpn J Pharmacol* **67,** 21-28.

Leppik JA, Aughey RJ, Medved I, Fairweather I, Carey MF & McKenna MJ. (2004). Prolonged exercise to fatigue in humans impairs skeletal muscle Na^+-K^+-ATPase activity, sarcoplasmic reticulum Ca^{2+} release, and Ca^{2+} uptake. *J Appl Physiol* **97,** 1414-1423.

Light PE, Bladen C, Winkfein RJ, Walsh MP & French RJ. (2000). Molecular basis of protein kinase C-induced activation of ATP-sensitive potassium channels. *Proceedings of the National Academy of Sciences of the United States of America* **97,** 9058-9063.

Light PE, Comtois AS & Renaud JM. (1994). The effect of glibenclamide on frog skeletal muscle: evidence for K_{ATP} channel activation during fatigue. *The Journal of physiology* **475,** 495-507.

Light PE, Kanji HD, Fox JE & French RJ. (2001). Distinct myoprotective roles of cardiac sarcolemmal and mitochondrial K_{ATP} channels during metabolic inhibition and recovery. *FASEB J* **15,** 2586-2594.

Lim KH, Javadov SA, Das M, Clarke SJ, Suleiman MS & Halestrap AP. (2002). The effects of ischaemic preconditioning, diazoxide and 5-hydroxydecanoate on rat heart mitochondrial volume and respiration. *J Physiol* **545,** 961-974.

Lindinger MI, Hawke TJ, Vickery L, Bradford L & Lipskie SL. (2001). An integrative, in situ approach to examining K^+ flux in resting skeletal muscle. *Canadian journal of physiology and pharmacology* **79,** 996-1006.

Lindinger MI & Heigenhauser GJ. (1988). Ion fluxes during tetanic stimulation in isolated perfused rat hindlimb. *The American journal of physiology* **254,** R117-126.

Lynch GS, Fary CJ & Williams DA. (1997). Quantitative measurement of resting skeletal muscle $[Ca^{2+}]_i$ following acute and long-term downhill running exercise in mice. *Cell Calcium* **22,** 373-383.

Mallouk N & Allard B. (2000). Stretch-induced activation of Ca^{2+}-activated K^+ channels in mouse skeletal muscle fibers. *American journal of physiology* **278,** C473-479.

Martins NM, Santos NA, Curti C, Bianchi ML & Santos AC. (2008). Cisplatin induces mitochondrial oxidative stress with resultant energetic metabolism impairment, membrane rigidification and apoptosis in rat liver. *J Appl Toxicol* **28,** 337-344.

Matar W, Lunde JA, Jasmin BJ & Renaud JM. (2001). Denervation enhances the physiological effects of the K_{ATP} channel during fatigue in EDL and soleus muscle. *Am J Physiol Regul Integr Comp Physiol* **281,** R56-65.

Matar W, Nosek TM, Wong D & Renaud J. (2000). Pinacidil suppresses contractility and preserves energy but glibenclamide has no effect during muscle fatigue. *American journal of physiology* **278,** C404-416.

Mattei A, Sutter PM, Marx A, Stierli P, Heberer M & Gurke L. (2000). Preconditioning with short cycles improves ischemic tolerance in rat fast- and slow-twitch skeletal muscle. *Eur Surg Res* **32,** 297-304.

McArdle F, Spiers S, Aldemir H, Vasilaki A, Beaver A, Iwanejko L, McArdle A & Jackson MJ. (2004). Preconditioning of skeletal muscle against contraction-induced damage: the role of adaptations to oxidants in mice. *The Journal of physiology* **561,** 233-244.

McCleskey EW. (1985). Calcium channels and intracellular calcium release are pharmacologically different in frog skeletal muscle. *The Journal of physiology* **361,** 231-249.

McComas AJ & Mrozek K. (1968). The electrical properties of muscle fiber membranes in dystrophia myotonica and myotonia congenita. *J Neurol Neurosurg Psychiatry* **31,** 441-447.

McKenna MJ. (1992). The roles of ionic processes in muscular fatigue during intense exercise. *Sports medicine (Auckland, NZ* **13,** 134-145.

McKenna MJ, Bangsbo J & Renaud JM. (2008). Muscle K^+, Na^+, and Cl^- disturbances and Na^+-K^+ pump inactivation: implications for fatigue. *J Appl Physiol* **104,** 288-295.

McKenna MJ, Medved I, Goodman CA, Brown MJ, Bjorksten AR, Murphy KT, Petersen AC, Sostaric S & Gong X. (2006). N-acetylcysteine attenuates the decline in muscle Na^+,K^+-pump activity and delays fatigue during prolonged exercise in humans. *The Journal of physiology* **576,** 279-288.

McPherson CD, Pierce GN & Cole WC. (1993). Ischemic cardioprotection by ATP-sensitive K^+ channels involves high-energy phosphate preservation. *The American journal of physiology* **265,** H1809-1818.

Merton PA. (1954). Voluntary strength and fatigue. *The Journal of physiology* **123,** 553-564.

Miki T, Liss B, Minami K, Shiuchi T, Saraya A, Kashima Y, Horiuchi M, Ashcroft F, Minokoshi Y, Roeper J & Seino S. (2001). ATP-sensitive K^+ channels in the hypothalamus are essential for the maintenance of glucose homeostasis. *Nature neuroscience* **4,** 507-512.

Miki T, Minami K, Zhang L, Morita M, Gonoi T, Shiuchi T, Minokoshi Y, Renaud JM & Seino S. (2002). ATP-sensitive potassium channels participate in glucose uptake in skeletal muscle and adipose tissue. *Am J Physiol Endocrinol Metab* **283,** E1178-1184.

Miki T, Nagashima K & Seino S. (1999). The structure and function of the ATP-sensitive K^+ channel in insulin-secreting pancreatic beta-cells. *Journal of molecular endocrinology* **22,** 113-123.

Miki T, Nagashima K, Tashiro F, Kotake K, Yoshitomi H, Tamamoto A, Gonoi T, Iwanaga T, Miyazaki J & Seino S. (1998). Defective insulin secretion and enhanced insulin action in K_{ATP} channel-deficient mice. *Proceedings of the National Academy of Sciences of the United States of America* **95,** 10402-10406.

Mikkelsen UR, Gissel H, Fredsted A & Clausen T. (2005). Excitation-induced cell damage and {beta}2-adrenoceptor agonist stimulated force recovery in rat skeletal muscle. *Am J Physiol Regul Integr Comp Physiol.*

Miledi R, Parker I & Schalow G. (1977). Calcium transients in frog slow muscle fibres. *Nature* **268,** 750-752.

Minners J, Lacerda L, Yellon DM, Opie LH, McLeod CJ & Sack MN. (2007). Diazoxide-induced respiratory inhibition - a putative mitochondrial K_{ATP} channel independent mechanism of pharmacological preconditioning. *Mol Cell Biochem* **294,** 11-18.

Mohanraj P, Merola AJ, Wright VP & Clanton TL. (1998). Antioxidants protect rat diaphragmatic muscle function under hypoxic conditions. *J Appl Physiol* **84,** 1960-1966.

Moldeus P, Cotgreave IA & Berggren M. (1986). Lung protection by a thiol-containing antioxidant: N-acetylcysteine. *Respiration* **50 Suppl 1,** 31-42.

Moopanar TR & Allen DG. (2005). Reactive oxygen species reduce myofibrillar Ca^{2+} sensitivity in fatiguing mouse skeletal muscle at 37 degrees C. *The Journal of physiology* **564,** 189-199.

Moopanar TR & Allen DG. (2006). The activity-induced reduction of myofibrillar Ca^{2+} sensitivity in mouse skeletal muscle is reversed by dithiothreitol. *The Journal of physiology* **571,** 191-200.

Moses MA, Addison PD, Neligan PC, Ashrafpour H, Huang N, Zair M, Rassuli A, Forrest CR, Grover GJ & Pang CY. (2005). Mitochondrial KATP channels in hindlimb remote ischemic preconditioning of skeletal muscle against infarction. *Am J Physiol Heart Circ Physiol* **288,** H559-567.

Murata M, Akao M, O'Rourke B & Marban E. (2001). Mitochondrial ATP-sensitive potassium channels attenuate matrix Ca^{2+} overload during simulated ischemia and reperfusion: possible mechanism of cardioprotection. *Circulation research* **89,** 891-898.

Murphy KT, Snow RJ, Petersen AC, Murphy RM, Mollica J, Lee JS, Garnham AP, Aughey RJ, Leppik JA, Medved I, Cameron-Smith D & McKenna MJ. (2004). Intense exercise up-regulates Na^+,K^+-ATPase isoform mRNA, but not protein expression in human skeletal muscle. *The Journal of physiology* **556,** 507-519.

Murphy RM, Dutka TL & Lamb GD. (2008). Hydroxyl radical and glutathione interactions alter calcium sensitivity and maximum force of the contractile apparatus in rat skeletal muscle fibres. *The Journal of physiology* **586,** 2203-2216.

Murphy RM, Goodman CA, McKenna MJ, Bennie J, Leikis M & Lamb GD. (2007). Calpain-3 is autolyzed and hence activated in human skeletal muscle 24 h following a single bout of eccentric exercise. *J Appl Physiol* **103,** 926-931.

Murphy RM & Lamb GD. (2009). Endogenous calpain-3 activation is primarily governed by small increases in resting cytoplasmic [Ca^{2+}] and is not dependent on stretch. *The Journal of biological chemistry* **284,** 7811-7819.

Murphy RM, Verburg E & Lamb GD. (2006). Ca^{2+} activation of diffusible and bound pools of mu-calpain in rat skeletal muscle. *The Journal of physiology* **576,** 595-612.

Murry CE, Jennings RB & Reimer KA. (1986). Preconditioning with ischemia: a delay of lethal cell injury in ischemic myocardium. *Circulation* **74,** 1124-1136.

Nethery D, Callahan LA, Stofan D, Mattera R, DiMarco A & Supinski G. (2000). PLA_2 dependence of diaphragm mitochondrial formation of reactive oxygen species. *J Appl Physiol* **89,** 72-80.

Nichols CG & Lederer WJ. (1991). Adenosine triphosphate-sensitive potassium channels in the cardiovascular system. *The American journal of physiology* **261,** H1675-1686.

Nichols CG, Ripoll C & Lederer WJ. (1991). ATP-sensitive potassium channel modulation of the guinea pig ventricular action potential and contraction. *Circulation research* **68,** 280-287.

Nielsen JJ, Kristensen M, Hellsten Y, Bangsbo J & Juel C. (2003). Localization and function of ATP-sensitive potassium channels in human skeletal muscle. *Am J Physiol Regul Integr Comp Physiol* **284,** R558-563.

Nielsen OB, Ortenblad N, Lamb GD & Stephenson DG. (2004). Excitability of the T-tubular system in rat skeletal muscle: roles of K^+ and Na^+ gradients and Na^+-K^+ pump activity. *The Journal of physiology* **557,** 133-146.

Noma A. (1983). ATP-regulated K^+ channels in cardiac muscle. *Nature* **305,** 147-148.

Nosek TM, Fender KY & Godt RE. (1987). It is diprotonated inorganic phosphate that depresses force in skinned skeletal muscle fibers. *Science (New York, NY* **236,** 191-193.

Nosek TM, Leal-Cardoso JH, McLaughlin M & Godt RE. (1990). Inhibitory influence of phosphate and arsenate on contraction of skinned skeletal and cardiac muscle. *The American journal of physiology* **259,** C933-939.

O'Rourke B. (2004). Evidence for mitochondrial K^+ channels and their role in cardioprotection. *Circulation research* **94,** 420-432.

Oldenburg O, Cohen MV, Yellon DM & Downey JM. (2002). Mitochondrial K_{ATP} channels: role in cardioprotection. *Cardiovasc Res* **55,** 429-437.

Oldenburg O, Qin Q, Krieg T, Yang XM, Philipp S, Critz SD, Cohen MV & Downey JM. (2004). Bradykinin induces mitochondrial ROS generation via NO, cGMP, PKG and mitoK_{ATP} channel opening and leads to cardioprotection. *Am J Physiol Heart Circ Physiol* **286,** H468-H476.

Oldenburg O, Yang XM, Krieg T, Garlid KD, Cohen MV, Grover GJ & Downey JM. (2003). P1075 opens mitochondrial K_{ATP} channels and generates reactive oxygen species resulting in cardioprotection of rabbit hearts. *J Mol Cell Cardiol* **35,** 1035-1042.

Oz M & Frank GB. (1991). Decrease in the size of tetanic responses produced by nitrendipine or by extracellular calcium ion removal without blocking twitches or action potentials in skeletal muscle. *J Pharmacol Exp Ther* **257,** 575-581.

Pang CY & Forrest CR. (1995). Acute pharmacological preconditioning as a new concept and alternative approach for prevention of skeletal muscle ischemic necrosis. *Biochem Pharmacol* **49,** 1023-1034.

Pang CY, Neligan P, Xu H, He W, Zhong A, Hopper R & Forrest CR. (1997a). Role of ATP-sensitive K^+ channels in ischemic preconditioning of skeletal muscle against infarction. *The American journal of physiology* **273,** H44-51.

Pang CY, Neligan P, Zhong A, He W, Xu H & Forrest CR. (1997b). Effector mechanism of adenosine in acute ischemic preconditioning of skeletal muscle against infarction. *The American journal of physiology* **273,** R887-895.

Pang CY, Yang RZ, Zhong A, Xu N, Boyd B & Forrest CR. (1995). Acute ischaemic preconditioning protects against skeletal muscle infarction in the pig. *Cardiovasc Res* **29,** 782-788.

Papanastasiou S, Estdale SE, Homer-Vanniasinkam S & Mathie RT. (1999). Protective effect of preconditioning and adenosine pretreatment in experimental skeletal muscle reperfusion injury. *Br J Surg* **86,** 916-922.

Pedersen TH, Clausen T & Nielsen OB. (2003). Loss of force induced by high extracellular [K^+] in rat muscle: effect of temperature, lactic acid and beta2-agonist. *The Journal of physiology* **551,** 277-286.

Pedersen TH, de Paoli F & Nielsen OB. (2005). Increased excitability of acidified skeletal muscle: role of chloride conductance. *The Journal of general physiology* **125,** 237-246.

Pedersen TH, de Paoli FV, Flatman JA & Nielsen OB. (2009). Regulation of ClC-1 and K_{ATP} channels in action potential-firing fast-twitch muscle fibers. *The Journal of general physiology* **134,** 309-322.

Pedersen TH, Nielsen OB, Lamb GD & Stephenson DG. (2004). Intracellular acidosis enhances the excitability of working muscle. *Science (New York, NY* **305,** 1144-1147.

Petersen AC, Murphy KT, Snow RJ, Leppik JA, Aughey RJ, Garnham AP, Cameron-Smith D & McKenna MJ. (2005). Depressed Na^+-K^+-ATPase activity in skeletal muscle at fatigue is correlated with increased Na^+-K^+-ATPase mRNA expression following intense exercise. *Am J Physiol Regul Integr Comp Physiol* **289,** R266-274.

Pette D & Vrbova G. (1992). Adaptation of mammalian skeletal muscle fibers to chronic electrical stimulation. *Rev Physiol Biochem Pharmacol* **120,** 115-202.

Piper HM & Garcia-Dorado D. (1999). Prime causes of rapid cardiomyocyte death during reperfusion. *Ann Thorac Surg* **68,** 1913-1919.

Porter JD, Merriam AP, Leahy P, Gong B, Feuerman J, Cheng G & Khanna S. (2004). Temporal gene expression profiling of dystrophin-deficient (mdx) mouse diaphragm identifies conserved and muscle group-specific mechanisms in the pathogenesis of muscular dystrophy. *Hum Mol Genet* **13,** 257-269.

Pusch M. (2002). Myotonia caused by mutations in the muscle chloride channel gene CLCN1. *Hum Mutat* **19,** 423-434.

Raymackers JM, Gailly P, Schoor MC, Pette D, Schwaller B, Hunziker W, Celio MR & Gillis JM. (2000). Tetanus relaxation of fast skeletal muscles of the mouse made parvalbumin deficient by gene inactivation. *The Journal of physiology* **527 Pt 2,** 355-364.

Reardon TF & Allen DG. (2009). Time to fatigue is increased in mouse muscle at 37 degrees C; the role of iron and reactive oxygen species. *The Journal of physiology* **587,** 4705-4716.

Reid MB. (2001a). Invited Review: redox modulation of skeletal muscle contraction: what we know and what we don't. *J Appl Physiol* **90,** 724-731.

Reid MB. (2001b). Nitric oxide, reactive oxygen species, and skeletal muscle contraction. *Medicine and science in sports and exercise* **33,** 371-376.

Renaud JM. (2002). Modulation of force development by Na^+, K^+, Na^+K^+ pump and K_{ATP} channel during muscular activity. *Can J Appl Physiol* **27,** 296-315.

Rios E & Pizarro G. (1991). Voltage sensor of excitation-contraction coupling in skeletal muscle. *Physiological reviews* **71,** 849-908.

Ruff RL. (1999). Effects of temperature on slow and fast inactivation of rat skeletal muscle Na^+ channels. *The American journal of physiology* **277,** C937-947.

Sacco P & Jones DA. (1992). The protective effect of damaging eccentric exercise against repeated bouts of exercise in the mouse tibialis anterior muscle. *Experimental physiology* **77,** 757-760.

Sandiford SD, Green HJ & Ouyang J. (2005). Mechanisms underlying increases in rat soleus Na^+-K^+-ATPase activity by induced contractions. *J Appl Physiol* **99,** 2222-2232.

Sandstrom ME, Zhang SJ, Bruton J, Silva JP, Reid MB, Westerblad H & Katz A. (2006). Role of reactive oxygen species in contraction-mediated glucose transport in mouse skeletal muscle. *The Journal of physiology* **575,** 251-262.

Sato T, O'Rourke B & Marban E. (1998). Modulation of mitochondrial ATP-dependent K^+ channels by protein kinase C. *Circulation research* **83,** 110-114.

Sato T, Saito T, Saegusa N & Nakaya H. (2005). Mitochondrial Ca^{2+}-activated K^+ channels in cardiac myocytes: a mechanism of the cardioprotective effect and modulation by protein kinase A. *Circulation* **111,** 198-203.

Seino S. (1999). ATP-sensitive potassium channels: a model of heteromultimeric potassium channel/receptor assemblies. *Annu Rev Physiol* **61,** 337-362.

Seino S & Miki T. (2003). Physiological and pathophysiological roles of ATP-sensitive K^+ channels. *Progress in biophysics and molecular biology* **81,** 133-176.

Senisterra GA, Huntley SA, Escaravage M, Sekhar KR, Freeman ML, Borrelli M & Lepock JR. (1997). Destabilization of the Ca2+-ATPase of sarcoplasmic reticulum by thiol-specific, heat shock inducers results in thermal denaturation at 37 degrees C. *Biochemistry* **36,** 11002-11011.

Sjogaard G, Adams RP & Saltin B. (1985). Water and ion shifts in skeletal muscle of humans with intense dynamic knee extension. *The American journal of physiology* **248,** R190-196.

Smith MA & Reid MB. (2006). Redox modulation of contractile function in respiratory and limb skeletal muscle. *Respir Physiol Neurobiol* **151,** 229-241.

Spruce AE, Standen NB & Stanfield PR. (1987). Studies of the unitary properties of adenosine-5'-triphosphate-regulated potassium channels of frog skeletal muscle. *The Journal of physiology* **382,** 213-236.

Standen NB, Quayle JM, Davies NW, Brayden JE, Huang Y & Nelson MT. (1989). Hyperpolarizing vasodilators activate ATP-sensitive K^+ channels in arterial smooth muscle. *Science (New York, NY* **245,** 177-180.

Steel RGD & Torrie JH. (1980). *Principles and procedures of statistics. A biometrical approach.* McGraw-Hill Book Company, New York.

Steele DS & Duke AM. (2003). Metabolic factors contributing to altered Ca^{2+} regulation in skeletal muscle fatigue. *Acta physiologica Scandinavica* **179,** 39-48.

Stoller D, Pytel P, Katz S, Earley JU, Collins K, Metcalfe J, Lang RM & McNally EM. (2009). Impaired exercise tolerance and skeletal muscle myopathy in sulfonylurea receptor-2 mutant mice. *Am J Physiol Regul Integr Comp Physiol* **297,** R1144-1153.

Street D, Nielsen JJ, Bangsbo J & Juel C. (2005). Metabolic alkalosis reduces exercise-induced acidosis and potassium accumulation in human skeletal muscle interstitium. *The Journal of physiology* **566,** 481-489.

Suzuki M, Li RA, Miki T, Uemura H, Sakamoto N, Ohmoto-Sekine Y, Tamagawa M, Ogura T, Seino S, Marban E & Nakaya H. (2001). Functional roles of cardiac and vascular ATP-sensitive potassium channels clarified by Kir6.2-knockout mice. *Circ Res* **88,** 570-577.

Suzuki M, Sasaki N, Miki T, Sakamoto N, Ohmoto-Sekine Y, Tamagawa M, Seino S, Marban E & Nakaya H. (2002). Role of sarcolemmal K(ATP) channels in cardioprotection against ischemia/reperfusion injury in mice. *J Clin Invest* **109,** 509-516.

Szentesi P, Zaremba R, van Mechelen W & Stienen GJ. (2001). ATP utilization for calcium uptake and force production in different types of human skeletal muscle fibres. *The Journal of physiology* **531,** 393-403.

Taborsky GJ, Jr., Ahren B & Havel PJ. (1998). Autonomic mediation of glucagon secretion during hypoglycemia: implications for impaired alpha-cell responses in type 1 diabetes. *Diabetes* **47,** 995-1005.

Tanabe T, Beam KG, Adams BA, Niidome T & Numa S. (1990a). Regions of the skeletal muscle dihydropyridine receptor critical for excitation-contraction coupling. *Nature* **346,** 567-569.

Tanabe T, Mikami A, Numa S & Beam KG. (1990b). Cardiac-type excitation-contraction coupling in dysgenic skeletal muscle injected with cardiac dihydropyridine receptor cDNA. *Nature* **344,** 451-453.

Thabet M, Miki T, Seino S & Renaud JM. (2005). Treadmill running causes significant fiber damage in skeletal muscle of KATP channel-deficient mice. *Physiol Genomics* **22,** 204-212.

Tricarico D, Capriulo R & Conte Camerino D. (1999a). Insulin modulation of ATP-sensitive K^+ channel of rat skeletal muscle is impaired in the hypokalaemic state. *Pflugers Arch* **437,** 235-240.

Tricarico D, Mele A & Conte Camerino D. (2005). Phenotype-dependent functional and pharmacological properties of BK channels in skeletal muscle: effects of microgravity. *Neurobiol Dis* **20,** 296-302.

Tricarico D, Mele A, Lundquist AL, Desai RR, George AL, Jr. & Conte Camerino D. (2006). Hybrid assemblies of ATP-sensitive K^+ channels determine their muscle-type-dependent biophysical and pharmacological properties. *Proceedings of the National Academy of Sciences of the United States of America* **103,** 1118-1123.

Tricarico D, Servidei S, Tonali P, Jurkat-Rott K & Camerino DC. (1999b). Impairment of skeletal muscle adenosine triphosphate-sensitive K^+ channels in patients with hypokalemic periodic paralysis. *J Clin Invest* **103,** 675-682.

Tucker SJ, Gribble FM, Zhao C, Trapp S & Ashcroft FM. (1997). Truncation of Kir6.2 produces ATP-sensitive K^+ channels in the absence of the sulphonylurea receptor. *Nature* **387,** 179-183.

Tusnady GE, Bakos E, Varadi A & Sarkadi B. (1997). Membrane topology distinguishes a subfamily of the ATP-binding cassette (ABC) transporters. *FEBS letters* **402,** 1-3.

Ueda K, Komine J, Matsuo M, Seino S & Amachi T. (1999). Cooperative binding of ATP and MgADP in the sulfonylurea receptor is modulated by glibenclamide. *Proceedings of the National Academy of Sciences of the United States of America* **96,** 1268-1272.

van der Poel C & Stephenson DG. (2002). Reversible changes in Ca^{2+}-activation properties of rat skeletal muscle exposed to elevated physiological temperatures. *The Journal of physiology* **544,** 765-776.

Van Lunteren E, Moyer M & Torres A. (1998). ATP-sensitive K^+ channel blocker glibenclamide and diaphragm fatigue during normoxia and hypoxia. *J Appl Physiol* **85,** 601-608.

Vercesi AE, Kowaltowski AJ, Grijalba MT, Meinicke AR & Castilho RF. (1997). The role of reactive oxygen species in mitochondrial permeability transition. *Biosci Rep* **17,** 43-52.

Vivaudou MB, Arnoult C & Villaz M. (1991). Skeletal muscle ATP-sensitive K^+ channels recorded from sarcolemmal blebs of split fibers: ATP inhibition is reduced by magnesium and ADP. *The Journal of membrane biology* **122,** 165-175.

Vollestad NK, Sejersted OM, Bahr R, Woods JJ & Bigland-Ritchie B. (1988). Motor drive and metabolic responses during repeated submaximal contractions in humans. *J Appl Physiol* **64,** 1421-1427.

Walker JE, Saraste M, Runswick MJ & Gay NJ. (1982). Distantly related sequences in the alpha- and beta-subunits of ATP synthase, myosin, kinases and other ATP-requiring enzymes and a common nucleotide binding fold. *The EMBO journal* **1,** 945-951.

Warren GL, Ingalls CP & Armstrong RB. (2002). Temperature dependency of force loss and Ca^{2+} homeostasis in mouse EDL muscle after eccentric contractions. *Am J Physiol Regul Integr Comp Physiol* **282,** R1122-1132.

Weselcouch EO, Sargent C, Wilde MW & Smith MA. (1993). ATP-sensitive potassium channels and skeletal muscle function in vitro. *J Pharmacol Exp Ther* **267,** 410-416.

Westerblad H & Allen DG. (1991). Changes of myoplasmic calcium concentration during fatigue in single mouse muscle fibers. *The Journal of general physiology* **98,** 615-635.

Westerblad H & Allen DG. (1993). The contribution of $[Ca^{2+}]_i$ to the slowing of relaxation in fatigued single fibres from mouse skeletal muscle. *The Journal of physiology* **468,** 729-740.

Westerblad H & Allen DG. (1994). Methods for calibration of fluorescent calcium indicators in skeletal muscle fibers. *Biophysical journal* **66,** 926-928.

Westerblad H, Bruton JD & Lannergren J. (1997). The effect of intracellular pH on contractile function of intact, single fibres of mouse muscle declines with increasing temperature. *The Journal of physiology* **500 (Pt 1),** 193-204.

Westerblad H, Lee JA, Lannergren J & Allen DG. (1991). Cellular mechanisms of fatigue in skeletal muscle. *The American journal of physiology* **261,** C195-209.

Zhang SJ, Andersson DC, Sandstrom ME, Westerblad H & Katz A. (2006a). Cross bridges account for only 20% of total ATP consumption during submaximal

isometric contraction in mouse fast-twitch skeletal muscle. *American journal of physiology* **291,** C147-154.

Zhang SJ, Bruton JD, Katz A & Westerblad H. (2006b). Limited oxygen diffusion accelerates fatigue development in mouse skeletal muscle. *The Journal of physiology* **572,** 551-559.

Zheng J, Wang R, Zambraski E, Wu D, Jacobson KA & Liang BT. (2007). Protective roles of adenosine A1, A2A, and A3 receptors in skeletal muscle ischemia and reperfusion injury. *Am J Physiol Heart Circ Physiol* **293,** H3685-3691.

Zingman LV, Hodgson DM, Bast PH, Kane GC, Perez-Terzic C, Gumina RJ, Pucar D, Bienengraeber M, Dzeja PP, Miki T, Seino S, Alekseev AE & Terzic A. (2002). Kir6.2 is required for adaptation to stress. *Proceedings of the National Academy of Sciences of the United States of America* **99,** 13278-13283.

Zuo L, Christofi FL, Wright VP, Liu CY, Merola AJ, Berliner LJ & Clanton TL. (2000). Intra- and extracellular measurement of reactive oxygen species produced during heat stress in diaphragm muscle. *American journal of physiology* **279,** C1058-1066.